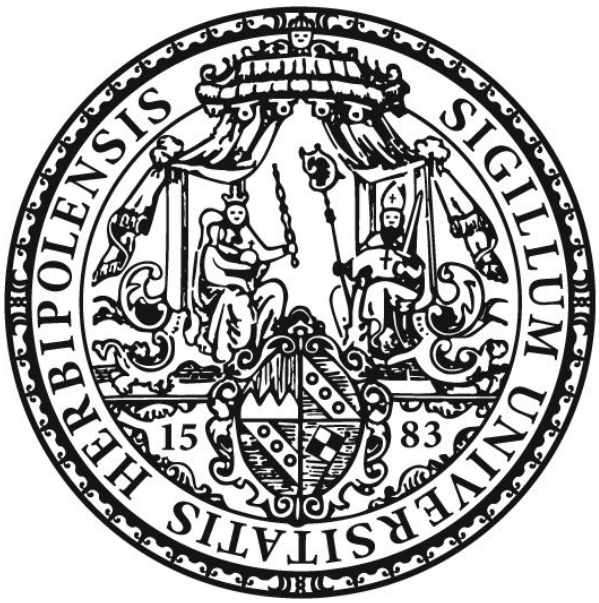

Influence of interleukin-6-type cytokine oncostatin M on murine aortic vascular smooth muscle cells

Einfluss des Interleukin-6-Typ Zytokins Oncostatin M auf murine vaskuläre glatte Muskelzellen der Aorta

Doctoral thesis for a doctoral degree at the Graduate School of Life Sciences, Julius-Maximilians-Universität Würzburg, Section Biomedicine

submitted by

Carmen Schäfer

from

Auerbach/Opf.

Würzburg, April 2016

Submission

Submitted on: .....

Members of the *Promotionskomitee*:

Chairperson: Prof. Dr. Manfred Gessler

Primary Supervisor: PD Dr. Heike Hermanns

Supervisor (Second): Prof. Dr. Bernhard Nieswandt

Supervisor (Third): Prof. Dr. Thomas Rudel

Date of public defence: .....

Date of receipt of Certificates: .....

For my family
especially
for my boyfriend Alex

"The most exciting phrase to hear in science, the one that heralds new discoveries, is not 'Eureka!' but 'That's funny...'"

–Isaac Asimov

Summary

Oncostatin M (OSM) is a cytokine of the interleukin-6 family and released in the early phase of inflammation by neutrophils, activated macrophages, dendritic cells, and T lymphocytes. Its roles in physiology and disease are not entirely understood yet. It has been shown recently that substantial amounts of OSM are found in atherosclerotic plaques.

The first part of this thesis addresses the effects of OSM on vascular smooth muscle cells (VSMCs). This cell type is known to contribute to atherogenesis and expresses the type I and type II OSM receptor complexes. This study revealed that OSM is a strong inducer of an array of genes which have recently been shown to play important roles in atherosclerosis. Investigation of VSMCs isolated from OSMRβ-deficient ($Osmr^{-/-}$) mice proved that the regulation of these target genes is entirely dependent on the activation of the type II OSMR complex. In addition to OSM, other cytokines expressed by T lymphocytes were found to contribute to plaque development. According to earlier publications, the influence of IL-4, IL-13, and IL-17 on the progression of plaques were discussed controversially. Nevertheless, for the regulation of investigated atherosclerotic target genes and receptor complexes in VSMCs, they seemed to play a minor role compared to OSM. Only the expression of the decoy receptor IL-13Rα2 - a negative feedback mechanism for IL-13-mediated signalling - was strongly induced after treatment with all mentioned cytokines, especially when VSMCs were primed with OSM before stimulation.

The second part of this thesis focuses on the role of OSM during the progression of atherosclerosis *in vivo*. Therefore, $Ldlr^{-/-}Osmr^{-/-}$ mice were generated by crossing $Ldlr^{-/-}$ mice - a typical mouse model for atherosclerosis - with $Osmr^{-/-}$ mice. These double-deficient mice together with $Ldlr^{-/-}Osmr^{+/+}$ mice were set on cholesterol rich diet (Western diet, WD) for 12 weeks before they were sacrificed. Determination of body and organ weight, staining of aortas and aortic roots as well as gene expression profiling

strongly suggested that *Ldlr*$^{-/-}$*Osmr*$^{-/-}$ mice are less susceptible for plaque development and weight gain compared to *Ldlr*$^{-/-}$*Osmr*$^{+/+}$ mice. However, further experiments and additional controls (*C57Bl/6* and *Osmr*$^{-/-}$ mice) on WD are necessary to clarify the underlying molecular mechanisms.

Taken together, the interleukin-6-type cytokine OSM is a strong inducer of an array of target genes involved in de-differentiation and proliferation of VSMCs, a process known to contribute substantially to atherogenesis. Further *in vivo* studies will help to clarify the role of OSM in atherosclerosis.

Zusammenfassung

Oncostatin M (OSM) gehört zur Familie der Interleukin-6-Typ Zytokine und wird in der frühen Phase der Inflammation von Neutrophilen, aktivierten Makrophagen, dendritischen Zellen und T-Lymphozyten freigesetzt. Seine Rolle in der Physiologie und Erkrankung ist noch nicht gänzlich verstanden. Vor kurzem konnte gezeigt werden, dass eine wesentliche Menge an OSM in arteriosklerotischen Plaques vorhanden ist.

Der erste Teil dieser Dissertation thematisiert den Effekt von OSM auf vaskuläre glatte Muskelzellen (*vascular smooth muscle cells*, VSMCs). Dieser Zelltyp trägt zur Entstehung der Arteriosklerose bei und exprimiert sowohl den Typ I als auch den Typ II OSM Rezeptor-Komplex. Diese Studie zeigt, dass OSM ein starker Induktor einer Reihe von Genen ist, von denen kürzlich gezeigt wurde, dass sie eine wichtige Rolle in der Arteriosklerose spielen. Eine Untersuchung an VSMCs, isoliert aus OSMRβ-defizienten ($OSMR^{-/-}$) Mäusen, bewies, dass die Regulation der Zielgene gänzlich von der Aktivierung des Typ II OSMR-Komplexes abhängig ist. Neben OSM wurden auch andere, von T-Lymphozyten exprimierte Zytokine gefunden, die zur Entwicklung von Plaques beitragen. Laut vorheriger Publikationen wurde der Einfluss von IL-4, IL-13 und IL-17 auf die Plaqueprogression kontrovers diskutiert. Dennoch scheinen diese Zytokine verglichen mit OSM für die Regulation der hier untersuchten, arteriosklerotischen Zielgene und Rezeptorkomplexe in VSMCs nur eine untergeordnete Rolle zu spielen. Lediglich die Expression des Köderrezeptors (*decoy receptor*) IL-13Rα2, der eine negative Rückkopplung der IL-13 vermittelten Signaltranduktion darstellt, wurde durch die Behandlung mit den oben genannten Zytokinen stark induziert. Dies geschieht insbesondere dann, wenn VSMCs vor der Stimulation mit OSM vorbehandelt wurden.

Der zweite Teil befasst sich mit der Rolle des OSM während der Enstehung von Arteriosklerose *in vivo*. Hierfür wurden $Ldlr^{-/-}Osmr^{-/-}$ Mäuse durch Kreuzung von $Ldlr^{-/-}$ - einem typischen Mausmodell für Arteriosklerose - mit $Osmr^{-/-}$ Mäusen generiert. Diese doppeldefizienten Mäuse zusammen mit $Ldlr^{-/-}Osmr^{+/+}$ Mäusen wurden für 12 Wochen

auf eine cholesterinreiche Diät (*Western diet*, WD) gesetzt bevor sie geopfert wurden. Die Bestimmung des Körpergewichts und des Gewichts der Organe, das Anfärben der Aorten und der Aortenwurzeln sowie das Erstellen eines Gen-Expressionsprofils wies stark darauf hin, dass $Ldlr^{-/-}Osmr^{-/-}$ Mäuse weniger anällig für die Ausbildung von Plaques und eine Gewichtszunahme sind als $Ldlr^{-/-}Osmr^{+/+}$ Mäuse. Dennoch sind weitere Experimente und zusätzliche Kontrollen (*C57Bl/6* und $Osmr^{-/-}$ Mäuse) nötig, um die zugrundeliegenden, molekularen Mechanismen aufzuklären.

Zusammenfassend ist das Interleukin-6-Typ Zytokin OSM ein starker Induktor einer Reihe an Zielgenen, die an der De-differenzierung und Proliferation von VSMCs beteiligt sind. Dieser Prozess könnte wesentlich zur Arteriogenese beitragen. Weitere *in vivo* Experimente werden helfen die Rolle des OSM in der Arteriosklerose zu verstehen.

Contents

1 Introduction

1.1 Oncostatin M, an IL-6-type cytokine

Oncostatin M (OSM) was initially described as a distinct cell growth regulator. It inhibits the replication of A375 melanoma and other solid human tumour cells [1]. However, studies within the last decade uncovered the pleiotropic character of OSM. The cytokine plays important roles in haematopoietic progenitor cell homoeostasis [2, 3], suppression of fetal liver haematopoiesis [4, 5], liver development [6, 7] and regeneration [8]. It influences also extrathymic T cell development [9, 10], angiogenesis [11] and is a major regulator of inflammatory processes. Various publications describe elevated protein levels of human OSM in arthritis, psoriasis and atherosclerosis [12, 13, 14, 15]. OSM is mainly produced by activated macrophages, dendritic cells, neutrophils, and T cells [1, 16, 17, 18]. There is a clear distinction between human (hOSM), murine (mOSM), rat (rOSM), and bovine OSM (bOSM). Furthermore, evolutionary relation and descent from a common ancestral gene were found for OSM, IL-6 and LIF [19].

OSM belongs to the interleukin 6 (IL-6) family which represents a group of pleiotropic cytokines. Additional members are IL-6, IL-11, leukaemia inhibitory factor (LIF), ciliary neurotrophic factor (CNTF), cardiotrophin-1 (CT-1), cardiotrophin-like cytokine (CLC), IL-27 (consisting of p28 and EBI-3), and neuropoietin (NP) [20, 21, 22, 23]. All of them use glycoprotein gp130 as a receptor subunit for signal transduction (Figure 1.1). IL-6-type cytokines are crucial for inflammation and the acute phase response [24, 25]. Furthermore, they are important for various biological processes including cardiovascular remodelling, neuronal differentiation, haematopoiesis, cell differentiation and proliferation [26]. Recently it was discovered that IL-35 signals through a unique heterodimer of receptor chains, IL-12Rβ2 and gp130 [27]. This is a good reason for IL-35 to be added to the family of IL-6-type cytokines. Based on the heterodimeric organisation of the cytokines, IL-35 as well as IL-27 appear to mark evolutionary bridges between the IL-6

and IL-12 family of cytokines. Additionally, IL-31 is sometimes included into this IL-6-type cytokine family, due to its binding to the OSMR and the IL-31-receptor (IL-31R) [28, 29]. Excellent reviews describe in detail the structure of the cytokines and their receptor complexes as well as the involved signalling pathways [20, 26, 30, 31, 32].

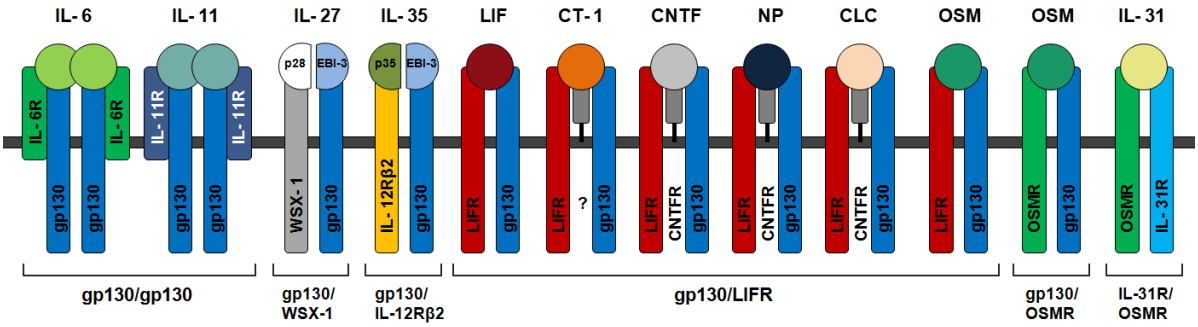

Figure 1.1: **The IL-6-type cytokine family and its receptor complexes.** IL-6-type cytokines signal through gp130 homo- or heterodimers. IL-6 and IL-11 use IL-6R/gp130 and IL-11R/gp130 receptor complexes for their signalling. Crystallographic data propose a hexameric structure for these receptors. IL-27 utilises gp130/WSX-1 and IL-35 binds to gp130/IL-12Rβ2. LIF, CT-1, CNTF, NP, CLC and OSM signal through gp130/LIFR heterodimers. OSM can additionally bind to gp130/OSMR and IL-31 is recruited to an IL-31R/OSMR heterodimer.

1.2 Species-specific receptor utilization by OSM and LIF

During the last decades, OSM from different species, human, mouse, rat, and bovine, has been cloned [7, 33, 34]. In contrast to other IL-6-type cytokines, the composition of the OSM receptor is different in the human and mouse system. Human OSM is able to bind the type I receptor complex consisting of LIFR and gp130 as well as the type II receptor complex composed of OSMRβ and gp130 heterodimers [35, 36, 37]. Murine OSM, however, only signals through the type II receptor complex since it lacks high affinity binding sites for the LIFR [38, 39]. This is an indication for a functional diversity in the biochemistry of the cytokine and a difference in the biology between species. Furthermore, rat OSM uses both receptor complexes, type I and type II, analogous to the human system [40]. This implies that studies of OSM in rats are more related to human OSM receptor function and biology *in vivo*. However, studies in mice might be more suitable to delineate the specific contributions of the specific OSMR subunit.

Further studies with human and mouse cells treated with OSM from both species reveal that hOSM was able to induce signalling in murine cells efficiently but only by activating the LIFR/gp130 (type I) complex [38, 39]. Consequently, studies using hOSM in mouse models for the reconstitution of human diseases only mimic the action of LIF, since no OSMR signalling is involved. Furthermore, mOSM is not able to stimulate human cells which is similar to findings for other IL-6 type cytokines [38].

LIF, another IL-6-type cytokine, is expressed by embryonic stem cells, megakaryocytes, osteoblasts and neuronal cells [41]. LIF and its receptor complex (LIFR/gp130) are present in both species, man and mouse [42, 43, 44]. Human and murine LIFR are to 76% identical while human and murine LIF share 78% of their amino acids. Despite this relatively high homology, their signalling is species specific. Due to the fact that mouse LIF is not able to stimulate human cells, its binding and activity is highly limited. Human LIF, however, can signal through both, human and mouse LIFR/gp130 complexes [45]. Interestingly, when human LIF is used to stimulate mouse LIFR, the affinity between cytokine and receptor is 100-500-fold higher than murine LIF and murine LIFR [45].

1.3 Activation of downstream signalling pathways by OSM

The first cytoplasmic proteins which are needed for the initiation of signal transduction after binding of cytokines to their receptors belong to the tyrosine kinases of the JAK (Janus kinase) family. In mammals four members of JAK proteins exist, JAK1, JAK2, JAK3, and (non-receptor) tyrosine-protein kinase 2 (TYK2) [46, 47, 48, 49] with molecular weight between 120 and 140 kilodalton (kDa). All members of the JAKs are very homologous. JAK1, JAK2 and TYK2 are present in a variety of tissues, whereas JAK3 is mainly expressed in haematopoietic cells. Mutations of JAK3 cause severe combined immunodeficiency syndrome [50, 51]. JAKs are involved in the signal transduction of many cytokines including interferons (IFNα, IFNβ, IFNγ) and IL-6-type cytokines. In the following parts, the signalling pathways of the OSM receptor type II (gp130/OSMR) through JAK/STAT activation are explained in detail.

1.3.1 JAK/STAT pathway

After cytokine binding and dimerisation, the signal-transducing receptor chains induce conformational changes. Thereby, receptor-associated JAK proteins are brought into close contact and become (auto-)phosphorylated [52, 53]. The activated JAKs are now able to phosphorylate specific tyrosine residues in the receptor chain of gp130 and OSMR which are then binding sites for proteins like SHP2 (SH2 domain-containing protein tyrosine phosphatase), Shc (SH2-and collagen-homology-domain-containing protein) or STATs (signal transducer and activator of transcription) at different tyrosine residues of the receptor complex (Figure 1.2) [54, 26]. Initial analysis showed that gp130 and LIFR recruit SHP2 for their downstream signalling to the MAPK pathway. OSMR, however, utilizes Shc as an adaptor protein for the induction of the Ras-Raf-MAPK cascade, not SHP2 [26, 55]. STATs are transcription factors (TFs) and become phosphorylated at tyrosine residues themselves. After homo- or heterodimerisation, they translocate into the nucleus for the transcription of target genes [54] (Figure 1.2 and 1.3). All IL-6-type cytokines activate STAT3, and to a minor extent STAT1, through their common receptor subunit gp130 [26, 20]. In the case of LIFR and OSMR, STAT3 and STAT1 as well as STAT5 activation has been observed [26, 56]. Furthermore, OSM regulates the activation of STAT6 in murine lung extracts [57] and induces STAT6 phosphorylation in fibroblasts [58].

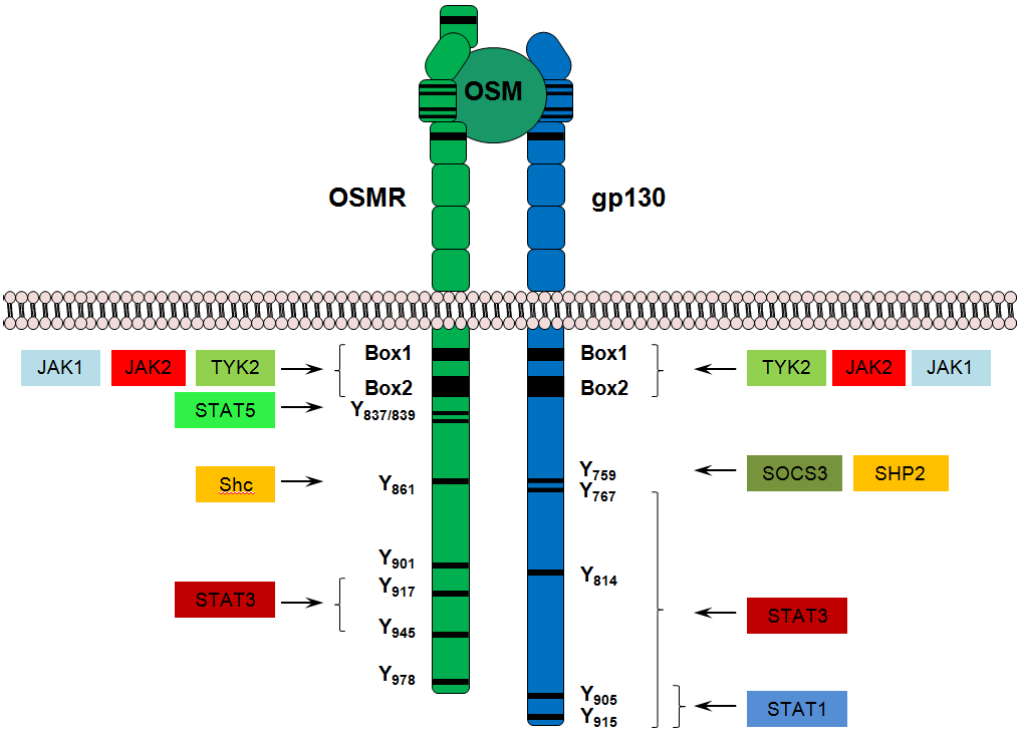

Figure 1.2: **OSMR/gp130-complex and binding sites for signalling proteins.** After OSM binding, the receptor chains gp130 and OSMR dimerize and initiate the JAK dependent phosphorylation of the indicated tyrosine residues. The box1 and box2 regions are important for JAK recruitment. STATs, SOCSs and SHP2 are recruited to their respective docking sites. After phosphorylation, STATs translocate into the nucleus, while SHP2 for gp130 and Shc for OSMR initiate the Ras-Raf-MAPK cascade. One of the STAT3 induced genes is *Socs3*, a feedback inhibitor of OSM-induced signalling pathways.

1.3.2 Ras-Raf-MAPK pathway

Most IL-6-type cytokines activate the Ras-Raf-MAPK pathway. In this case, the recruitment of an adaptor protein to the phosphorylated receptor tyrosines is necessary to allow the initiation of this cascade. As mentioned before, the phosphatase SHP2 uses its SH2 (Src homology 2) domains for binding to gp130 or LIFR [59, 60]. Therefore, tyrosine (Y) 759 of gp130 and Y974 of the LIFR are crucial [61]. OSMR, however, does not utilize SHP2 for the activation of the Ras-Raf-MAPK cascade, but an adaptor protein called Shc which is recruited to Y861 in the OSMR [55] (Figure 1.2). After its own phosphorylation by JAKs, Shc interacts with Grb2 (growth factor receptor-bound protein 2). Grb2 contains an SH2 and two SH3 (Src homology 3) domains without catalytic activity [55, 59]. Via its SH3 domains, it is associated with the guanine nucleotide exchange factor SOS (son of sevenless) which by receptor recruitment of Grb2 translocates from the cytoplasm to the plasma membrane for the activation of the GTPase Ras. After activation of the MAP kinase kinase kinase (MAP3K) Raf by Ras, MEK1/2 (MAP2K) are phosphorylated and activate the MAPKs ERK1/2 [62]. The stress-activated MAPK JNK1/2/3 are phosphorylated by MKK4/7 and p38 by MKK3/6 [62]. Upon activation, ERK1/2, p38 and JNK migrate into the nucleus to modify various transcription factors (Figure 1.3).

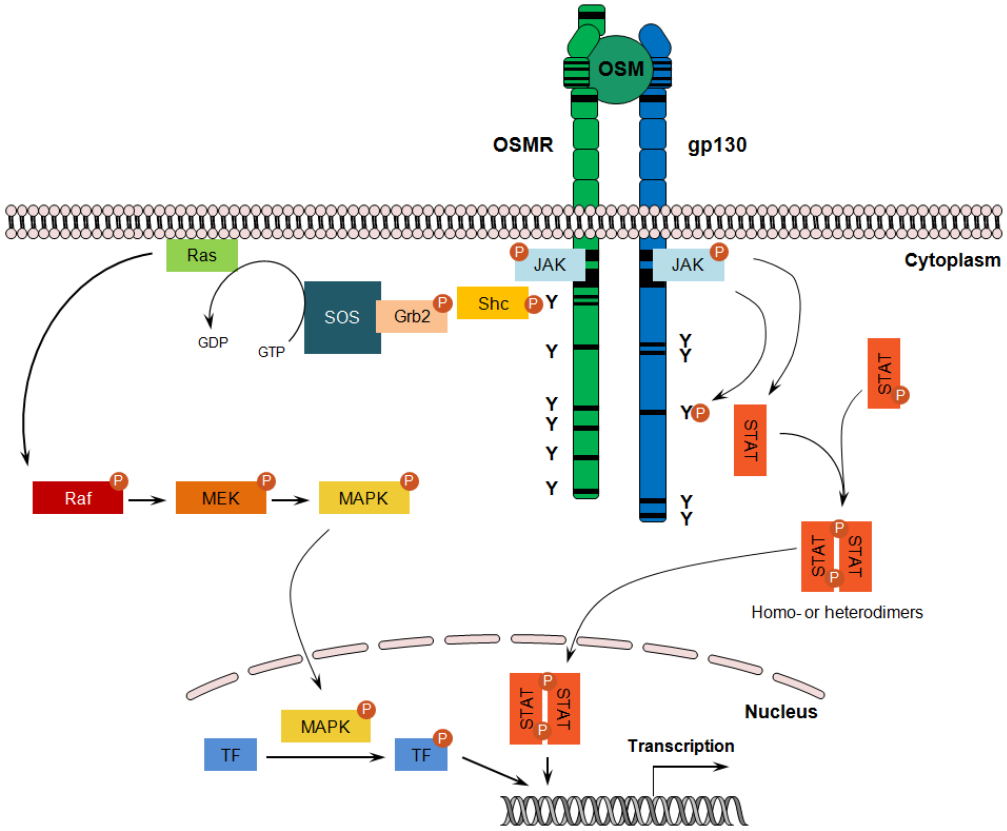

Figure 1.3: **OSM activates the JAK/STAT pathways and the MAPK cascade.** After OSM binding and dimerisation of the receptor type II (OSMR/gp130), two major pathways are initiated, the JAK/STAT pathway and the Ras-Raf-MAPK cascade. STATs are recruited to specific phospho-tyrosine residues in the intracellular part of the receptor and additionally phosphorylated by JAKs. Then they dimerise to form homo- or heterodimers and translocate into the nucleus for the induction of gene transcription. The adaptor protein Shc is also recruited to phospho-tyrosines, where it interacts with additional proteins to allow the induction of the Ras-Raf-MAPK pathway. Phosphorylated MAPKs like ERK1/2 can translocate into the nucleus for the activation of specific transcription factors (TFs).

1.3.3 PI3K/Akt pathway

Another signalling pathway which is activated by many IL-6-type cytokines, is called the PI3K (phosphatidyl-inositol 3 kinase) cascade. This enzyme modifies certain phosphatidylinositides, so that the protein kinase B/AKR thymoma oncogene homologue (PKB/Akt) is recruited to the plasma membrane, where it becomes phosphorylated by PDK1 (phosphoinositide-dependent kinase-1) [26]. Substrates of Akt include the forkhead transcription factor FKHR and the pro-apoptotic factor Bad (Bcl-2/Bcl-xL-antagonist, causing cell death), whose phosphorylation is associated with inactivation and increased survival or cell growth [26]. In basal carcinoma cells the PI3K pathway is crucially involved in the IL-6-mediated prevention of apoptosis which coincides with the up-regulation of the anti-apoptotic protein Mcl-1 [26, 63]. The IL-6-type cytokine induced activation of PI3K is cell-type specific. For instance, human HepG2 hepatoma cells do not activate Akt when treated with IL-6 [64]. The complete PI3K/Akt pathway after receptor dimerisation is not fully understood. After stimulation, the adaptor protein Gab1 (Grb2-associated binding protein 1) appears to be involved which interacts with PI3K [26, 60] finally leading to the activation of Akt [65].

1.4 General view of atherosclerosis

Atherosclerosis is a chronic inflammatory disorder of the arterial vessel wall. It is considered to be the main cause for morbidity and mortality in the western world ([66], [67], [68]). Reduction in vessel lumen associated with increased risk for plaque rupture is characteristic for the progression of atherosclerosis. This causes coronary artery disease (CAD), acute coronary syndrome (ACS), myocardial infarction or ischemic stroke [69, 70]. Many risk factors are known to be involved in the development of atherosclerosis. Hypertension increases the arterial wall tension followed by disturbed repair and aneurysm formation. Angiotensin II incites leukocytes for adhesion on the vessel wall, which is the first step for plaque formation. Cigarette smoking and diabetes also affect vascular biology, but these mechanisms are less well understood. The role of cholesterol, however, is described in great detail. This knowledge could be helpful for prevention strategies [66, 68].

1.4.1 Lipids and atherosclerotic plaque formation

A vascular vessel wall contains three different layers: The inner layer, the *tunica intima*, contains an endothelial cell layer which is in contact with blood. The middle layer, the *tunica media*, consists of smooth muscle cells (SMCs) embedded in extracellular matrix. The outer layer, called *tunica adventitia*, includes mast cells, nerve endings, and microvessels (Figure 1.4 A). Clinical and experimental data confirms that high blood lipid and cholesterol levels promote atherosclerosis. In the blood system, cholesterol is carried by low-density lipoproteins (LDL). These carriers consist of esterified or unmodified cholesterol, triglycerides, phospholipids and apolipoprotein B100 (ApoB100) and accumulate in the intima by binding to proteoglycans of the extracellular matrix (ECM) [67, 71, 72, 69]. After retention and accumulation, LDL particles undergo oxidative modifications that can lead to activation of endothelial cells or macrophages. Thereby, the oxidation level can range between low or even highly oxidized covering a broad spectrum of chemical modifications [67]. LDL and oxidized LDL (oxLDL) trigger the expression of adhesion molecules at the cell surfaces of the endothelial monolayer enabling leukocytes to migrate from the blood stream into the plaque area [69]. Furthermore, migrated leukocytes promote plaque growth by contributing to lipid accumulation [67, 73]. The so-called fatty streaks in early plaques consist of activated T cells and lipid-laden monocyte and macrophage (foam cells) driving advanced lesion formation (Figure 1.4 B). The migration of smooth muscle cells (SMCs) from the media into the intima, increased adherence of platelets to the dysfunctional endothelium, exposed collagen or macrophages and continuous recruitment of leukocytes contributes to inflammation and promotes advanced lesion formation [68] (Figure 1.4 C). In the progression of advanced atheromas (mature plaques), leukocytes, lipids, cholesterol crystals, apoptotic cells as well as cell debris can be found in a necrotic core covered by a fibrous cap of collagen and smooth muscle cells [66, 68, 74]. Enzymes, metalloproteinases (MMPs) and other pro-inflammatory mediators, released from infiltrating T and mast cells, lead to the formation of an unstable plaque [74, 75]. When the fibrous cap ruptures, pro-thrombotic plaque material interacts with blood material triggering thrombus formation by activating the coagulation cascade. Vascular occlusion follows that can lead to myocardial infarction or ischemic stroke [66, 68, 67, 74, 76] (Figure 1.4 D).

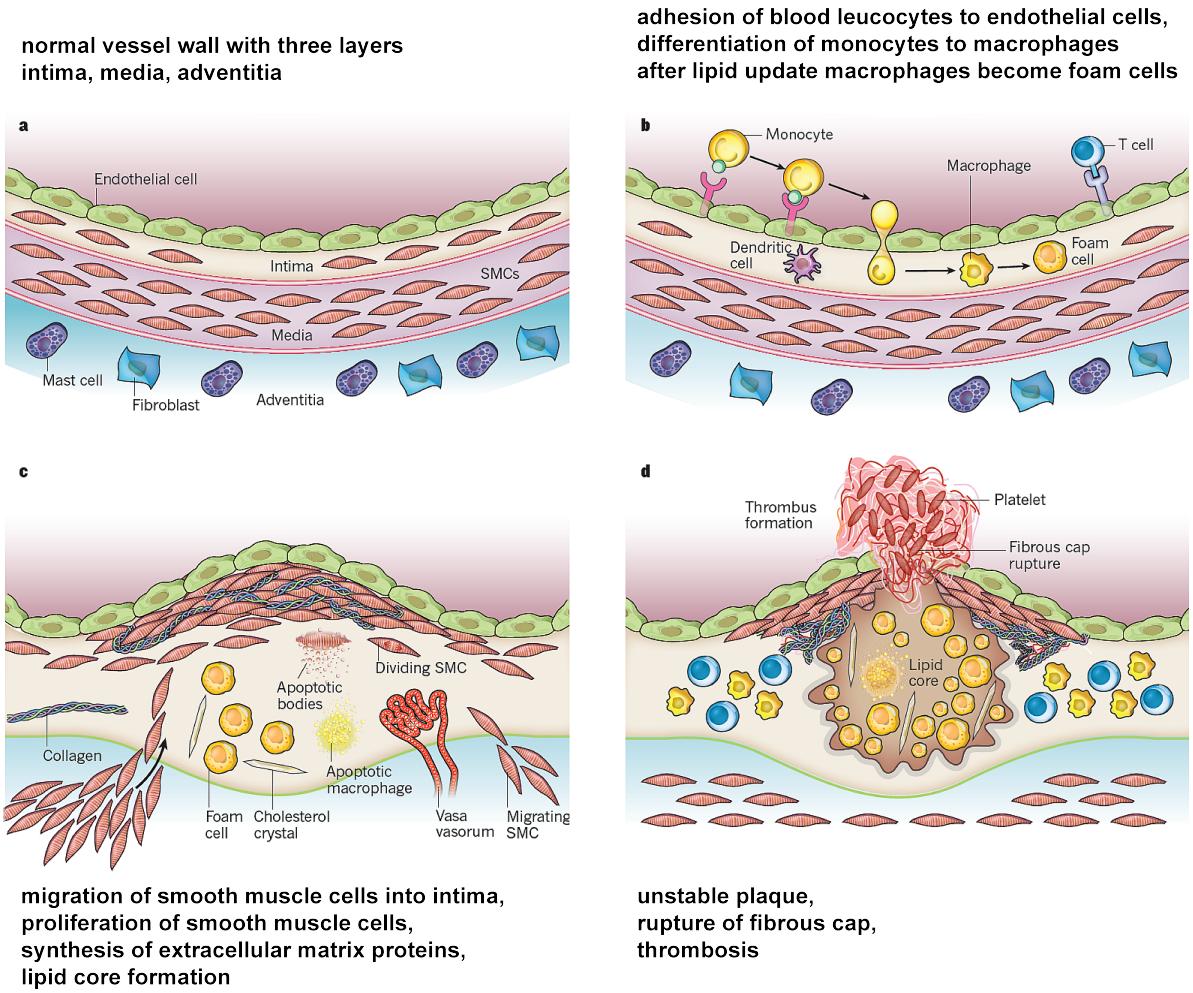

Figure 1.4: **Progression of atherosclerotic plaque development. A**, A normal vessel wall contains three layers, the inner (*intima*), the medial (*media*), and the outer layer (*adventitia*). **B**, Adhesion of blood leukocytes to endothelial cells and their differentiation after migration into the *intima* represent the first step for plaque development. **C**, Migration of smooth muscle cells together with apoptotic cells and synthesis of extracellular matrix proteins lead to the formation of a fibrous cap and a lipid core. **D**, When the plaque becomes unstable and the fibrous cap ruptures, thrombosis occurs by contact of blood compounds to the pro-thrombotic plaque material. Source: adapted from Libby et al. [66]

1.4.2 Atherosclerosis in mice

Mouse models for the investigation of cellular and molecular mechanisms of atherosclerosis are well established. Nevertheless, atherosclerosis is different in men and mice. For example, lesion distribution is not identical. In humans, lesions occur in the coronary arteries, carotids and peripheral vessels whereas in mice, aortic root, aortic arch and innominate artery are affected [77]. Additionally, plaque rupture and thrombosis formation is rare in mice models and cannot be analysed [78]. However, most patients are treated when symptoms are already present. A mouse model characterising this late stage of the disease would be of advantage. Nonetheless, the two most important murine atherosclerosis models give insight into the development and progress of plaque lesions and numerous critical processes shared between mice and men [77].
In ApoE deficient (*Apoe-/-*) mice, reduced and blocked clearance of plasma lipoproteins through the LDL receptor (LDLR) and the LDL receptor-related protein causes massive accumulation of cholesterol-rich VLDL on a normal low-fat chow diet [79, 80]. Additionally, the rate of atherogenesis can be notably accelerated by feeding a high-fat and high-cholesterol Western diet (WD) (21% milk fat, 0.2% cholesterol) [77, 81]. However, ApoE affects also factors of the immune system - such as macrophage and adipose biology - which could be of disadvantage for the *Apoe-/-* mouse model [77, 82]. Transferred ApoE from bone marrow derived cells (macrophage/monocytes) of *Apoe-/-* mice into wild type mice lead to an increase in aortic root atherosclerosis independent of the amount of plasma lipids [77, 83, 84].
In *Ldlr-/-* mice lipoproteins cannot be cleared through the LDLR which leads to moderate accumulations of LDL on normal chow diet and severe hypercholesterolemia on a high-fat diet [78, 85]. Although lesion development is less pronounced compared to *Apoe-/-* mice, the lipid profile of *Ldlr-/-* is more similar to the human system. Therefore, *Ldlr-/-* mice have been chosen for experimental analysis of atherosclerosis in this thesis. In contrast to *Apoe-/-* mice, atherosclerotic lesions are developed at an older age in *Ldlr-/-* mice, but feeding a high-fat, high-cholesterol Western diet (WD) accelerates this effect. Unfortunately, high-fat diets are not standardized. Therefore, studies of plaque morphologies are often not comparable [77, 78].
Nevertheless, these atherosclerotic mouse models uncover the complex network of immune cells that play a crucial role in the development of atherosclerosis.

1.4.3 Role of OSM in atherosclerosis

Inflammation is a major factor in atherosclerosis, even though the process is not fully understood yet. IL-1 and TNF released from macrophages are involved in the development of atherosclerosis in mouse models [86]. IL-6 has been found to be involved as well [87, 88] depending on the experimental model. Macrophages can be found in early as well as in ruptured plaques [89, 90], cells which secrete large amounts of OSM [91, 92] and IL-6. Therefore, a potential involvement of OSM in atherogenesis seems to be realistic. Several studies have examined the impact of an OSM stimulation of endothelial cells, including the increased expression of IL-6 [93, 94]. Furthermore, OSM is a mitogen for rabbit aortic vascular smooth muscle cells [95] and promotes their proliferation. An OSM ligand was also found in human aortic aneurysm tissue [96] and more recently in both human and ApoE atherosclerotic lesions [15]. This data implies that OSM might be pro-atherosclerotic, but its precise function in atherosclerosis is not understood.

1.5 Role of vascular smooth muscle cells in atherosclerosis and the impact of immune cell-derived cytokines in their phenotypic changes

Vascular smooth muscle cells (VSMCs) maintain the vascular tone in vessel walls [97]. Therefore, VSMCs show a contractile behaviour characterised by the expression of proteins favouring myofilament structure and function. Furthermore, VSMCs can neither proliferate nor switch phenotype when surrounded by ECM proteins [98]. After injury or in case of atherosclerotic plaque development, VSMCs become activated, migrate into the intima and de-differentiate into a proliferating and non-contractile cell type with a strong change in gene expression [97, 99, 100]. In the progress of plaque development, VSMCs as well as secreted extracellular matrix proteins form a fibrous cap that acts as a barrier to shield the plaque core from blood flow [97, 101]. Calcification of the vessel wall plays a major part in advanced atherosclerotic lesions. Decreased elasticity and hemodynamic changes are the consequences leading to hypertrophy, oxidative stress, and diastolic dysfunction[102, 103].

During atherogenesis, VSMCs are able to respond to several cytokines which are released by plaque macrophages, dendritic cells, and T cells. The predominant cell

type in atherosclerotic plaques are macrophages [67, 104] which are able to produce OSM [1]. Studies using M-CSF deficient mice with reduced macrophage levels demonstrate an athero-protective phenotype [105]. This indicates the immense importance of macrophages in disease development. After differentiation from monocytes, their proliferation and apoptosis contribute to lesion formation [106, 107]. During atherosclerotic plaque formation, macrophages are able to ingest oxLDL or LDL and become foam cells. Several studies verified the presence of so called M1 and M2 macrophages in human and murine atherosclerosis. M1 macrophages are categorized as inflammatory cells whereas M2 macrophages are reparative cells [104, 108, 109]. The wound-healing M2 macrophages are able to release anti-inflammatory cytokines including IL-4, IL-10 and IL-13. These cytokines diminish endothelial and smooth muscle cell activation, and induce smooth muscle cell proliferation and formation of anti-inflammatory Th2 and regulatory T cells (Tregs) in atherosclerosis [104, 110]. M2 macrophages are less susceptible to foam cell formation compared to M1 macrophages, since their phagocytosis and uptake of oxLDL is less pronounced. M1 macrophages are able to secrete pro-inflammatory cytokines including TNFα, IL-1β and IL-6 which induce endothelial cell activation and dysfunction as well as smooth muscle cell activation [104]. This may aggravate the progression of atherosclerosis.

Dendritic cells (DCs), together with macrophages, are specialised antigen-presenting cells (APCs) having the ability to stimulate naïve T cells indicating an important link between the innate and adaptive immune system [111, 112]. DCs are present in the atherosclerotic lesions of mice and human [113, 114]. Here, DCs are either recruited into vascular lesions or they derive from Ly6C^{hi} or Ly6C^{lo} monocytes which are already located in the intima [115]. In this context, lipid accumulation and differentiation into foam cells is also possible for residential intimal DCs leading to lesion formation in the early state of atherosclerosis [116]. Evidence for the importance of DCs during the development of atherosclerosis can be found in several research studies [117, 118, 119]. In addition, DCs are able to release cytokines including OSM, TNFα, IL-6, and IL-12 [18, 117]. The latter plays an important role for Th1 cell induction. Furthermore DCs modulate Th17 differentiation through the secretion of cytokines IL-23 and IL-27 [120, 121].

Since atherosclerosis represents a T cell driven disease, T helper cells - especially Th1 cells - play an important role [74, 122, 123, 124]. Previous publications describe OSM as a Th1 cytokine [2, 17, 125]. T cells constitute about 10% of all cells in atherosclerotic

lesions [74], the majority of them are of αβ TCR type ($CD4^+$ T cells and $CD8^+$ T cells) [74]. After presentation of athero-specific antigens such as oxLDL by migrating APCs, $CD4^+$ T cells differentiate into T helper cells (Th cells) whereas $CD8^+$ T cells form cytotoxic T lymphocytes (CTLs) [126, 127].
Evidence of the importance of Th1 cells has been derived from experiments using atherosclerotic mouse models combined with a deficiency in Th1-related genes. Deletion of *Il12* or *Il18*, both genes encoding for important Th1 inducing cytokines, or deletion of *Tbx21*, the gene for the main Th1 differentiation transcription factor T-bet, result in reduced atherosclerosis [128, 129, 130]. Moreover, treatment with IL-12, IL-18 or IFNγ promotes lesion formation in mice [131, 132, 133].
Th2 and Th17 cells are also present in atherosclerotic plaques. Their role, however, is still disputed and needs further investigations [67]. Th2 cells produce IL-4, IL-5 and IL-13 [134]. However, some studies postulate a pro-atherosclerotic effect for IL-4 [129], whereas others found no changes [135]. IL-5 and IL-13 seem to protect from atherogenesis [136, 137].
IL-17 is mainly produced by Th17 cells (IL-17A and IL-17F) [138], but also $CD8^+$ T cells [139], γδ T cells, natural killer (NK) and natural killer T cells (NKT) [140] as well as neutrophils [141] are able to secrete IL-17. It plays a role in the pathogenesis of a number of autoimmune diseases including rheumatoid arthritis (RA), asthma, psoriasis and multiple sclerosis (MS) [142, 143]. Additionally, IL-17 expressing T cells have been found in atherosclerotic lesions of humans and mice [144, 145]. Eid *et al.* could show that IL-17 is produced together with IFNγ by infiltrating T cells. Both cytokines act synergistically to induce proinflammatory responses in vascular smooth muscle cells [146]. Nevertheless, the role of IL-17 is still disputed. Some studies assumed that IL-17 is protective [147, 148], while others postulate that it acts pathogenic [146, 149, 150] or has no effect at all on the alteration of plaque burden [151, 152].

In the context of this thesis, previous findings for the role of OSM in VSMC responses and its cross-talk with other inflammatory cytokines are of importance. In summary, OSM exerts a number of different effects on smooth muscle cells. For instance, it enhances vascular endothelial growth factor (VEGF) expression in human VSMCs contributing to plaque angiogenesis and destabilization [153]. Moreover, it may promote smooth muscle cell proliferation, migration and extracellular matrix protein synthesis through the JAK/STAT pathway, since OSM was expressed in atherosclerotic lesions of human patients [15]. Recently, it was described that the phenotype of SMCs can be modulated by downstream proteins STAT1 and STAT3 of the OSM signalling pathway. Thereby, when

the balance of both transcription factors shifted towards STAT1, more de-differentiated SMCs were generated [154]. Kakutani *et al.* could show that the expression of two osteblastic differentiation markers, alkaline phosphatase (ALP) and runt-related transcription factor 2 (Runx2), were stimulated by OSM through JAK3/STAT3 pathway promoting mineralisation of human VSMCs [155].

OSM primes the response of VSMCs alone or in combination with other cytokines, such as IL-4, IL-13 or IL-17. For instance, OSM regulates the expression of IL-6, MCP-1, and different receptors (*Osmr*, *Il6st*, *Il4r*) in human airway smooth muscle cells (HASMCs) [156]. This OSM-induced expression pattern of IL-6 and MCP-1 can be enhanced in synergy with IL-17A [156]. IL-17A interacts with a receptor complex composed of IL-17RA/IL-17RC, which is expressed generally on a wide variety of cell types including SMCs [156, 157].

Pretreatment of fibroblasts and SMCs with OSM followed by stimulation with IL-4 or IL-13 regulates the eotaxin-1 response and the expression of IL-4Rα in a synergistic manner [156, 158, 159]. On cells of non-hematopoietic stem cell origin, including fibroblasts and SMCs, IL-4 as well as IL-13 can use the type II complex, comprising IL-4Rα and IL-13Rα1 [160, 161, 162] (Figure 1.5). In contrast, the type I receptor complex - consisting of IL-4Rα and the common gamma-chain (γc) - can only be formed by IL-4 and is important for the regulation of the Th2 development [160]. After binding to the type II receptor complex, IL-4 or IL-13 activate the Janus kinases JAK1 and TYK2 to induce the phosphorylation of STAT6 at tyrosine residue 641 (Y641) by activating JAKs. Two tyrosine-phosphorylated STAT6 proteins form a homodimer and translocate into the nucleus where they bind to promoter/enhancer regions of IL-4/IL-13 responsive target genes (Figure 1.5).

IL-13 receptor alpha 2 (IL-13Rα2) - another receptor subunit - recruits only IL-13 with high affinity [163, 164, 165], but the function of this receptor remains a controversial issue. Due to its short cytoplasmatic region (human: 17 amino acids; mouse: 28 amino acids) without any obvious signalling motif, IL-13Rα2 is thought to act as a non-signalling "decoy" receptor [165, 166, 167]. Fichtner-Feigl *et al.* postulated, however, that IL-13 signals through IL-13Rα2 and thereby induces TGFβ1 production in macrophages in a STAT6-independent manner leading to collagen deposition *in vivo* [168]. IL-13Rα2 exists as membrane bound protein as well as an alternatively spliced soluble receptor in mice [169, 170, 171, 172] (Figure 1.5). However, soluble IL-13Rα2 (sIL-13Rα2) was not found in humans [173].

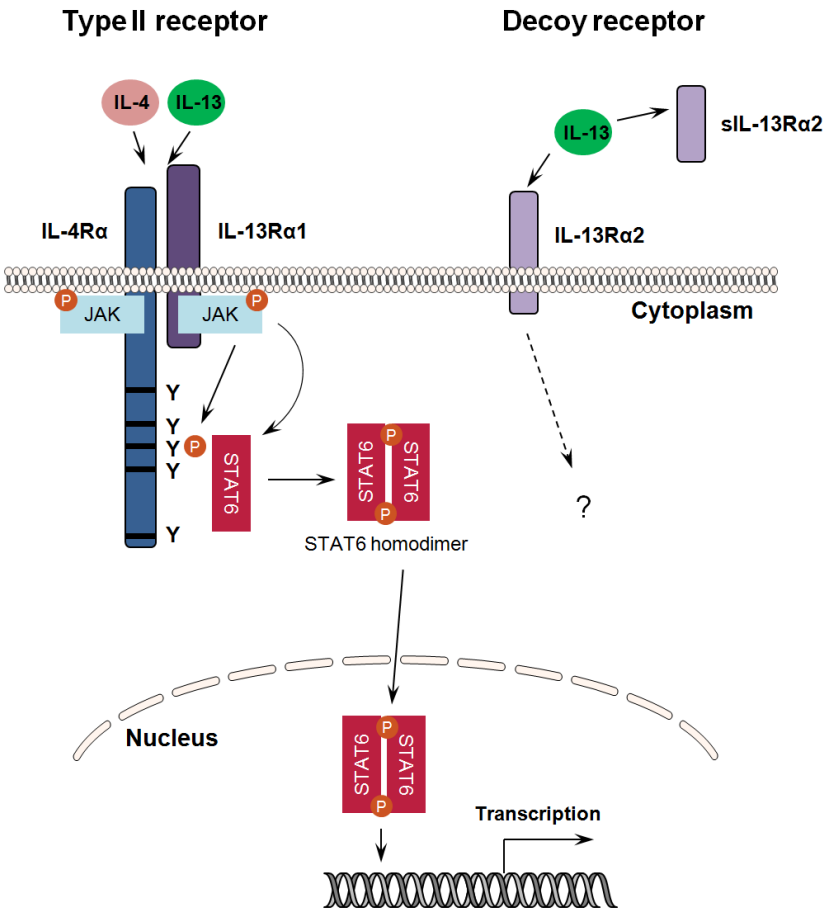

Figure 1.5: **IL-4/IL-13 activate the type II receptor complex whereas the decoy receptor IL-13Rα2 can only bind IL-13.** After binding of IL-4 or IL-13 and dimerisation of IL-4Rα and IL-13Rα1, the JAK/STAT pathway is initiated. Different to OSM signalling, only STAT6 is recruited to the receptor complex and phosphorylated. The homodimer of two tyrosine-phosphorylated STAT6 molecules translocates into the nucleus to initiate gene transcription. The decoy receptor IL-13Rα2 binds with high affinity to IL-13, but not IL-4. Its short cytoplasmic region is devoid of box 1/2 binding sites for JAKs and allows no STAT6 activation. In the murine system, a soluble form of IL-13Rα2 was found (sIL-13Rα2).

1.6 Aim of this study

OSM - an IL-6-type cytokine with pleiotropic character - is involved in numerous physiological and pathophysiological processes including inflammation, haematopoiesis, tissue remodelling, cell growth, and cardiovascular diseases. OSM is released by infiltrating and neutrophils, macrophages, dendritic cells and activated T lymphocytes. Most tissue resident cell types including VSMCs express the OSM receptor complex and are consequently responsive to OSM. Moreover, OSM was identified in human and murine atherosclerotic lesions as well as in peripheral blood mononuclear cells (PBMCs) from patients with stable coronary artery disease (CAD). However, the function of OSM in the cardiovascular system is not completely understood, especially concerning the effect on cells of the vessel wall.

Here, the contributions of OSM to vascular changes observed during atherogenesis is shown by investigating atherosclerotic target gene expression and signalling pathways in VSMCs isolated from the aorta of *C57Bl/6J* (wild-type) and OSMRβ knock-out ($Osmr^{-/-}$) mice. Furthermore, the cross-talk of OSM with other cytokines identified in atherosclerotic lesions - particularly the Th2 and Th17 cytokines IL-4, IL-13, and IL17 - on VSMCs is corroborated. The last part of this thesis describes a newly generated transgenic mouse line in which $Ldlr^{-/-}$ mice were crossed with $Osmr^{-/-}$ mice helping to reveal important aspects of OSM during atherogenesis *in vivo*.

2 Material

2.1 Antibodies

2.1.1 Antibodies for immunofluorescence staining

Primary antibodies

All listed antibodies detect mouse epitopes.

Antibody	Host sp.	Clone	Dilution	Manufacturer
actin, α-smooth muscle (SMA)	mouse	1A4	1:200	Sigma-Aldrich (Taufkirchen, Germany)
smooth muscle protein 22-alpha (SM22α)	rabbit	polyclonal	1:300	Abcam (Cambridge, UK)

Secondary antibodies

Antibody	Host sp.	Dilution	Manufacturer
anti mouse Alexa Fluor 488	goat	1:500	Life Technologies (Darmstadt, Germany)
anti rabbit Alexa Fluor 488	goat	1:500	Life Technologies (Darmstadt, Germany)

2.1.2 Antibodies for flow cytometry

Primary antibodies

Antibody	Fluoro-phore	Clone	Host species	Manufacturer
CCR1	-	643854	rat	R&D Systems (Wiesbaden-Nordenstadt, Germany)
IL-4R	PE	mIL4R-M1	rat	BD (Heidelberg, Germany)
OSMRβ	-	30-1	rat	MBL (Woburn, MA, USA)
Isotype control IgG2a	-	RTK2758	rat	Biolegend (Fell, Germany)
Isotype control IgG2b	-	RTK4530	rat	
Isotype control IgG2a	PE	eB149/10H5	rat	eBiosciences (Frankfurt, Germany)

Secondary antibody

Antibody	Host species	Manufacturer
anti rat-PE (Fab fragment)	goat	Jackson Immuno Research/ Dianova (Hamburg, Germany)

2.1.3 Antibodies for Western Blot analysis

Primary antibodies

Antibody	Clone	Host species	Dilution	Product number	Manufacturer
actin, α-smooth muscle	1A4	mouse	1:4000	A5228	Sigma-Aldrich (Taufkirchen, Germany)
phospho-Akt (S473) XP	D9E	rabbit	1:2000	4060	Cell Signaling (Frankfurt, Germany)
Akt	polyclonal	rabbit	1:1000	9272	Cell Signaling (Frankfurt, Germany)
GAPDH	14C10	rabbit	1:2000	2118	Cell Signaling (Frankfurt, Germany)
gp130 (M-20)	polyclonal	rabbit	1:250	sc-656	Canta Cruz Biotechnology, Inc. (Heidelberg, Germany)
IL-4Rα (M-300)	polyclonal	rabbit	1:1000	sc-25474	Canta Cruz Biotechnology, Inc. (Heidelberg, Germany)
LIFR (C-19)	polyclonal	rabbit	1:200	sc-659	Canta Cruz Biotechnology, Inc. (Heidelberg, Germany)
phospho-MK2 (T334)	27B7	rabbit	1:1000	3007	Cell Signaling (Frankfurt, Germany)
MK2	polyclonal	rabbit	1:1000	3042	Cell Signaling (Frankfurt, Germany)

OSMR	polyclonal	goat	1:1000	AF662	R&D Systems (Wiesbaden-Nordenstadt, Germany)
phospho-p38	28B10	mouse	1:2000	9216	Cell Signaling (Frankfurt, Germany)
phospho-p38 XP	D3F9	rabbit	1:1000	4511	Cell Signaling (Frankfurt, Germany)
p38 XP	D13E1	rabbit	1:1000	8690	Cell Signaling (Frankfurt, Germany)
phospo-p44/42 MAPK (Erk1/2) (T202/Y204)	E10	mouse	1:2000	9106	Cell Signaling (Frankfurt, Germany)
p44/42 MAPK (Erk1/2)	polyclonal	rabbit	1:1000	9102	Cell Signaling (Frankfurt, Germany)
phospho-STAT1 (Y701)	D4A7	rabbit	1:1000	7649	Cell Signaling (Frankfurt, Germany)
STAT1	polyclonal	rabbit	1:1000	9172	Cell Signaling (Frankfurt, Germany)
phospho-STAT3 (Y705)	3E2	mouse	1:1000	9138	Cell Signaling (Frankfurt, Germany)
STAT3	124H6	mouse	1:1000	9139	Cell Signaling (Frankfurt, Germany)
phospho-STAT6 (Y641)	J71-773.58.11	mouse	1:1000	558241	BD (Heidelberg, Germany)
STAT6	polyclonal	rabbit	1:1000	9362	Cell Signaling (Frankfurt, Germany)

α-tubulin	B-5-1-2	mouse	1:3000	T 6074	Sigma-Aldrich (Taufkirchen, Germany)
VEGF Receptor 2	55B11	rabbit	1:1000	2479	Cell Signaling (Frankfurt, Germany)

Secondary antibodies

Antibody	Host species	Dilution	Order number	Manufacturer
anti biotin HRP linked	goat	1:3000	7075	Cell Signaling (Frankfurt, Germany)
anti goat IgG HRP linked	rabbit	1:2000	P 0449	DakoCytomation (Hamburg, Germany)
anti mouse IgG HRP linked	horse	1:2000	7076	Cell Signaling (Frankfurt, Germany)
anti rabbit IgG HRP linked	goat	1:2000	7074	Cell Signaling (Frankfurt, Germany)

2.2 Recombinant cytokines and inhibitors

Cytokine/Inhibitor	Concentration	Manufacturer
murine IL-4	10 (2.5, 1.0) ng/ml	Peprotech
murine IL-13	10 (2.5, 1.0) ng/ml	(Hamburg, Germany)
murine IL-17A	10 ng/ml	
murine OSM	10 ng/ml	R&D Systems (Wiesbaden-Nordenstadt, Germany)
MEK 1/2 III (inhibitor)	1 µM	Calbiochem/Merck/Millipore (Darmstadt, Germany)
SB203580 (inhibitor)	5 µM	Axon Medchem (Groningen, Netherlands)

2.3 Primer

2.3.1 Primer for genotyping

These primer were used for genotyping of *C57Bl/6*, *Osmr*$^{-/-}$, *Ldlr*$^{-/-}$*Osmr*$^{-/-}$ and *Ldlr*$^{-/-}$*Osmr*$^{+/+}$ mice. They were ordered from Eurofins Genomics (Ebersberg, Germany).

Gene	**Name**	**Sequence (5' →3')**
Osmr	OSMR 1	GTAATCAGACCAATGGCTTTCTC
	OSMR 2	GATCCAACAGAGCAATCATGAAGC
	OSMR 3	GCACATCTGAACTTCAGC
Ldlr	IMRO 0092	AATCCATCTTGTTCAATGGCCGATC
	IMRO 3349	CCATATGCATCCCCAGTCTT
	IMRO 3350	GCGATGGATACACTCACTGC

2.3.2 Primer for quantitative RT-PCR (qRT-PCR)

All primer, recognizing murine genes, are designed using the Universal ProbeLibrary Assay Design Center from Roche (Basel, Switzerland) and ordered from Eurofins Genomics (Ebersberg, Germany).

Gene Name	**Primer Name**	**Sequence (5' →3')**
ATP-binding cassette	mABCA1 fw	ggacatgcacaaggtcctga
protein A1	mABCA1 rev	cagaaaatcctggagcttcaaa
Acetyl-coenzyme A	mACC fw	gccattggtattggggcttac
carboxylase	mACC rev	cccgaccaaggactttgttg
Bile salt export pump	mBSEP fw	aagctacatctgccttagacacagaa
	mBSEP rev	caatacaggtccgaccctctct
C-C chemokine	mCCR1 fw	ctctggaaacacagactcactg
receptor type 1	mCCR1 rev	ctccatcctttgctgaggaac
Collagen type I alpha 1	mCol1α1 fw	gactggcaacctcaagaagg
	mCol1α1 rev	gtgcagccgtccacaagg
Collagen type I alpha 2	mCol1α2 fw	gccaacaagcatgtctggttagg
	mCol1α2 rev	aggacacccttctacgttgt

Collagen type III alpha 1	mCol3α1 fw	gcacagcagtccaacgtaga
	mCol3α1 rev	gacatctctagactcataggactgacc
Cholesterol 7 alpha-	mCYP7A1 fw	aacgggttgattccatacctgg
hydroxylase	mCYP7A1 rev	gtggacatatttccccatcagtt
Elastin	mEln fw	cctgggagttggtggaaaa
	mEln rev	agcccccaccttggtatcc
Elongation of very long	mELOVL6 fw	ccttgtgctcttctgccatt
chain fatty acids protein 6	mELOVL6 rev	tactcagccttcgtggcttt
Fatty acid synthase	mFASN fw	ttcggctgctgttggaagtcag
	mFASN rev	acccacccagacgccagtgttc
Farnesoid X receptor	mFXR fw	cttgatgtgctacaaaagctgtg
	mFXR rev	actctccaagacatcagcatctc
Glycoprotein 130	mu gp130 fw	tcccatgggcaggaatatag
	mu gp130 rev	ccattggcttcagaaagagg
Hypoxanthine-guanine	mHPRT for	tcctcctcagaccgctttt
phosphoribosyltransferase	mHPRT rev	cctggttcatcatcgctaatc
Interleukin-4 receptor	mIL4R fw	tggatagcgctgtggactg
	mIL4R rev	ggatgcatgtgaggttttca
Interleukin-13 receptor	mIL13Rα1 fw	caagccctgacacacactatactc
alpha 1	mIL13Rα1 rev	gatgttttcacattgacgactttt
Interleukin-13 receptor	mIL13Rα2 fw	actggctattctttggagataaaagt
alpha 2	mIL13Rα2 rev	aaccaagtaatccaggatccaa
Leukemia inhibitory	mLIFR for	aaagctaattccaagaaagaagtga
factor receptor	mLIFR rev	gcaacatggtaagttgaatcctc
Low-density	mLDLR fw	gatggctatacctacccctcaa
lipoprotein receptor	mLDLR rev	tgctcatgccacatcgtc
Sodium-taurocholate	mNTCP fw	gaagtccaaaaggccacactatgt
cotransporting polypeptide	mNTCP rev	acagccacagagagggagaaag
Osteoprotegerin	mOPG fw	gagacacagctcacaagagcaa
	mOPG rev	gctttcacagaggtcaatgtctt
Oncostatin M receptor	mOSMR for	ccaaaaagagttcagcacacc
	mOSMR rev	ccgaccacacttgtctccat
Stearoyl-coenzyme A	mSCD1 fw	ccggagacccttagatcga
desaturase 1	mSCD1 rev	tagcctgtaaaagatttctgcaaacc

Plasminogen activator inhibitor 2	mSerpinb2 fw	tagtgaatccagggcgtctt
	mSerpinb2 rev	aaagttcttccattgtttcaatcc
Small heterodimer partner	mSHP fw	cgatcctcttcaacccagatg
	mSHP rev	agggctccaagacttcacaca
Osteopontin	mSpp1 fw	ggaggaaaccagccaaggac
	mSpp1 rev	tgccagaatcagtcactttcac
Thrombospondin-4	mThbs4 fw	atgggacggctgaacaaa
	mThbs4 rev	gttgaacaccaccagatggat
Tenascin	mTnc fw	gtcagtgccatagcaacaaca
	mTnc rev	actctccacctgagcagtaggt

2.4 Reaction kits

Name	Manufacturer
RNeasy Mini Kit QIAshredder RNase-Free DNase Set	QIAGEN (Hilden, Germany)
FastStart Universal SYBR Green Master (Rox) Transcriptor First Strand cDNA Synthesis Kit	Roche (Penzberg, Germany)

2.5 Protein and DNA ladder

Ladder for SDS gels and Western blot analysis

Name	Manufacturer
PageRuler™ Plus Prestained Protein Ladder (10-250 kDa)	Fermentas/Life Technologies (Darmstadt, Germany)
Biotinylated Protein Ladder (9-200 kDa)	Cell Signaling (Frankfurt, Germany)

Ladder for DNA agarose gels

Name	Manufacturer
GeneRuler™ 1 kb DNA Ladder (up to 10 kbp)	Fermentas/Life Technologies (Darmstadt, Germany)

2.6 Eukaryotic cells

***wt* VSMCs**	vascular smooth muscle cells, adherent, isolated from the aorta of *C57Bl/6J* (*B6*) mice
***Osmr-/-* VSMCs**	vascular smooth muscle cells, adherent, isolated from the aorta of *Osmr*$^{-/-}$ mice (*C57Bl/6J* background)
MS1 (MILE SVEN 1)	endothelial cells, adherent, located in pancreas/islet of Langerhans; mus musculus (*C57Bl/6J* strain); ATCC CRL-2279 (kindly provided by AG Nieswandt, Department of Experimental Biomedicine, Vascular Medicine, University Hospital Würzburg)

2.7 Mice

Name	Short Name	Breeding location
C57Bl/6JRj	*C57Bl/6 or B6*	Janvier Labs (Le Genest-Saint-Isle, France) and self breeding, RVZ Würzburg
B6.Osmr^{tm1Mtan} (*C57Bl/6J* background)	*Osmr$^{-/-}$*	self breeding, RVZ Würzburg
B6.129S7-Ldlr^{tm1Her}/J (*C57Bl/6J* background)	*Ldlr$^{-/-}$*	self breeding, RVZ Würzburg
B6.Ldlr$^{-/-}$Osmr$^{-/-}$ (*C57Bl/6J* background)	*Ldlr$^{-/-}$Osmr$^{-/-}$*	self breeding, RVZ Würzburg
B6.Ldlr$^{-/-}$Osmr$^{+/+}$ (*C57Bl/6J* background)	*Ldlr$^{-/-}$Osmr$^{+/+}$*	self breeding, RVZ Würzburg

Breeding of mice is explained in section 3.1.

2.8 Chemicals

Acid aldehyde	Sigma-Aldrich (Taufkirchen)
Acrylamide solution (30%), Mix 37, 5:1	AppliChem (Darmstadt)
Agarose	Peqlab (Erlangen)
Aminocaproic acid	AppliChem (Darmstadt)
Amphotericin B	Life Technologies (Darmstadt)
Ampicillin	Roth (Karlsruhe)
Aprotinin	AppliChem (Darmstadt)
Bromophenol blue	AppliChem (Darmstadt)
4,6-Diamidino-2-phenylindole (DAPI)	AppliChem (Darmstadt)
Dimethyl sulfoxide (DMSO)	AppliChem (Darmstadt)

Ethanol	Roth (Karlsruhe)
Ethanol absolute	AppliChem (Darmstadt)
Ethidium bromide	AppliChem (Darmstadt)
Fibronectin solution, bovine (1 mg/ml)	PromoCell (Heidelberg)
Glycerol	AppliChem (Darmstadt)
Glycine	AppliChem (Darmstadt)
Isopropyl alcohol	Roth (Karlsruhe)
Leupeptin	AppliChem (Darmstadt)
2-Mercaptoethanol	AppliChem (Darmstadt)
Methanol	AppliChem (Darmstadt)
Non-fat dry milk powder, blotting grade	AppliChem (Darmstadt)
Nuclease free H_2O	QIAGEN (Hilden)
Oil-Red-O	Sigma-Aldrich (Taufkirchen)
Paraformaldehyde	AppliChem (Darmstadt)
Penicillin (5000 U/ml)/Streptomycin (5 mg/ml)	Life Technologies (Darmstadt)
Pepstatin A	Merck (Darmstadt)
Phenylmethylsulfonyl fluoride (PMSF)	AppliChem (Darmstadt)
Potassium chloride (KCl)	AppliChem (Darmstadt)
Potassium dihydrogen phosphate (KH_2PO_4)	AppliChem (Darmstadt)
Saturated aqueous picric acid	Sigma-Aldrich (Taufkirchen)
Sirius red	Sigma-Aldrich (Taufkirche)
Sodium acetate	AppliChem (Darmstadt)
Sodium chloride (NaCl)	AppliChem (Darmstadt)
Sodium dihydrogen phosphate (Na_2HPO_4)	Roth (Karlsruhe)
Sodium dodecyl sulfate (SDS)	AppliChem (Darmstadt)
Sodium fluoride (NaF)	AppliChem (Darmstadt)
Sodium hydrogen carbonate ($NaHCO_3$)	Sigma-Aldrich (Taufkirchen)
Sodium hydroxide (NaOH)	AppliChem (Darmstadt)
Sodium orthovanadate (Na_3VO_4)	AppliChem (Darmstadt)
50x TAE buffer	AppliChem (Darmstadt)
Tetramethylethylenediamine (TEMED)	AppliChem (Darmstadt)
Triton X-100	AppliChem (Darmstadt)
Tris(hydroxymethyl)aminomethane (Tris)	AppliChem (Darmstadt)
Trypan blue for Countess®	Life Technologies (Darmstadt)
Tween 20	AppliChem (Darmstadt)

Xylene	Carl Roth (Karlsruhe)

2.9 Buffers, solutions and prepared culture media

10x PBS:	1.37 M	NaCl
	27 mM	KCl
	100 mM	Na_2HPO_4
	20 mM	KH_2PO_4
	pH	7.4
1x PBS:	137 mM	NaCl
	2.7 mM	KCl
	10 mM	Na_2HPO_4
	2 mM	KH_2PO_4
	pH	7.4
2x Laemmli buffer:	125 mM	Tris-HCl (pH 6.8)
	20%	Glycerol
	10%	2-Mercaptoethanol
	4%	SDS
	0.004%	Bromophenol blue
4x Laemmli buffer:	250 mM	Tris-HCl (pH 6.8)
	40%	Glycerol
	20%	2-Mercaptoethanol
	8%	SDS
	0.004%	Bromophenol blue
Triton X-100 lysis buffer:	20 mM	Tris-HCl pH 7.5
	150 mM	NaCl
	10 mM	NaF
	1%	Triton X-100

protease and phosphatase inhibitors:	1 mM	Na_3VO_4
	1 mM	PMSF
	5 µg/ml	Aprotinin
	5 µg/ml	Leupeptin
	3 µg/ml	Pepstatin
Tris-buffered saline Tween 20 (1xTBS-T):	137 mM	NaCl
	20 mM	Tris
	0.1%	Tween 20
	pH	7.6
Running buffer (1x):	25 mM	Tris
	192 mM	Glycin
	3.5 mM	SDS
10% Separating gel:	5.9 ml	H_2O (Millipore)
	5.0 ml	30% Acrylamide solution
	3.8 ml	1.5 M Tris-HCl (pH 8.8)
	150 µl	10% SDS
	12 µl	TEMED
	75 µl	APS
3% Stacking gel:	3.4 ml	H_2O (Millipore)
	830 µl	30% Acrylamide solution
	630 µl	2.0 M Tris-HCl (pH 6.8)
	50 µl	10% SDS
	5 µl	TEMED
	40 µl	APS
Anode I buffer: (for Western Blotting)	300 mM	Tris
	20%	Methanol
Anode II buffer: (for Western Blotting)	25 mM	Tris
	20%	Methanol

Cathode buffer:	40 mM	Aminocaproic acid
(for Western Blotting)	20%	Methanol
Stripping buffer:	62.5 mM	Tris
	2%	SDS
	pH	6.7
	0.78%	2-Mercaptoethanol (freshly added)
6x DNA sample buffer:	15%	Ficoll®400
	0.25%	Bromophenol blue
	0.25%	Xylene cyanol FF
Collagenase solution:	10 mg	Collagenase Type II
(sterile filtered prior to use)	10 mg	Trypsin inhibitor
	300 mg	BSA
	10 ml	HBSS
Gelatine solution:	0.75 mg	Gelatine powder
(dissolving by autoclaving)	100 ml	PBS
VSMC culture medium:	5% (25 ml)	FBS
	5% (25 ml)	Mouse serum
	5 ml	Penicillin/Streptomycin
	1 ml	Amphotericin B
	ad 500 ml	DMEM
VSMC isolation medium:	10% (50 ml)	FBS
	10% (50 ml)	Mouse serum
	5 ml	Penicillin/Streptomycin
	1 ml	Amphotericin B
	ad 500 ml	DMEM

0.5% Trypsin solution:		2.5% Trypsin solution
	1:5	in PBS
Freezing medium:	40%	Respective medium
	50%	FBS
	10%	DMSO
PHEM buffer:	60 mM	PIPES
	25 mM	HEPES
	10 mM	EGTA
	2 mM	$MgCl_2$
	pH	6.9
	4%	PFA
	1%	IGEPAL®CA-630 (supplemented)
Mouse tissue lysis buffer:	10 mM	TRIS, pH 8.0
	10 mM	Na_2EDTA, pH 8.0
	10 mM	NaCl
	0.5%	SDS
Red blood cell lysis buffer:	155 mM	NH_4Cl
	10 mM	$KHCO_3$
	0.1 mM	EDTA
Aldehyde-Fuchsin solution:		
Stock solution:	70%	Ethanol
	0.5%	Aldehyde fuchsin
Working solution:	50 ml	Stock solution
(solution on RT o/n,	2.5 ml	Acid aldehyde
filtered prior to use)	1 ml	Conc. Hydrochloric acid

Kaiser's glycerin jelly:		
Stock solution:	4 g	Gelatine
	21 ml	ddW
	25 ml	Glycerin
Working solution:	3 Parts	Stock solution
	7 Parts	ddW
Oil-Red-O (ORO)		
Lipid Staining solution:		
Stock solution:	0.5%	Oil-Red-O
		Isopropanol
Working solution:	180 ml	Stock solution
(incubation 1h at RT	120 ml	ddW
followed by filtration)		
Picrosirius Red solution:	0.1%	Picrosirius red
(solution mixed thoroughly		Saturated aqueous
filtered prior to use)		Picric acid

2.10 Cell culture reagents

Name	Manufacturer
2.5% Trypsin (no phenol red) Amphotericin B DMEM, high glucose, GlutaMAX™ Hank's balanced salt solution (HBSS) Penicillin/Streptomycin	Life Technologies (Darmstadt, Germany)
Bovine serum albumin (BSA) Fetal bovine serum (FBS)	Sigma-Aldrich (Taufkirchen, Germany)
Mouse serum	GE Healthcare Life Sciences (Freiburg, Germany)
Soybean Trypsin-Inhibitor	Worthington (Lakewood, NJ, USA)

2.11 Molecular biology reagents

Name	Manufacturer
Bovine serum albumin (BSA), blotting grade	AppliChem (Darmstadt, Germany)
Collagenase Type II	Worthington (Lakewood, NJ, USA)
RNase-Free DNase Set	QIAGEN (Hilden, Germany)
Fluroshield with Dapi Goat serum	Sigma-Aldrich (Taufkirchen, Germany)
Proteinase K	Thermo Scientific (Schwerte, Germany)
Tissue-Tek® O.C.T. compound	Sakura Finetek (Staufen, Germany)
Vitro Clud	R. Langenbrinck (Emmendingen, Germany)

2.12 Consumables

Consumable	Manufacturer
1.5/2 ml caps 5/10/25 ml serological pipettes 6-well plates 10/20/100/200/1000 µl tips 10/20/100/200/1000 µl filter tips 15 ml/ 50 ml tubes Cryotubes Cuvettes EDTA-coated tubes FACS tubes PCR tubes Serum gel tubes	Sarstedt (Nümbrecht, Germany)

10 ml wide mouth pipettes 1/20 ml syringe	BD (Heidelberg, Germany)
70 µm cell strainer	Falcon, A Corning Brand (Tewksbury, USA)
Filter 0.2 µm	Sartorius AG (Göttingen, Germany)
Injection needles (26 gauge)	Neoject, Dispomed (Gelnhausen, Germany)
MicroAmp® Optical 384-Well R. Plate MicroAmp® Optical Adhesive Film	Life Technologies (Darmstadt, Germany)
Microscope slides, superfrost	Thermo Scientific (Braunschweig, Germany)
Poly-L-lysin glass slides	Menzel GmbH (Braunschweig, Germany)
Coverslips PVDF membrane	VWR (Ismaning, Germany)
Western diet (21% or 15% milk fat, 0.15% cholesterol, 19.5% casein)	Altromin (Lage, Germany)
Whatman paper	Whatman (Kent, UK)

2.13 Laboratory equipment

Apparatus	**Manufacturer**
ABI PRISM® 7900HT, real time PCR cycler	Life Technologies (Darmstadt, Germany)
Adjustable casting chamber (JustCast)	Peqlab (Erlangen, Germany)
Agarose gel electrophoresis chambers	
AxioObserver.Z1, fluorescence microscope	Zeiss (Jena, Germany)
Benchtop shakers, magnetic stirrers and overhead stirrers	Heidolph (Schwabach, Germany)
Biometra Multigel and Maxigel, protein gel electrophoresis system	Analytik Jena (Jena, Germany)
BioPhotometer plus	Eppendorf (Hamburg, Germany)
Benchtop centrifuges	
CONTOUR® glucometer	Bayer (Leverkusen, Germany)
Countess®, automated cell counter	Life Technologies (Darmstadt, Germany)

EVOS® fl Microscope	Peqlab (Erlangen, Germany)
FluorChem Q, Western blot Imager	PoteinSimple (Santa Clara, USA)
Freezer and refrigerators	Liebherr (Bulle, Switzerland)
Gel documentation system	Herolab (Wiesloch, Germany)
Heraeus HERAcell 240®, cell incubator	Thermo Fisher Scientific Inc. (Waltham, USA)
Heraeus HERAfreeze, -80C freezer	
Leica upright microscope DM4000 B	Leica (Wetzlar, Germany)
Mastercycler® pro, thermal PCR cycler	Eppendorf (Hamburg, Germany)
Microwave oven	Privileg (Stuttgart, Germany)
NanoPhotometer® P 300	Implen (Westlake Village, USA)
Single channel and multichannel pipettes	Eppendorf (Hamburg, Germany) Brand (Wertheim, Germany)
pH sensor, FE20 - FiveEasy™pH	Mettler-Toledo (Giessen, Germany)
Pipetus®, electronic pipette controller	Hirschmann Laborgerte (Eberstadt, Germany)
Power supplies for electrophoresis	Consort (Turnhout, Belgium)
QIAgility, automated pipetting robot	QIAGEN (Hilden, Germany)
Sterile benches for cell culture, BDK-S 1200	BDK Luft- und Reinraumtechnik (Sonnenbühl, Germany)
Sysmex KX-21N	Sysmex (Norderstedt, Germany)
Thermomixer compact/comfort	Eppendorf (Hamburg, Germany)
Transmitted light microscope, Leica DMIL	Leica (Wetzlar, Germany)
Vortex-Genie® 2; vortex mixer	Scientific Industries (Bohemia, USA)
Water bath	GFL - Gesellschaft für Labortechnik (Burgwedel, Germany)
Western blot chamber, semi-dry blotting	Peqlab (Erlangen, Germany)

3 Methods

3.1 Mice

C57Bl/6JRj (B6) mice were obtained from Janvier Labs. *B6.Osmr^{tm1Mtan} (Osmr$^{-/-}$)* mice were kindly provided by Prof. Dr. Koji Nakamura (LivTech Inc., Japan), Prof. Dr. Thomas Braun and Dr. Thomas Kubin (Max Planck Institute for Heart and Lung Research, Bad Nauheim, Germany). *B6.129S7-Ldlr$^{tm1Her/J}$ (Ldlr$^{-/-}$)* mice were received from Prof. Dr. Alma Zernecke-Madsen (Institute of Clinical Biochemistry and Pathobiochemistry, Würzburg). For Western diet (WD) experiments, *Ldlr$^{-/-}$* mice were crossed with *Osmr$^{-/-}$* mice to obtain *Ldlr$^{-/-}$Osmr$^{-/-}$* and *Ldlr$^{-/-}$Osmr$^{+/+}$* mice. Both single knock out mice were on *C57Bl/6* background. All mice were bred and maintained in the animal facility of the Rudolf-Virchow-Zentrum (RVZ), Josef-Schneider-Straße 2, 97080 Würzburg. All WD experiments were approved by local authorities (Regierung von Unterfranken; Az 55.2-2531.01-27/14).

3.1.1 Isolation of genomic DNA (gDNA)

Ear marks were collected in 1.5ml tubes. 190µl of tissue lysis buffer together with 10µl of proteinase K was added into each tube. The mouse tissue was incubated in a thermo block at 56°C with 14000 rpm over night. Afterwards, the digested tissue was centrifuged at 20000g for 10 minutes and the supernatant was transferred into a new 1.5 ml tube. In the next step, 300µl of tissue lysis buffer together with 50µl 3M NaOAc was added to the supernatant and mixed by shaking the tube up and down. 450µl of isopropanol was added to the mixture and shaken gently until thin fibres of gDNA could be seen (at this step, the tubes can be stored at -20°C). Next, the mixture was centrifuged at 20000g for 30 minutes. After adding of 500µl of 70% ethanol to the pellet, the tube was centrifuged again at 20000g for 20 minutes. When the pellet was dried at room temperature, the

DNA was eluated in 70 to 100µl TAE buffer. The DNA eluate was stored at 4°C for several days or at -20°C for longer terms.

3.1.2 Genotyping of Ldlr and Osmr

For determination of the genotype, isolated gDNA from ear marks was used. The PCR master mix (total amount 22µl) consisted of 12.5µl 2x PCR master mix (Fermentas), 1.5µl of each primer (concentration: 10µM) and 5µl nuclease free water. The master mix was transferred into a PCR tube together with 3µl of gDNA. After mixing and spinning down all liquid, the PCR was carried out with the following settings:

For *Ldlr*:

Temperature	**Duration**	**Cycle**
94°C	3 min.	no
94°C	30 sec.	35x
61°C	1 min.	
72°C	1 min.	
72°C	2 min.	no
4°C	hold	no

For *Osmr*:

Temperature	**Duration**	**Cycle**
94°C	5 min.	no
94°C	1 min.	35x
60°C	1 min.	
72°C	90 sec.	
72°C	5 min.	no
4°C	hold	no

expected sizes of DNA fragments are:

***Ldlr*$^{+/+}$:**	167 bp	***Osmr*$^{+/+}$:**	364 bp
***Ldlr*$^{-/-}$:**	350 bp	***Osmr*$^{-/-}$:**	750 bp
***Ldlr*$^{+/-}$:**	167 and 350 bp	***Osmr*$^{+/-}$:**	364 and 750 bp

3.1.3 Agarose gel electrophoresis (DNA electrophoresis)

DNA fragments were separated according to their size using 1% agarose gel electrophoresis. For producing gels, an appropriate amount of agarose was dissolved in 1x TAE buffer (diluted from 50x TAE buffer) and heated in a microwave. After cooling down, ethidium bromide (0.3-0.5µg/ml) was added. Ethidium bromide intercalates between both DNA strands thus visualising the DNA under UV light (λ=312 nm). The agarose gel was cast using the adjustable casting chamber and the appropriate combs (Peqlab, Erlangen). The DNA samples were diluted with 6x DNA loading buffer and - together with an appropriate DNA ladder (Section 2.5) - were loaded onto the gel. The electrophoresis chamber was filled with 1x TAE buffer and electrophoresis performed at 80-100 V.

3.2 Cell culture

3.2.1 Isolation and cultivation of vascular smooth muscle cells (VSMCs)

Primary aortic VSMCs were isolated from five female *C57Bl/6* and *OSMR*$^{-/-}$ mice each. After euthanasia, the chest was opened and rib cage, heart, lungs and oesophagus were removed. The aortas were cut along the anterior end by moving gently toward the posterior end. Aortas of the respective genotypes were pooled in ice-cold HBSS. Blood and fatty layer were removed and after shortly washing in 70% ethanol and HBSS, the aortas were put into an empty well of a six well dish followed by cutting into small pieces. Together with 15 ml HBSS, the aorta pieces were transferred into a 15 ml tube. After spinning at 1000 rpm for five minutes, the supernatant was discarded and the aorta pieces were digested in 5 ml of sterile filtered collagenase solution for two hours at 37°C. During this procedure, one six well was coated with 500µl of gelatine solution which, after two hours, was replaced by 3 ml of VSMC isolation medium (DMEM, 10% FBS, 10% mouse serum, penicillin/streptomycin and amphotericin B). The digestion of the aortas was stopped with 10 ml DMEM containing 10% FCS followed by centrifugation at 1000 rpm for five minutes. The cell pellet was gently resuspended in 1ml of VSMC isolation medium. The cell suspension was added to the pre-coated, medium-filled six well. After three days of culture at 37°C and 5% CO_2, smooth muscle cells adhered to

the bottom of the well and started to proliferate. At day four, the supernatant containing dead cells was removed and refreshed with 4 ml of VSMC isolation medium. When VSMCs were confluent, the cells were split by using 0.5% trypsin solution. Freezing and thawing of VSMCs is described in subsection 3.2.2. After passage 2, the isolation medium was replaced with VSMC culture medium (DMEM, 5% FBS, 5% mouse serum, penicillin/streptomycin and amphotericin B, Section 2.9) for slowing down cell-growth. For experiments, VSMCs between passage 2 and 6 were used. 24 hours before stimulation, the cells were starved with DMEM containing 1% FBS, penicillin/streptomycin and amphotericin B. In the following sections, VSMCs are termed as *wt* VSMCs (from *B6* mice) and *Osmr-/-* VSMCs (from *Osmr*$^{-/-}$ mice).

3.2.2 Freezing and thawing of VSMC

VSMCs were removed from the cell dishes by using a 0.5% trypsin solution and centrifuged at 1000 rpm for five minutes. After resuspending in 1ml cold freezing medium, the cell solution was pipetted into a cryotube. Cryotubes were immediately stored in a cryo-freezing container. An isopropanol filled box allows a slow and gentle freezing procedure by cooling down with a rate of -1°C/min when put into a -80°C freezer. After 24 hours, the cryotubes were transferred to the liquid nitrogen tank for long term storage.

Thawing cells was performed by warming cryotubes in a water bath at 37°C. When almost thawed, the cell suspension was diluted by using 1ml warm VSMC culture medium (DMEM, 5% FBS, 5% mouse serum, penicillin/streptomycin and amphotericin B). After pipetting into a 15 ml tube containing another 9 ml VSMC culture medium, the cells suspension was centrifuged at 1000 rpm at room temperature for five minutes. The pellet was resuspended in 1 ml VSMC culture medium and then added into wells of a gelatine-coated six well dish.

3.3 Microscopy

3.3.1 Analysis of VSMCs by light microscopy

The phenotype of VSMCs was monitored by using an EVOS® fl Microscope for light microscopy. Therefore, cultured *wt* VSMCs and *Osmr-/-* VSMCs were photographed from passage 0 to 6 and compared with the morphology of endothelial cells (MS1). For more detailed characterization of VSMCs, smooth muscle markers for immunofluorescence and Western Blot analysis were used.

3.3.2 Staining of VSMCs by immunofluorescence

For the detection and localization of smooth muscle actin (SMA) and smooth muscle protein 22-alpha (SM22α), *wt* VSMCs (from *B6* mice) and *Osmr-/-* VSMCs (from *Osmr*$^{-/-}$ mice) were stained with specific antibodies for immunofluorescence. 5x10^4 cells were seeded on cover slips and the following day starved in DMEM containing 1% FBS, penicillin/streptomycin and amphotericin B overnight. For staining, the cells were washed with PBS followed by fixation and permeabilization with PHEM buffer for 30 minutes at room temperature. After blocking with 5% BSA/5% goat serum/PBS for 60 minutes at room temperature, VSMCs were incubated with primary antibodies for SMA or SM22α diluted in 5% BSA/PBS for 1-2 hours at room temperature. After washing the cells in PBS three times for ten minutes, incubation with a secondary antibody coupled to Alexa Fluor 488 was carried out for one hour at room temperature in the dark. After washing again in PBS three times for ten minutes and in the dark, the cells were mounted with Fluoroshield™ containing DAPI (Sigma-Aldrich). The slides were stored at 4°C in the dark and were analysed by fluorescence microscopy on the next day.

3.3.3 Aorta en face staining

En face staining of the aorta was kindly performed by AG Zernecke, Institute for Clinical Biochemistry and Pathobiochemistry, University Hospital Würzburg. Briefly, after euthanasia the mice were re-perfused with PBS followed by trans-cardial perfusion with 4% PFA in PBS. Before dissecting and mounting on gummed glass slides, the aorta

was cleaned by removing excessive fat and tissue. Slides were left in 4% PFA in PBS overnight and adventitial tissue was removed before oil-red-o staining was performed.

For the oil-red-o lipid staining, samples were washed in PBS for five minutes. Then they were dipped in 60% isopropanol ten times, followed by 15 minutes incubation in oil-red-o working solution. After additional ten dips in 60% isopropanol, samples were mounted in Kaisers glycerin jelly and images were recorded with a Leica DMLB microscope.

3.3.4 Aortic root staining

Hearts were dissected after fixation by re-perfusion with 4% PFA in PBS. For cryo-protection, the fixing solution was exchanged against 30% sucrose solution in PBS for 24 hours before freezing in 1:1 O.C.T. (optimum cutting temperature)/PBS mixture compound. The frozen hearts were cut in 5 µm serial sections through the aortic root. The cryo sections were washed twice for five minutes in PBS before immunohistochemical staining was performed.

For the collagen and elastin staining, aortic root sections were rehydrated in 70% ethanol followed by staining in aldehyde fuchsin working solution for 15 minutes at room temperature. Then, slides were dipped five times in 70% ethanol and placed in deionized water for five minutes. After staining for 90 minutes in sirius red solution at RT, the slides were incubated for one minute in 0.01 M hydrochloric acid at RT. After dehydration via an ascending alcohol series to xylen, the slides were dried and mounted with Vitro-Clud.

3.3.5 Analysis of plaque area in the aorta and aortic root

For the quantification of the *en face* and aortic root stainings, Diskus image analysis software was used. The total area of the whole aorta as well as the whole aortic root and the plaque area was marked per slide. Plaque area in the aortic roots was analysed in three sections per animal.

3.4 Molecular biological methods

3.4.1 Cell stimulation and RNA/protein extraction

The VSMCs were stimulated with murine Oncostatin M (mOSM), Interleukin 4 (mIL-4), Interleukin 13 (mIL-13) and Interleukin 17A (mIL-17A) (10ng/ml each). For inhibitor experiments, VSMCs were treated with 1µM MEK 1/2 III or 5µM SB203580. When VSMCs were double stimulated, they were pretreated with mOSM (10ng/ml) before stimulation with mIL-4 or mIL-13 under suboptimal conditions (1 and 2.5ng/ml).

RNA extraction from VSMCs was conducted using the RNeasy Mini Kit (QIAGEN) and from liver tissue (50mg) the NucleoSpin® RNA kit (Macherey-Nagel) according to the manufacturer's instructions.

Protein lysates were generated using Triton X-100 lysis buffer containing protease and phosphatase inhibitors (Section 2.9). All handling with Triton X-100 lysis buffer had to be done on ice. The cells were washed with cold PBS before 100µl of cold lysis buffer was added. After dissociation with a scraper from the bottom of the well, the cell lysate was transferred into a 1.5ml cap and incubated for 30 minutes on ice. After spinning for 15 minutes at 14000 rpm, the supernatant was collected in a fresh 1.5 ml cap and the pellet was discarded.

3.4.2 Quantitative real time PCR (qRT-PCR)

Quantitative analysis of gene expression was assessed by quantitative real time RT-PCR (qPCR) analysing the mRNA expression levels. After isolation of total RNA using RNeasy Mini Kit (QIAGEN), reverse transcription PCR was performed using the Transcriptor First Strand cDNA Synthesis Kit (Roche). The following pipetting scheme was used: 400 ng RNA (in 10µl final volume) were mixed with 1µl anchored-oligo(dT)18 primers, 2 µl random hexamer primers, 4 µl Transcriptor RT reaction buffer, 0.5 µl Protector RNase inhibitor, 2 µl dNTP-Mix and 0.5 µl Transcriptor reverse transcriptase. Then the samples were centrifuged and transferred to the Eppendorf Mastercycler Pro. The run was performed as described in the following steps:

Temperature	Duration	Comment
50°C	60 min.	reverse transcription
85°C	5 min.	inactivation
4°C	hold	

The resulting cDNA was used to perform real time PCR with FastStart Universal Sybr Green Master (Rox) Mix from Roche. Primers applied in qPCR experiments are mentioned in subsection 2.3.2. Serial dilutions of template cDNAs were used to verify primer efficiency. For each target gene to be analysed, the Master Mix was prepared as follows: 5µl of Sybr Green master mix, 400 nM of each primer (0.4 µl of a 10 µM stock), 2.2 µl nuclease free H_2O and 2 µl of the respective cDNA were mixed on a 384 well plate in duplicates using the automated liquid handling robot QIAgility®. Real time PCR was performed on a real time PCR cycler (ABI PRISM® 7900HT) using the following conditions:

Comment	Temperature	Duration	Cycle
initial activation	95°C	10 min.	no
denaturation	95°C	15 sec.	40x
hybridisation	60°C	20 sec.	
elongation	60°C	20 sec.	
final elongation	65°C	15 sec.	no
melting curve	95°C	15 sec.	no
	60°C	15 sec.	no
-	4°C	hold	no

Quantification of amplified cDNA was performed according to Pfaffl [174].

3.4.3 PCR array for atherosclerosis

An RT² Profiler PCR™ array (Format E) was purchased from QIAGEN/SABiosciences. This array contains primer assays for 84 mouse genes related to atherosclerosis, spotted in four replicates on a 384 well plate (4x96). Additionally, primer for five housekeeping genes and seven control genes were included. The qRT-PCR was performed in accordance with the RT² Profiler PCR™ array handbook.

3.4.4 SDS-PAGE (Sodium dodecyl sulfate polyacrylamide gel electrophoresis)

The separation of polypeptides by mass was performed using denaturating SDS-PAGE under reducing conditions, as described by Laemmli [175]. SDS gels were cast according to the gel formula mentioned under section 2.9. The separating gel was cast between both glass plates (provided with the Biometra gel systems) and covered with isopropyl alcohol. After polymerisation of the gel, the isopropyl alcohol was discarded and the plates were dried. Then the stacking gel was cast and the appropriate comb was inserted immediately. After polymerisation of the stacking gel the pockets were washed and the gel chamber filled with 1x running buffer. For the experiments, only 10% separation gels and 3% stacking gels were produced. After loading of the samples, the PageRuler™ Plus Prestained Protein Ladder and the biotinylated Protein Ladder, electrophoresis was performed at 25-50 mA for 2-3 hours. The anionic charge of the detergent SDS masks the individual electrical charges of the protein. Therefore, by addition of SDS, proteins can be separated according to their size irrespective of their own charges. Moreover, SDS interrupts hydrogen bonds and denatures polypeptides in combination with β-mercaptoethanol.

3.4.5 Semi-dry Western Blot

After SDS-PAGE, the separated proteins were transferred onto a PVDF (polyvinylidene difluoride) membrane via semi-dry Western blotting. The membrane and the Whatman papers were cut to required gel sizes. The PVDF-membrane was activated through immersion in 100% methanol for a few seconds. Afterwards, the membrane was washed shortly in H_2O (Millipore) and equilibrated in anode II buffer. Meanwhile, the gel was released from the glass plates and equilibrated in cathode buffer. The Whatman papers were equilibrated in the appropriate buffers and the assembly was performed according to Figure 3.1 (from the bottom (anode) to the top (cathode)).

Power was applied for one hour. The applied amperage was defined as follows: 0.8 mA x area of the membrane (cm^2) = used amperage (mA).

After protein transfer, the membrane was blocked in 10% BSA dissolved in 1x TBS-T for 40 minutes and incubated overnight with indicated primary antibodies at 4°C on a

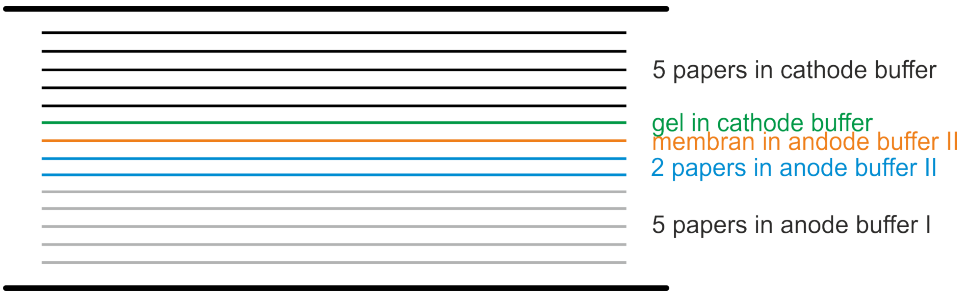

Figure 3.1: **Arrangement of the western blot apparatus.**

shaker. On the next day, the membranes were washed three times for 10 minutes in 1x TBS-T. Then, the membranes were incubated with the respective horseradish peroxidase (HRP) conjugated secondary antibody for one hour at room temperature, followed by three washing steps. Protein detection was conducted using the chemiluminescence kit (Thermo Fisher Scientific Inc.) according to the manufacturer's instructions. Quantification of the chemiluminescence signal was carried out on the FluorChemQ™ using the Alpha View® software (ProteinSimple, San Jose, USA). Equal loading of the gel was verified by stripping the membrane with stripping buffer at 70°C for 20 minutes and re-detection with antibodies recognizing the protein irrespective of its phosphorylation status as well as by detection of GAPDH or tubulin as house keeping proteins.

3.4.6 FACS analysis

Wild-type and *Osmr-/-* VSMCs were cultured in 6 well tissue culture plates under normal culture conditions. At 70% confluency, the cells were stimulated with mOSM (10 ng/ml) for 2.5 and 20 hours. Cells were washed in PBS, released from the six well by incubation in 2 ml PBS/EDTA for five minutes and stained with antibodies detecting OSMR, IL-4R or CCR1 for 30 min at 4°C using dilutions according to the manufacturer's instructions. Appropriate isotype controls were included. After washing in PBS/5% FCS/NaN3 cells were analysed by flow cytometry using a FACSCalibur (BD Biosciences). Data was processed using the FlowJo software.

3.5 Data analysis

Data representing mean ± SEM were analysed by Students t-test or Mann-Whitney test, as appropriate using GraphPad Prism 6.0 software. Differences with $p < 0.05$ were considered to be statistically significant.

4 Results

4.1 Characterisation of VSMCs in cell culture

4.1.1 Light microscopy and immunofluorescence analysis of VSMCs

After isolating smooth muscle cells (VSMCs) from the murine aorta, the cells were taken into culture. The procedure is described in subsection 3.2.1. For the characterisation of their morphology, VSMCs were observed initially by light microscopy from passage zero to seven (p0 to p7) (Figure 4.1).

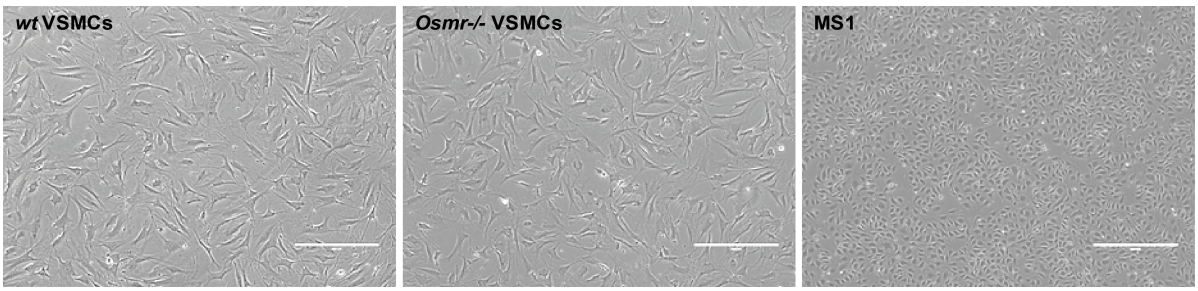

Figure 4.1: **Characterisation of *wt* VSMCs and *Osmr-/-* VSMCs by light microscopy.** Cells from passage zero to seven (p0 - p7) were analysed by light microscopy. Shown are representative pictures of VSMCs from p3. MS1 endothelial cells served as a control. Scale bar: 400µm.

Light microscopy confirmed that the cell growth behaviour of VSMCs differs substantially from fibroblasts or endothelial cells since they form overlapping layers, a characteristic property of smooth muscle cell culture. In comparison, MS1 endothelial cells also preferred cell contact, but they displayed the cobblestone-like morphology typical for endothelial cells and grew in one monolayer. In early passages, VSMCs were smaller and grew faster than in later passages. After passage seven, the cells mostly stopped proliferating and went into growth arrest. For experimental analysis, VSMCs were used

between passage two and six. No difference in the morphological phenotype between *wt* VSMCs and *Osmr-/-* VSMCs could be seen.

Staining for smooth muscle markers by immunofluorescence was used for further characterisation of VSMCs. Typical markers are smooth muscle actin (SMA) and SM22-alpha (SM22α) (Figure 4.2).

All seeded *wt* VSMCs and *Osmr-/-* VSMCs in passage three to six stained positive for smooth muscle markers in green. The cells did not loose their smooth muscle characteristics from p0 to p6 and were not overgrown by other cell types negative for the smooth muscle markers, but positive for the nuclear dye DAPI. This shows that no cell contamination occurred during cell culturing.

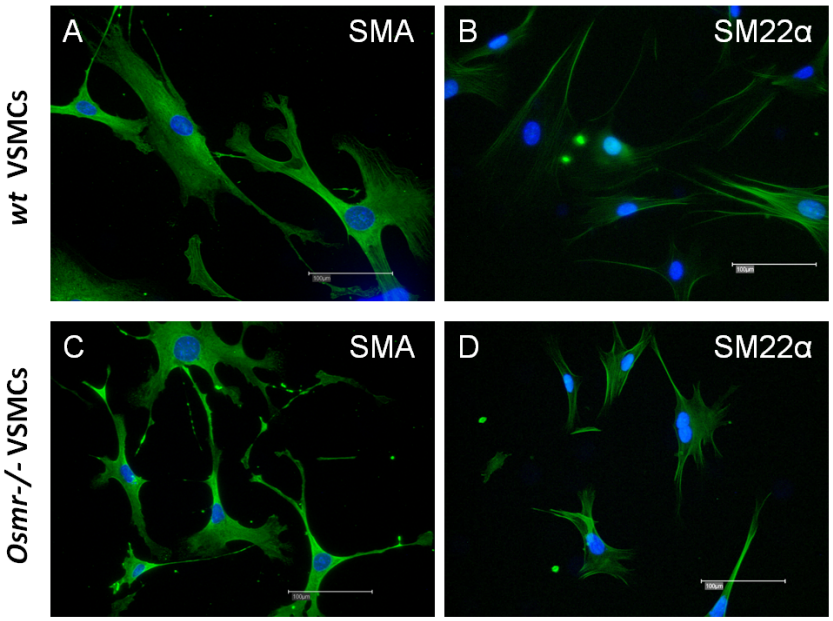

Figure 4.2: **Characterisation of *wt* VSMCs and *Osmr-/-* VSMCs for the expression of smooth muscle markers by immunofluorescence.** Cells were seeded on cover slips. The binding of antibodies directed against SMA (A and C) and SM22α (B and D) and labelled with Alexa Fluor 488 was determined and is shown in green. Staining with the nuclear dye DAPI is shown in blue. The experiments were carried out for VSMCs from passage three to six. Scale bar = 100 µm.

4.1.2 Western Blot analysis of VSMCs

The smooth muscle marker SMA was used for Western blot analysis to determine the purity of *wt* VSMCs and *Osmr-/-* VSMCs. MS1 endothelial cells and vascular endothelial growth factor receptor 2 (VEGFR2), an endothelial cell marker, served as controls. MS1 cells and VSMCs from passage two to six were lysed in Triton X-100 lysis buffer (Figure 4.3).

VEGFR2 was detected only in extracts from MS1, whereas SMA was only detectable in VSMC lysates. Additionally, SMA was consistently present in every passage of *wt* and *Osmr-/-* lysates. Therefore, contamination of both cell cultures, *wt* VSMCs and *Osmr-/-* VSMCs, with endothelial cells could be excluded. No differences in SMA expression were observed in VSMCs during the passages and p2 to p6 could be used for experiments.

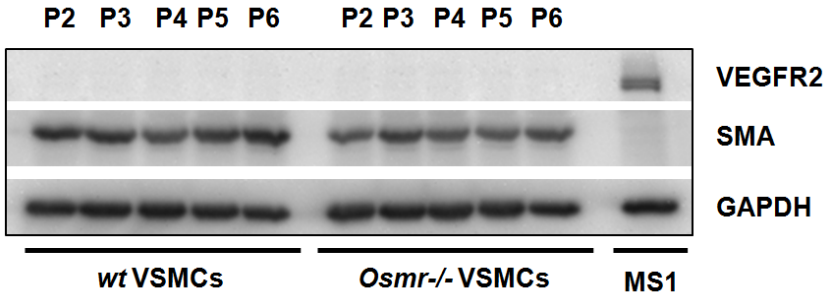

Figure 4.3: **Characterisation of *wt* VSMCs and *Osmr-/-* VSMCs for smooth muscle marker SMA.** Cells were lysed in every passage (p2 - p6). SMA (for VSMCs), and VEGFR2 (for endothelial cells, MS1) were determined by Western blot analysis. The house keeping protein GAPDH was used as a loading control. One representative out of three independent experiments is shown.

4.2 Determination of OSM receptor complex expression on VSMCs

4.2.1 Analysis of expression levels of the OSM receptors in VSMCs by real-time PCR

In the human system, human OSM (hOSM) is able to bind two receptor complexes: OSM receptor type I containing the LIF receptor beta (LIFRβ) and gp130, OSM receptor type II containing OSM receptor beta (OSMRβ) and gp130. Both receptor complexes use gp130 for their signalling. In the murine system, murine OSM (mOSM) signals mainly through the type II complex (gp130/OSMRβ). In order to determine if both receptor complexes are expressed on murine VSMCs, the mRNA from unstimulated VSMCs was isolated and analysed by qRT-PCR for *Osmr*, *IL6st* and *Lifr* expression. The *Il6st* gene encodes for the gp130 protein.

Figure 4.4 shows the "cycle of threshold" (ct) value distribution of the three receptors. For comparison, house-keeping gene hypoxanthine guanine phosphoribosyl transferase (*Hprt*) was included. *Osmr* and *IL6st* with a ct value of 21.6 ± 0.19 and 20.2 ± 0.33 showed a strong expression in VSMCs. *Lifr*, however, was presented at a lower level than the other two receptors (ct value of 25.1 ± 0.45). Therefore, at least on mRNA level, more *Osmr* than *Lifr* was expressed in VSMCs.

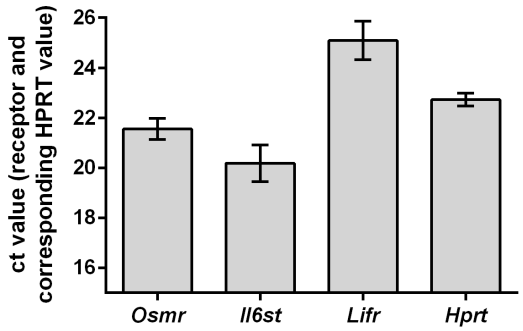

Figure 4.4: **Basal cycle of threshold (ct) values of *Osmr*, *Il6st*, *Lifr* and *Hprt*.** Transcription of each target gene in *wt* VSMCs was analysed by qRT-PCR. Shown are the mean values (n=3-5) with standard error of the mean (SEM). A high ct value indicates a low mRNA expression and *vice versa*.

4.2.2 OSM regulates the expression of its own receptors in VSMCs

In order to find out if OSM is able to regulate the expression of the type I receptor complex (LIFRβ/gp130) and the type II receptor complex (OSMRβ/gp130), *wt* VSMCs and *Osmr-/-* VSMCs were stimulated with mOSM for one hour, eight and 24 hours. The mRNA transcription of the genes *Osmr*, *Lifr*, and *Il6st* (Interleukin-6 receptor subunit beta, encoding for the gp130 protein) was analysed by qRT-PCR (Figure 4.5).

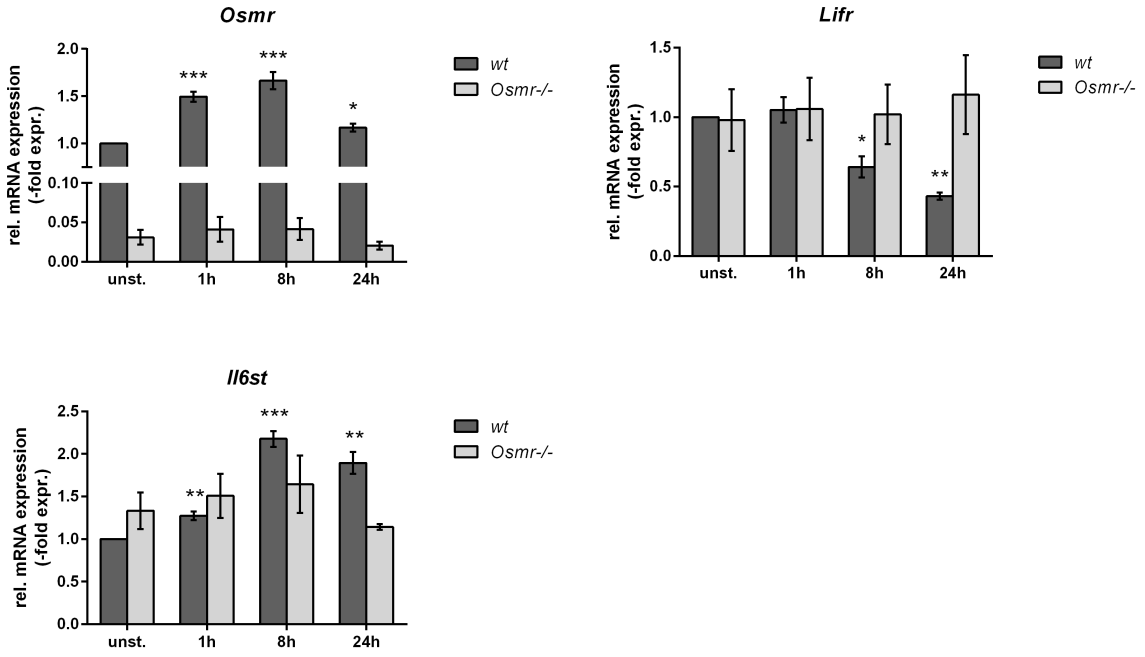

Figure 4.5: **OSM enhances the mRNA expression of *Osmr*, *Lifr* and *Il6st* in VSMCs.** *Wt* and *Osmr-/-* VSMCs were stimulated for 1 hour, 8 and 24 hours with mOSM (10ng/ml). Transcription of *Osmr*, *Lifr* and *Il6st* (encoding for gp130 protein) was analysed by qRT-PCR. Data represent mean-fold changes in mRNA levels normalized to untreated *wt* sample and house-keeping gene *Hprt* (n=3-8) with standard error of the mean (SEM). $^{*}p < 0.05$, $^{**}p < 0.01$, $^{***}p < 0.001$ stimulated vs. unstimulated.

In *wt* VSMCs, *Osmr* and *Il6st* mRNA expression was significantly enhanced whereas the *Lifr* expression decreased about 50% after OSM stimulation for 24 hours. This indicates that OSM regulates its own receptor expression on mRNA level. Furthermore, the expression of the type II receptor (OSMRβ/gp130) appears to be transiently enhanced, while the expression of the type I receptor (LIFR/gp130) remains unchanged at early times and is even downregulated upon prolonged exposure of the cells to OSM.

As expected, in *Osmr-/-* VSMCs, only traces of *Osmr* were detectable. *Lifr* was expressed in *Osmr-/-* VSMCs but remained on basal level even after OSM stimulation. Additionally, the mRNA amount of *Lifr* was equal in *wt* VSMCs and *Osmr-/-* VSMCs. This suggests that the loss of OSMR in knock-out cells was not compensated by a higher LIFR expression. *Il6st* was slightly (1.3-1.5-fold) but not significantly stronger expressed in *Osmr-/-* VSMCs than in *wt* VSMCs and remained at this level even after OSM stimulation.

Western Blot analyses were carried out to determine the expression level of all three OSM receptors on protein level. Therefore, *wt* VSMCs and *Osmr-/-* VSMCs were stimulated for 30 minutes, two, five and 24 hours with mOSM (Figure 4.6 A and B). In *wt* VSMCs, the protein amount of OSMR remained almost unaltered with a slight but significant decrease after 24 hours of mOSM stimulation. It was verfied that the OSMR was not expressed in *Osmr-/-* VSMCs despite the traces of mRNA detected by qPCR. In *wt* VSMCs, gp130 was expressed stronger after five up to 24 hours of mOSM stimulation. Furthermore, gp130 was expressed stronger in *Osmr-/-* VSMCs than in *wt* VSMCs but unaltered after mOSM stimulation. The same effect could be seen on mRNA level as shown in Figure 4.5. According to the mRNA results, the expression of LIFR was weak in *wt* VSMCs. Unlike what was observed on mRNA level, a stronger expression of LIFR was seen in *Osmr-/-* VSMCs. Similar to the mRNA results in Figure 4.5, the protein amount of LIFR was decreased after 24 hours of mOSM stimulation.

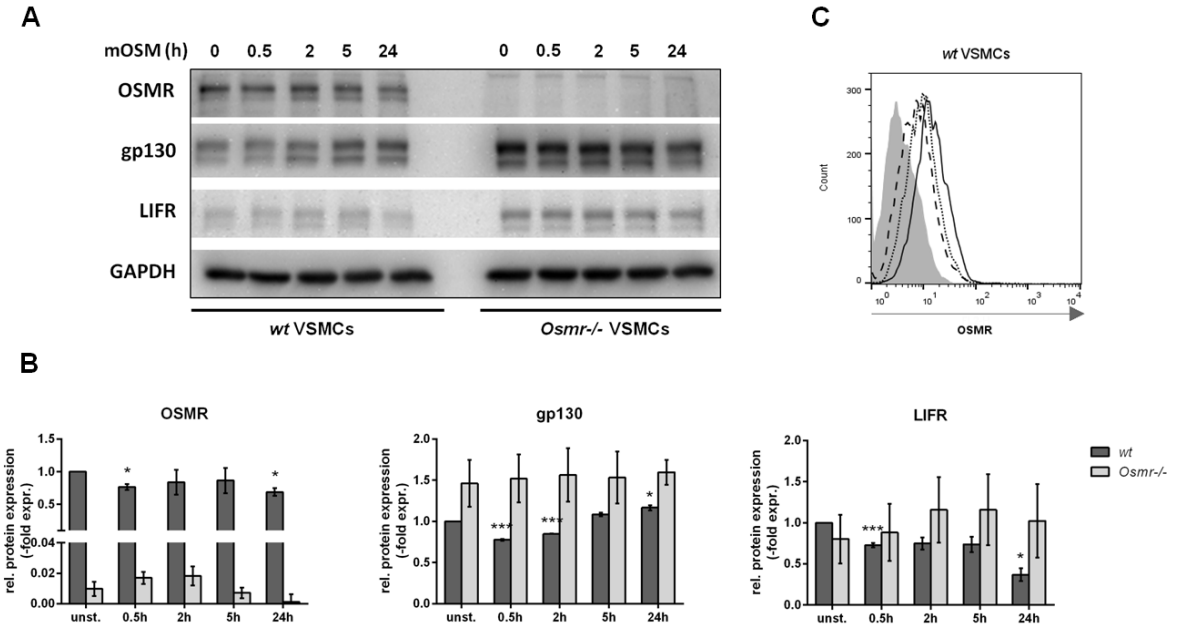

Figure 4.6: **Protein expression of OSMR, gp130 and LIFR after mOSM stimulation. A**, *Wt* and *Osmr-/-* VSMCs were stimulated for 30 minutes, two, five and 24 hours with mOSM (10ng/ml). OSMR, gp130 and LIFR were determined by Western blot analysis. House-keeping protein GAPDH was used as a loading control. One representative out of three independent experiments is shown. **B**, Relative protein expression of OSMR, gp130 and LIFR after Western Blot analysis. Shown are the mean expression levels normalized to the untreated *wt* VSMCs samples with standard error of the mean (SEM). $^{*}p < 0.05$, $^{***}p < 0.001$ stimulated vs. unstimulated. **C**, Cell surface expression of OSMR after FACS analysis in *wt* VSMCs. Cells were stimulated for 2.5 (dotted line) and 20 hours (dashed line) with mOSM (10ng/ml). Expression levels of unstimulated cells are shown as a solid line and isotype control as a grey-filled histogram. One representative out of three independent experiments is shown.

Furthermore, FACS analyses were accomplished in *wt* VSMCs to determine the behaviour of OSMR expression on the cell surface. The cells were stimulated for 2.5 and 20 hours with mOSM (Figure 4.6 C). In contrast to the slight increase of OSMR transcription in *wt* VSMCs in response to mOSM stimulation (Figure 4.5), the amount of OSMR on the cell surface decreased after stimulation for 2.5 hours (dotted line) and 20 hours (dashed line) with mOSM. Earlier studies described an internalisation of OSMR, LIFR and gp130 [176] after ligand binding. This internalisation is mediated by di-leucine motif in the cytoplasmatic region of gp130 and the LIFR [177, 178, 179]. Therefore, in this experiment, it is likely that mOSM induces the internalisation of OSMR in VSMCs.

The LIFR cell surface expression could not be analysed, because no specific antibody for FACS analysis was available throughout the time period of this thesis.

Taken together, mOSM is able to regulate the mRNA and protein expression of OSMR, LIFR and gp130 in VSMCs. Additionally, LIFR seems to be less involved in mOSM signalling than OSMR.

4.2.3 Analysis of OSM-activated signalling pathways in VSMCs

OSM, as a pleiotropic cytokine, is able to activate several signalling pathways in different cell types. Therefore, *wt* and *Osmr-/-* cells were stimulated for 30 minutes, two, eight and 24 hours with mOSM to determine the signalling cascade in VSMCs. Cell lysis was described under subsection 3.4.1. The phosphorylation status of the transcription factors STAT1, STAT3 and STAT6, the mitogen-activated protein kinases (MAPK) ERK1/2 and p38 as well as the serine/threonine kinase PKB/Akt was detected via Western blot analysis (Figure 4.7).

The murine OSM induced phosphorylation of all mentioned proteins in *wt* VSMCs. The tyrosine phosphorylation of STAT3 (Y705) persisted for 24 hours. The tyrosine phosphorylation of STAT1 (Y701) showed its maximum at 30 minutes, but was still detectable at five hours after stimulation. The tyrosine phosphorylation of STAT6 (Y641), threonine/tyrosine phosphorylation of ERK1/2 (T202/Y204) and p38 (T180/Y182) as well as serine phosphorylation of PKB/Akt (S473) were only detectable for 30 minutes. No phosphorylation could be seen in *Osmr-/-* VSMCs. Nevertheless, a slight increase in the basal phosphorylation was detectable for all proteins except of STAT6 in *Osmr-/-* VSMCs compared to *wt* VSMCs (Figure 4.7).

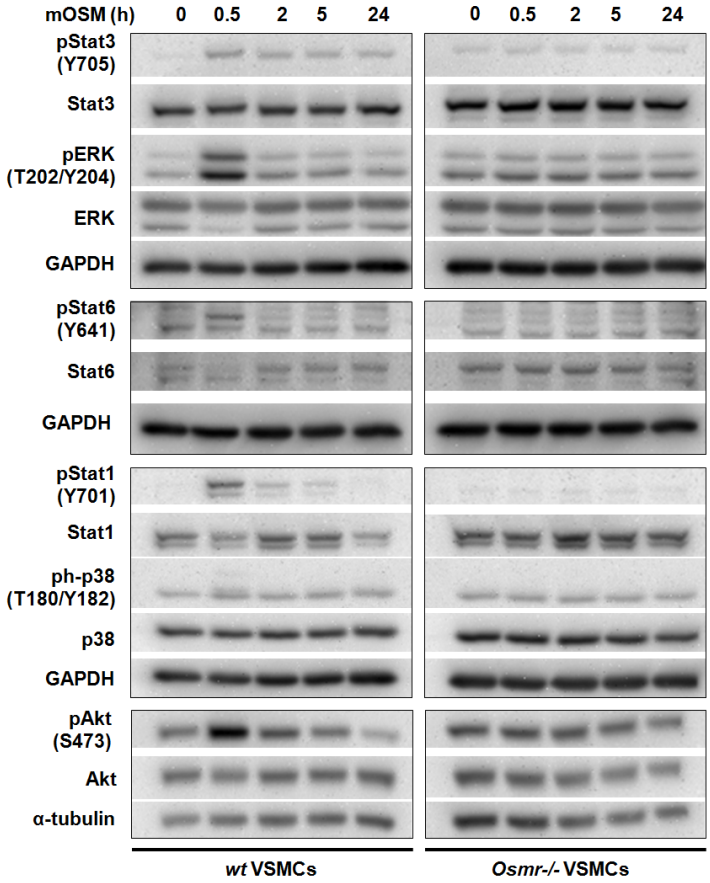

Figure 4.7: **OSM induces the activation of the JAK/STAT, MAPK and PI3K pathway in VSMCs.** *Wt* and *Osmr-/-* VSMCs were stimulated for 30 minutes, two, five and 24 hours with mOSM (10ng/ml). Specific antibodies against the described activatory phosphorylation site of STAT1, STAT3, STAT6, ERK, p38 and Akt as well as against the total proteins were used. House-keeping proteins GAPDH and α- tubulin were used as loading controls. One representative out of three independent experiments is shown.

4.3 Atherosclerotic target gene expression regulated by OSM in VSMCs

Earlier studies already described the expression of OSM in atherosclerotic lesions from human carotid plaques [15]. However, the function of OSM remained elusive. As seen before, VSMC express high mRNA and protein levels of gp130 and the OSMRβ (Figure 4.5 and 4.6), in contrast to immune cells. Furthermore, these tissue cells are well known to contribute to atherosclerotic plaque development. We therefore carried out RT^2 Profiler PCR™ Array analyses in VSMC to investigate the influence of OSM on genes involved in atherogenesis.

4.3.1 Identification of atherosclerotic target genes by PCR array

To identify possible atherosclerotic target genes regulated by OSM in VSMCs, an RT^2 Profiler PCR™ Array analysis (QIAGEN/SABiosciences) was performed. It is designed to analyse a panel of genes related to the investigated disease state, for example genes involved in the processes of blood coagulation and circulation, in cell-adhesion, and in lipid transport and metabolism. Genes involved in stress response, cell growth and proliferation, and apoptosis are represented as well. This array contains primer assays for 84 mouse genes related to atherosclerosis, spotted in four replicates on a 384 well plate (4x96). The remaining wells contain several controls verifying a successful and valid PCR run. They include five house-keeping genes, three reverse transcription controls, three positive PCR controls and one control for mouse genomic DNA contamination also spotted in four replicates.

Two 384 well plates were used, one for untreated vs. two hours of OSM treatment (as technical replicates, data not shown) and one for untreated vs. 24 hours of OSM treatment (Figure 4.8). 14 genes were up-regulated and four genes were down-regulated (black arrows) by OSM, each of them more than four fold.
For further experiments, we focused on ten atherosclerotic target genes for which expression levels were determined by classical real-time PCR. One group contains genes involved in regulation and composition of extracellular matrix (ECM) and cell adhesion. The other group includes genes involved in immune response.

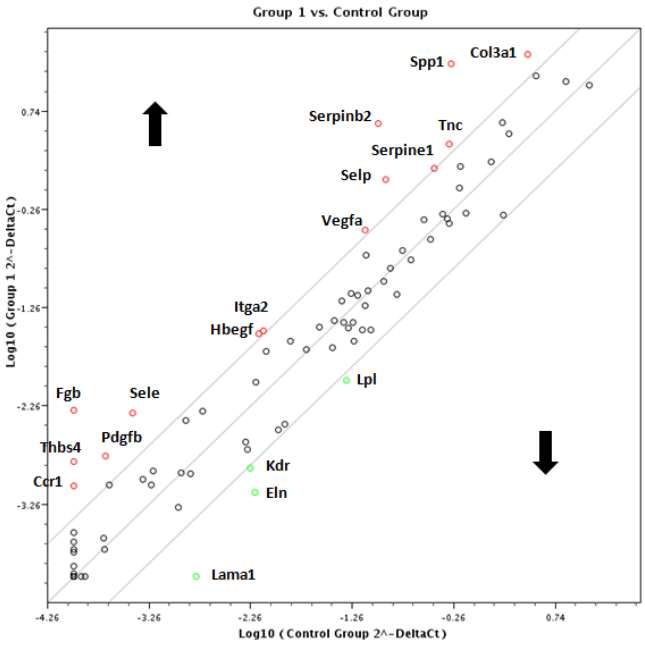

Figure 4.8: **RT² Profiler PCR™ Array analysis of 84 genes involved in atherosclerosis in VSMCs.** *Wt* VSMCs were stimulated with mOSM (10ng/ml) for 24 hours or remained untreated. Total RNA was reverse transcribed and selected target genes analysed by qRT-PCR. Only target genes regulated more than 4-fold upon OSM treatment are marked, indicated by the outer grey lines. Red circles: up-regulated target genes, green circles: down-regulated target genes.

Group 1:

Elastin is an extracellular matrix (ECM) protein secreted by VSMCs in the arterial media, and contributes up to 50% of the vessel's dry weight [180]. Elastin is expressed as a soluble monomer, called tropoelastin [180, 181]. This monomer is modified post-translationally and cross-linked by lysyl oxidase followed by organisation into elastin polymers that form concentric rings of elastic lamellae around the arterial lumen [180]. Each elastic lamella alternates with a ring of smooth muscle cells forming a lamellar unit, considered the functional and structural unit of the arterial wall [180, 182]. Collagen type I and III are also major components of the vessels wall and are situated as an interlamellar matrix between the elastic fibers and smooth muscle cells providing tensile strength [183, 184]. They belong to the fibrillar collagen family and are composed of a triple helix of three polypeptide α chains, each with a Gly-X-Y (X and Y representing any amino acid) repeating sequence [184, 185, 186, 187]. Elastin and collagens ensure

flexibility and stability of the vessels to withstand the normal blood pressure. Besides collagen type III (collagen 3 alpha 1, *Col3a1*) included in the RT^2 Profiler PCR™ Array, genes encoding for collagen type I (collagen 1 alpha 1, *Col1a1*, and collagen 1 alpha 2, *Col1a2*) were chosen for PCR analysis.

The glycoprotein thrombospondin-4 (*Thbs4*) is one of five members of the Thbs family (Thbs-1 to Thbs-5) and is secreted as an ECM protein [188]. These proteins have many physiological roles including activities in wound healing and angiogenesis, vessel wall biology, and connective tissue organisation [188]. The pentameric structure of Thbs-4 binds to the extracellular matrix and regulates cell-to-cell and cell-to-matrix interactions [189]. Furthermore, Thbs-4 is expressed and secreted by VSMCs and endothelial cells of large blood vessels and in capillaries [190]. Its mRNA expression is limited to heart, brain, and skin of adults [191]. Multiple reports have documented a genetic association between Thbs-4 and accelerated atherogenesis [192, 193, 194, 195]. In addition, Thbs4 deficient mice show a reduction in the development and inflammation of atherosclerotic lesions [196].

Tenascin C (*Tnc*) is a large extracellular matrix glycoprotein and was the first member identified of a family of four structurally similar proteins [197]. TnC plays an important role in myocardial and vascular remodelling and it is a marker of progressive destabilization of the aortic wall [198]. The TnC polypeptide contains a number of different domains: tenascin assembly domain (TA), epidermal growth factor-like domains, fibronectin type III (FN III) domains and a fibrinogen-homology domain. Through alternative splicing, a number of various isoforms exist which contain one to six extra FN III domains [197, 199]. These isoforms of TnC appear to have a number of pathophysiological effects [197]. In this study primer sets were used to amplify *Tnc* mRNA which detects the variable spliced A to D FN III repeats (exactly AD2 to C). This region is known to bind to annexin II localized to the extracellular leaflet of the plasma membrane, whereby cell adhesion is inhibited [197, 199].

Osteopontin (OPN) - encoded by gene *Spp1* - is a glycoprotein which has been found in atherosclerotic arteries and its elevated serum levels are associated with vascular calcifications [200]. When OPN is phosphorylated, it acts as a calcification inhibitor in VSMCs [201, 202]. In contrast, cleaved OPN acts as a pro-inflammatory cytokine facilitating vascular mineralization [201, 203, 204]. Several studies confirmed, that OPN is involved in diseases related to inflammation such as atherosclerosis, obesity and autoimmune diseases [203, 205, 206, 207].

Osteoprotegerin (OPG), encoded by gene *Tnfrsf11b*, was initially described as a decoy receptor for RANKL (receptor activator of NFκB ligand). However, further studies reveal that this glycoprotein is involved in vascular, bone, immune and tumour biology as well [208]. Moreover, OPG is considered as a protective factor against vascular calcification by blocking the bone remodelling process in the tissue [201]. Therefore, OPG was chosen for further analysis even though it was not one of the 84 target genes included in the RT^2 Profiler PCR™ Array.

Group 2:

SerpinB2 (Serine peptidase inhibitor, clade B, member 2, gene: *Serpinb2*) also known as PAI-2 (Plasminogen activator inhibitor-2) belongs to the clade B family of serine protease inhibitors and is one of the most up-regulated proteins following cellular stress [209]. It is expressed in several cell types, e.g. in monocytes/macrophages, fibroblasts, and endothelial cells after inflammation, infection or injury [209]. However, SerpinB2 can also be found in smooth muscle cells [210, 211, 212]. The principle role of SerpinB2 is the inhibition of urokinase plasminogen activator (uPA) and tissue plasminogen activator (tPA). Nevertheless, the majority of SerpinB2 is not secreted since intracellular binding partners have been found (reviewed in [213]). Therefore, its function inside the cell needs further investigations.

CCR1 (C-C chemokine receptor type 1, gene: (*Ccr1*) acts as receptor for the chemokines CCL3/MIP-1α, CCL4/MIP-1β, CCL5/RANTES [214, 215]. All chemokine receptors belong to the superfamily of G protein-coupled receptors. They were initially thought to be expressed in monocytes and T lymphocytes to allow their transendothelial migration. However, it is known now that various chemokine receptors are present on different cells leading to selective chemokine function [216, 217]. They have been shown to be secreted from VSMCs where they play an important role in the proliferation and migration of VSMCs from the media to the intima [218].

4.3.2 Regulation of atherosclerotic target gene expression by OSM

After performing the RT^2 Profiler PCR™ Array analyses, the results for the target genes *Col1a1*, *Col1a2*, *Col3a1*, *Eln*, *Tnfrsf11b*, *Spp1*, *Thbs4*, and *Tnc* (group 1) as well as for *Ccr1* and *Serpinb2* (group 2) had to be confirmed by qRT-PCR. Therefore, primer sets for these ten genes were designed and the qRT-PCR of cDNA reverse transcribed from

RNA obtained from mOSM stimulated *wt* and *Osmr-/-* VSMCs. The qRT-PCR was performed as described in subsection 3.4.2 and the results are depicted in Figure 4.9 and 4.10.
Col1a1 and *Col1a2* mRNA expression was slightly decreased after mOSM stimulation. In contrast to *Col1a2*, this effect on the *Col1a1* transcription did not persist for long, since after 24 hours of mOSM treatment, the mRNA amount of *Col1a1* returned back to its basal level. While the mRNA expression of *Col1a1* and *Col1a2* was decreased, the *Col3a1* mRNA, however, was increased significantly after mOSM stimulation. Furthermore, *Eln* was down-regulated by mOSM as well. Its mRNA amount diminished stronger than *Col1a1* or *Col1a2* with a loss of about 50% after eight hours and persisted at least 24 hours upon mOSM stimulation. All other genes of group 1, *Tnfrsf11b*, *Spp1*, *Thbs4*, and *Tnc* showed an increase of mRNA expression in *wt* VSMCs. The mRNA of *Thbs4* was enhanced continuously by mOSM stimulation with a maximum of a 150-fold up-regulation at 24 hours. Thus, out of the genes analysed, *Thbs4* was regulated strongest by this IL-6-type cytokine. The mRNA levels of *Spp1* [1] and *Tnc* showed their maximum regulation at 24 hours of mOSM stimulation. *Tnfrsf11b* [2] was increased transiently with its maximum at five hours of mOSM stimulation (Figure 4.9).
The mRNA levels of the genes *Ccr1* and *Serpinb2* (group 2), which both are involved in immune response, were increased transiently in response to mOSM. Thereby, the *Ccr1* mRNA amount reached its maximum at five hours and the mRNA of *Serpinb2* at eight hours of mOSM stimulation. After its maximum transcription, the *Ccr1* mRNA amount reached a plateau five-fold above the basal level (Figure 4.10).
Moreover, the use of *Osmr-/-* VSMCs showed clearly that none of these examined genes was regulated by mOSM in the absence of OSMR expression.

For the analysis of *Eln* expression by qRT-PCR, an additional note has to be made. VSMCs in cell culture do express elastin. However, immediately after harvesting or passaging (16 to 24 hours after seeding), *Eln* mRNA was not detectable in VSMCs indicated by high ct values (30 or more). However, 48 to 72 hours after cell seeding, substantial amounts of *Eln* mRNA could be measured again (ct value of about 26 $\pm$ 1) after reproducing. Thus, for experimental analyses of the *Eln* mRNA expression, VSMCs were kept in culture for at least two days before treatment and harvesting of the cells started (data not shown).

[1] protein name: Osteopontin (OPN)
[2] protein name: Osteoprotegerin (OPG)

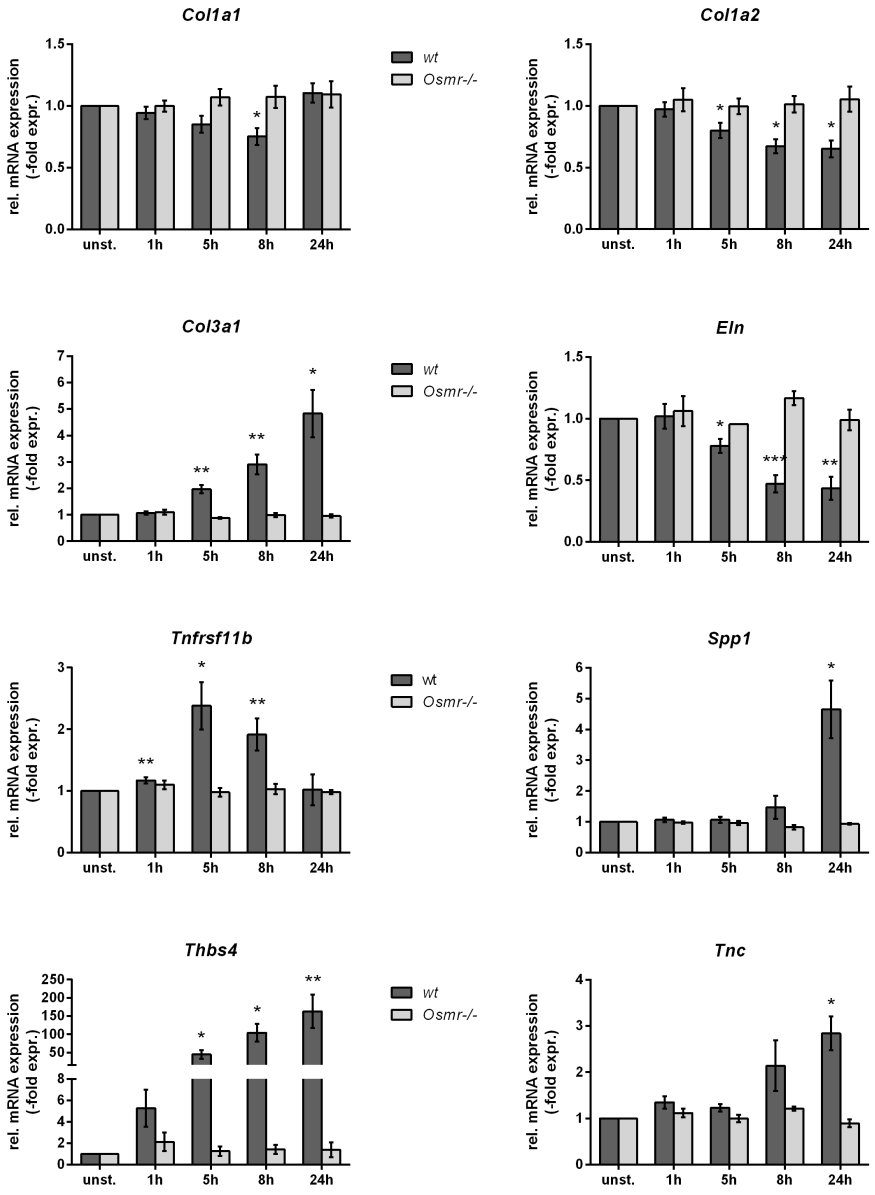

Figure 4.9: **Changes in mRNA expression levels of atherosclerotic target genes involved in the regulation and composition of ECM in response to OSM.** *Wt* and *Osmr-/-* VSMCs were treated for one hour, five, eight and 24 hours with mOSM (10ng/ml). Transcription of *Col1a1*, *Col1a2*, *Col3a1*, *Eln*, *Tnfrsf11b*, *Spp1*, *Thbs4* and *Tnc* were analysed by qRT-PCR. Data represent mean-fold changes in mRNA levels normalized to untreated *wt* or *Osmr-/-* VSMCs, and house-keeping gene *Hprt* (n=3-9) with standard error of the mean (SEM). $*p < 0.05$, $**p < 0.01$, $***p < 0.001$ stimulated vs. unstimulated VSMCs.

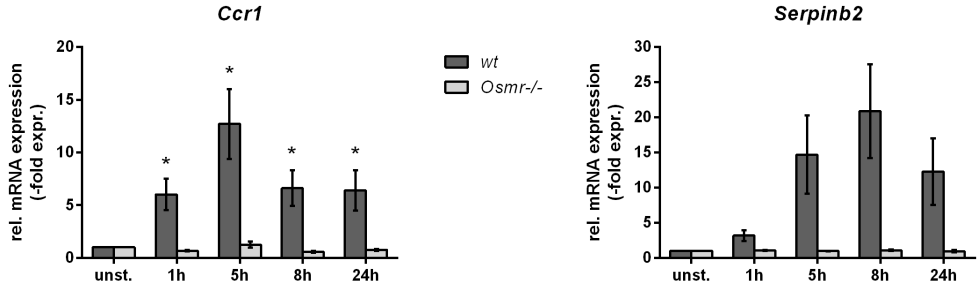

Figure 4.10: **Changes in mRNA expression levels of atherosclerotic target genes involved in innate and adaptive immunity in response to OSM.** *Wt* and *Osmr-/-* VSMCs were treated for one hour, five, eight and 24 hours with mOSM (10ng/ml). Transcription of *Ccr1* and *Serpinb2* were analysed by qRT-PCR. Data represent mean-fold changes in mRNA levels normalized to untreated *wt* or *Osmr-/-* VSMCs and house-keeping gene *Hprt* (n=3-9) with standard error of the mean (SEM). $*p < 0.05$ stimulated vs. unstimulated VSMCs.

Unfortunately, the investigation of these genes regarding their protein levels has proved difficult. In this thesis, several commercially available antibodies were tested, but turned out to be unspecific with the exception of antibodies for CCR1 by flow cytometry. Therefore, FACS analyses were performed to determine the cell surface expression of CCR1 on *wt* VSMCs stimulated with mOSM (10ng/ml) for 2.5 (dotted lines) and 20 hours (dashed lines). Unstimulated cells (solid lines) and the isotype control (grey-filled histograms) were included (Figure 4.11).

Within the VSMC culture, two cell populations expressing low levels and high levels of CCR1 exist and can be identified by two peaks in the histogram. Upon OSM stimulation of *wt* VSMCs, the mean fluorescence was strongly increased indicating that CCR1 is up-regulated (Figure 4.11). One possible reason for detecting two cell populations expressing CCR1 in distinct amounts could be found in the publication by Shimizu et al. [217]. There, VSMCs were isolated from the intima and from the media layer and FACS analysis of CCR1 showed different expression pattern in the histogram. The method used for VSMCs isolation in this thesis did not distinguish between VSMCs from intima or media and therefore, both VSMC populations appear to be present in FACS analyses performed here.

Besides OSM, other IL-6 type cytokines like leukaemia inhibitory factor (LIF) and interleukin-6 (IL-6) were tested for the involvement in atherosclerotic target gene ex-

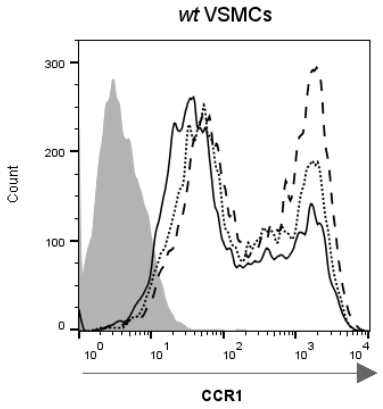

Figure 4.11: **OSM regulates the cell surface expression of CCR1 on VSMCs.** Cell surface expression of CCR1 was determined by FACS analysis. *Wt* VSMCs were stimulated with mOSM (10ng/ml) for 2.5 hours (dotted line) and 20 hours (dashed line). Expression levels of unstimulated cells are shown as solid lines and isotype control as a grey-filled histogram. One representative out of three independent experiments is shown.

pression on mRNA level (Figure 1.1). After binding of IL-6 to non-signalling IL-6Rα, the ligand-receptor-complex binds to the signal transducing receptor gp130. Recruiting and binding of another gp130 molecule results in a hexameric complex composed of two gp130, two IL-6Rα, and two IL-6 molecules [219, 220, 221, 222, 223]. VSMCs naturally do not express the membrane bound IL-6 receptor (IL-6Rα). To stimulate these cells, different possibilities exist: First, stimulation with IL-6 and soluble IL-6R (sIL-6R). Thereby, the transmembrane and cytoplasmic parts of sIL-6R is missing [224, 225]. However, binding of IL-6/sIL-6R complex to gp130 and the following signal transduction is unaffected. A second possibility would be the stimulation with hyperIL-6 which was designed by Fischer and Rose-John *et al.* [226]. HyperIL-6 is a fusion protein consisting sIL-6R covalently linked to IL-6. This complex can also bind to gp130 and activate signalling pathways but generally stronger than IL-6 and sIL-6R alone. IL-6/sIL-6R, hyperIL-6, and additionally LIF were tested on VSMCs but in contrast to OSM, none of the ten target genes was regulated (data not shown).

4.3.3 OSM-mediated signalling pathways involved in atherosclerotic target gene expression in VSMCs

The previous subsections described the role of OSM as a strong activator of the JAK/STAT, Ras-Raf-MAPK, and PI3K/Akt pathways in VSMCs (Figure 4.7). Additionally, OSM regulates the mRNA expression of target genes involved in the regulation and composition of ECM (Figure 4.9) and in the innate and adaptive immunity (4.10). In order to identify whether MAPK signalling pathways might be involved in the OSM-regulated transcription of these target genes, *wt* VSMCs were treated with MEK inhibitor III (MEK1/2-III) or p38 MAPK inhibitor (SB203580) 30 minutes prior to stimulation with OSM. Figure 4.12 shows the OSM induced phosphorylation status of STAT1 (Y701), STAT3 (Y705), ERK1/2 (T202/Y204), Akt (S473), and MK2 (T334) as well as their total protein amount after pre-incubation with inhibitors. In addition, Figure 4.13 and 4.14 depict the OSM regulated mRNA expression of *Thbs4*, *Ccr1*, *Col3a1*, and *Eln* again after pre-incubation with both inhibitors.

Western blot analyses verified that MEK1/2 inhibition did not influence OSM-mediated activation of STAT1, STAT3 or Akt, while it completely prevented OSM-mediated activation of ERK1/2 (Figure 4.12 A). Inhibition of p38 MAPK activation by pre-treatment with SB203580 for 30 minutes resulted in abrogation of OSM-mediated MK2 phosphorylation (Figure 4.12 B).

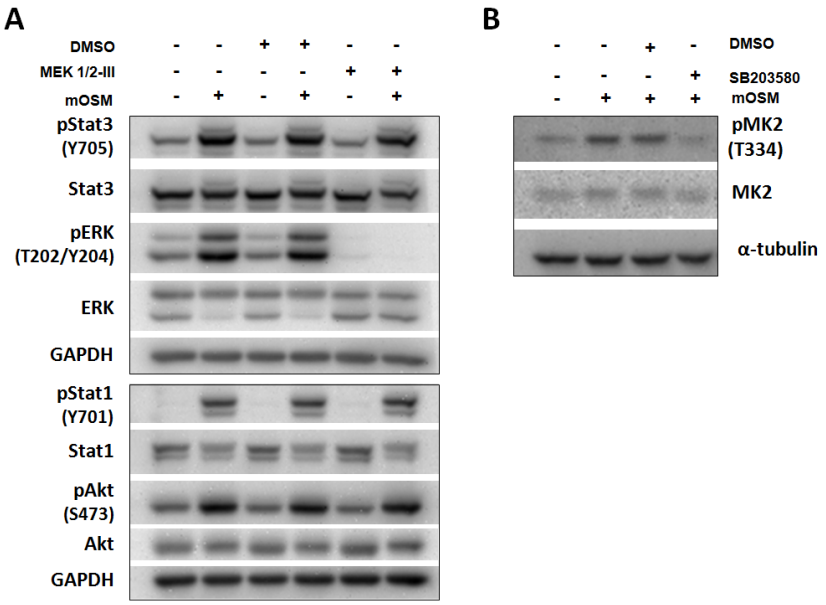

Figure 4.12: **OSM-induced phosphorylation of ERK1/2 and MK2 is abrogated by MEK1/2-III or SB203580 pretreatment, respectively, in VSMCs.** *Wt* VSMCs were left untreated or treated with 1µM MEK 1/2-III (**A**), 5µM SB203580 (**B**) or the solvent DMSO for 30 minutes prior to mOSM stimulation (10ng/ml) for additional 30 minutes. Specific antibodies against the activatory phosphorylation site of STAT1, STAT3, ERK1/2, Akt, and MK2 as well as the total proteins were used for Western blot analysis. House-keeping proteins GAPDH and α tubulin were included as loading controls. One representative out of three (MEK1/2-III) and out of two (SB203580) independent experiments is shown.

Inhibition of ERK1/2 activation by MEK1/2 inhibitor III completely abrogated the OSM-mediated up-regulation of *Thbs4* and *Ccr1* gene expression. Interestingly, this effect was not observed for the expression of *Col3a1* and *Eln*. Basal as well as OSM-stimulated transcription of *Col3a1* increased upon inhibition of MEK1/2 activity, indicating a suppressive activity of this pathway on *Col3a1* expression. Also the slightly enhanced basal and OSM stimulated *Eln* mRNA expression after MEK1/2-III treatment suggests a suppression of ERK1/2 in VSMCs (Figure 4.13).

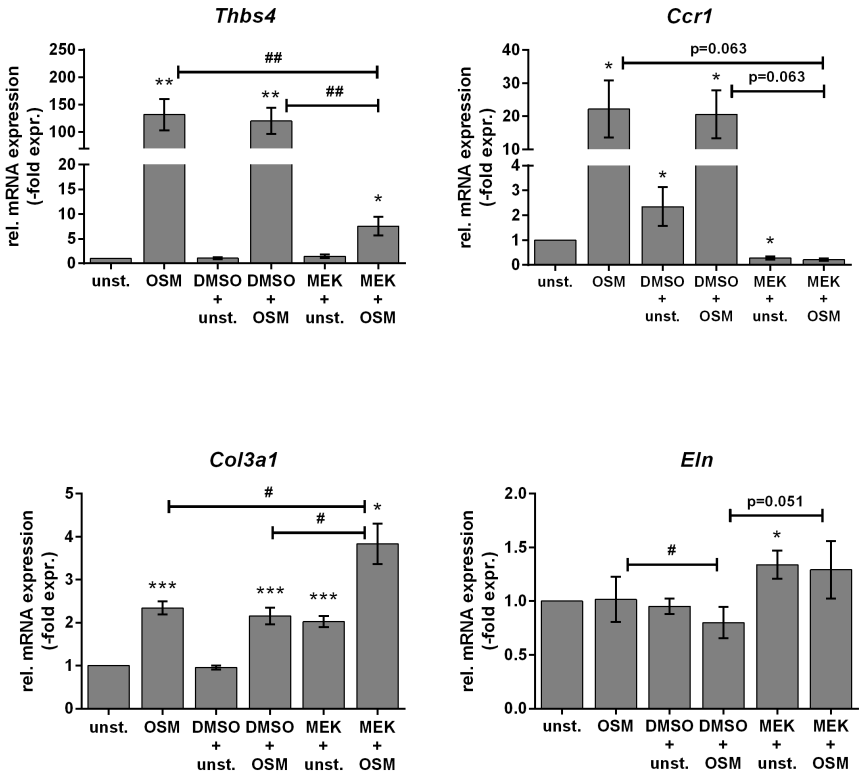

Figure 4.13: **Changes of OSM-induced mRNA expression levels of atherosclerotic target genes after pretreatment with MEK 1/2 inhibitor III.** *Wt* VSMCs were left untreated or treated with 1µM MEK 1/2-III or solvent DMSO for 30 minutes prior to mOSM stimulation (10ng/ml) for additionally five hours. Transcription of *Thbs4*, *Col3a1*, *Ccr1* and *Eln* was analysed by qRT-PCR. Data represent mean-fold changes in mRNA levels normalized to untreated cells and house-keeping gene *Hprt* (n=5-7) with standard error of the mean (SEM). $*p < 0.05$, $**p < 0.01$, $***p < 0.001$ treated vs. unstimulated , $\#p < 0.05$, $\#\#p < 0.01$ OSM vs. MEK+OSM/DMSO+OSM or DMSO+OSM vs. MEK+OSM.

The p38 MAPK inhibitor SB203580 had no or only a marginal effect on basal or OSM-modified *Thbs4* or *Col3a1* expression, while the mRNA amount of *Ccr1* from cells treated with SB+OSM was even higher than with OSM alone (24-fold vs. 16-fold). The OSM-reduced *Eln* mRNA expression, seemed to be not affected by the SB203580 pre-incubation. However, basal transcription decreased upon inhibition of p38 MAPK activity with SB203580 (Figure 4.14).

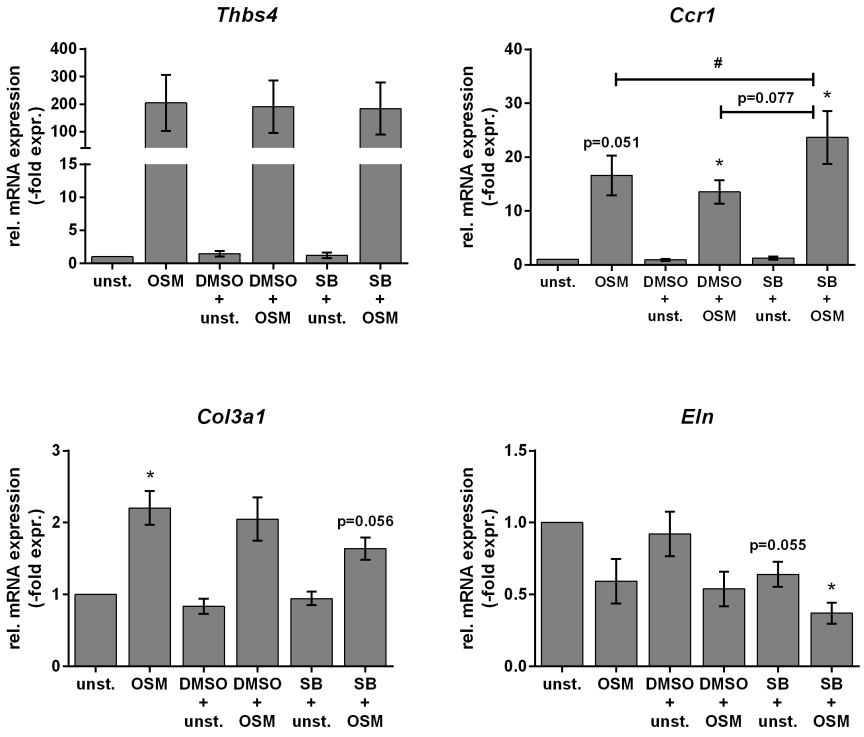

Figure 4.14: **Changes of OSM-induced mRNA expression levels of atherosclerotic target genes after pretreatment with p38 MAPK inhibitor.** *Wt* VSMCs were left untreated or treated with 5µM SB203580 or solvent DMSO for 30 minutes prior to mOSM stimulation (10ng/ml) for additionally five hours. Transcription of *Thbs4*, *Col3a1*, *Ccr1* and *Eln* was analysed by qRT-PCR. Data represent mean-fold changes in mRNA levels normalized to the untreated sample and house-keeping gene *Hprt* (n=3) with standard error of the mean (SEM). $^*p < 0.05$ treated vs. unstimulated , $\#p < 0.05$ OSM vs. SB+OSM.

4.4 Cross-talk between OSM, IL-4 and IL-13

In addition to OSM, many other cytokines and chemokines as well as their receptors play a role in atherosclerosis [227]. They are mainly produced by cells located in atherosclerotic plaques, particularly T cells, monocytes and macrophages. Their functions range from protective to pathogenic. Hofbauer et al. postulate that IL-4 and IL-13, which are produced by Th2 cells and which can be found in aortic plaques, modulate osteoprotegerin (OPG) expression of human coronary artery smooth muscle cells (CASMC) [228]. Furthermore, it has also been shown that other cytokines in combination with IL-4 and IL-13 prime the response of treated cells. For example, pretreatment of fibroblasts with OSM followed by stimulation with IL-4 or IL-13 regulates the synergistic eotaxin-1 response and the expression of the IL-4Rα in a synergistic manner [158]. To study the role of these Th2 cytokines and their crosstalk with OSM in VSMCs, receptor and atherosclerotic target gene expressions were determined after stimulation with OSM, IL-4 and IL-13 as well as after OSM pretreatment followed by stimulation with IL-4 or IL-13 (OSM+IL-4 and OSM+IL-13). Additionally, the signalling pathway used by IL-4 and IL-13 was investigated in VSMCs.

4.4.1 Analysis of the OSM and IL-4/IL-13 receptor expression in VSMCs

It was already shown that OSM regulates the IL-4/IL-13 receptor expression in fibroblasts and in human airway smooth muscle cells (HASMCs) [158, 156]. Therefore, this experiments were recapitulated in murine VSMCs by stimulating with mOSM, mIL-4 or mIL-13 (10ng/ml each) for one hour, five, eight and 24 hours. The gene transcription of the OSM receptor complex type II (*Osmr/Il6st*) and IL-4 receptor complex type II (*Il4r/Il13ra1*) was determined by qRT-PCR (Figure 4.15).

As seen before (subsection 4.2.2), the mRNA expression of *Osmr* and *Il6st* was enhanced 2-fold after mOSM stimulation. Similar to this results, the mRNA expression of *Il4r* and *Il13ra1* appears to be transiently enhanced with a maximum expression for *IL4r* after five hours of mOSM stimulation (about 7-fold) and for *Il13ra1* after eight hours of mOSM stimulation (about 8-fold). IL-4 and IL-13 alone showed no effect on the receptor expression (Figure 4.15).

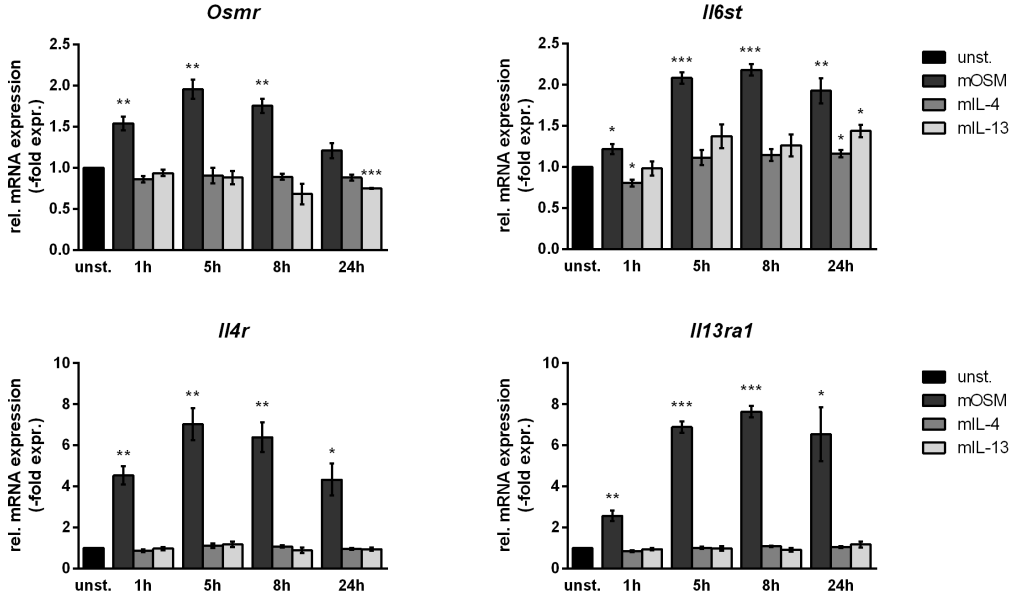

Figure 4.15: **OSM and not IL-4/IL-13 regulates the mRNA expression of OSM receptor complex type II and IL-4/IL-13 receptor complex type II in VSMCs.** *Wt* VSMCs were stimulated with mOSM, mIL-4 and mIL-13 (10ng/ml each) for one hour, five, eight and 24 hours. Transcription of *Osmr, Il6st, Il4r* and *Il13ra1* was analysed by qRT-PCR. Data represent mean-fold changes in mRNA levels normalized to untreated cells and housekeeping gene *Hprt* (n=3-4) with standard error of the mean (SEM). $^{*}p < 0.05$, $^{**}p < 0.01$, $^{***}p < 0.001$ stimulated vs. unstimulated VSMCs.

FACS analyses were carried out to determine the cell surface expression of IL-4R. Therefore, *wt* VSMCs were stimulated with mOSM for 2.5 (dotted line) and 20 hours (dashed line). Expression levels of unstimulated cells are shown as a solid line and isotype control as a grey-filled histogram. Similar results were obtained for Western blot analyses (Data not shown). The IL-4R cell surface expression was enhanced in response to OSM treatment (Figure 4.16).
The IL-13Rα1 protein expression level could not be analysed, because no specific antibody for Western blot and FACS analysis was available within the time frame of this thesis.

Taken together, mOSM does not only regulate its own receptor complex expression in VSMCs but also receptor subunits used by IL-4. However, both cytokines - IL-4 and IL-13 - are not involved in this regulation process.

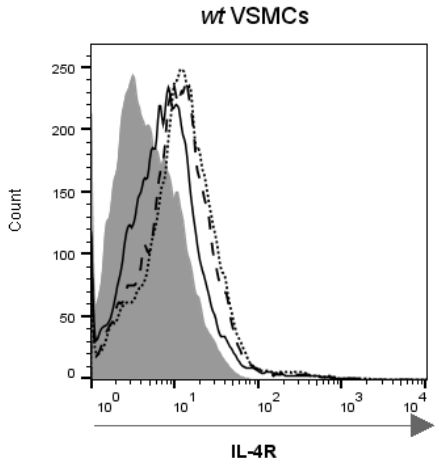

Figure 4.16: **OSM regulates the cell surface expression of IL-4R in VSMCs.** Cell surface expression of IL-4R in *wt* VSMCs was determined by FACS analysis. VSMCs were stimulated with mOSM (10ng/ml) for 2.5 (dotted line) and 20 hours (dashed line). Expression levels of unstimulated cells are shown as a solid line and isotype control as a grey-filled histogram. One representative out of three independent experiments is shown.

4.4.2 Regulation of atherosclerotic target gene expression by OSM, IL-4 and IL-13

To investigate the effect of OSM, IL-4 and IL-13 treatment on atherosclerotic target genes, mRNA expression of Collagen3α1 (*Col3a1*), elastin (*Eln*) and Osteoprotegerin (*Tnfrsf11b*) was analysed. These genes are known to be involved in atherosclerosis and are regulated by mOSM in VSMCs (subsection 4.3.1 and 4.3.2).

VSMCs isolated from wild-type mice were stimulated with mOSM, mIL-4, mIL-13, mOSM+mIL-4 and mOSM+mIL-13 (10ng/ml each) for one hour, five, eight and 24 hours. *Col3a1*, *Eln* and *Tnfrsf11b* mRNA levels were determined by qRT-PCR (Figure 4.17).

As seen before in subsection 4.3.2, the mRNA level of *Col3a1* was significantly increased over time, *Eln* was decreased and *Tnfrsf11b* showed a maximum expression after five hours of mOSM stimulation. Both Th2 cytokines, mIL-4 and mIL-13, had little or no effect on mRNA expression of atherosclerotic target genes when compared to mOSM. The mRNA of *Tnfrsf11b* was not regulated by mIL-4 or mIL-13, whereas the mRNA

expression of *Col3a1* showed a small but significant increase after 24 hours of mIL-4 and mIL-13 stimulation (about 2-fold). The mRNA expression of *Eln* was actually decreased about 50% compared to basal level after 24 hours of mIL-13 stimulation. A synergistic or additive effect on the transcription of *Col3a1*, *Eln* and *Tnfrsf11b* could not be seen when VSMCs were treated with mOSM+mIL-4 or mOSM+mIL-13 (Figure 4.17).

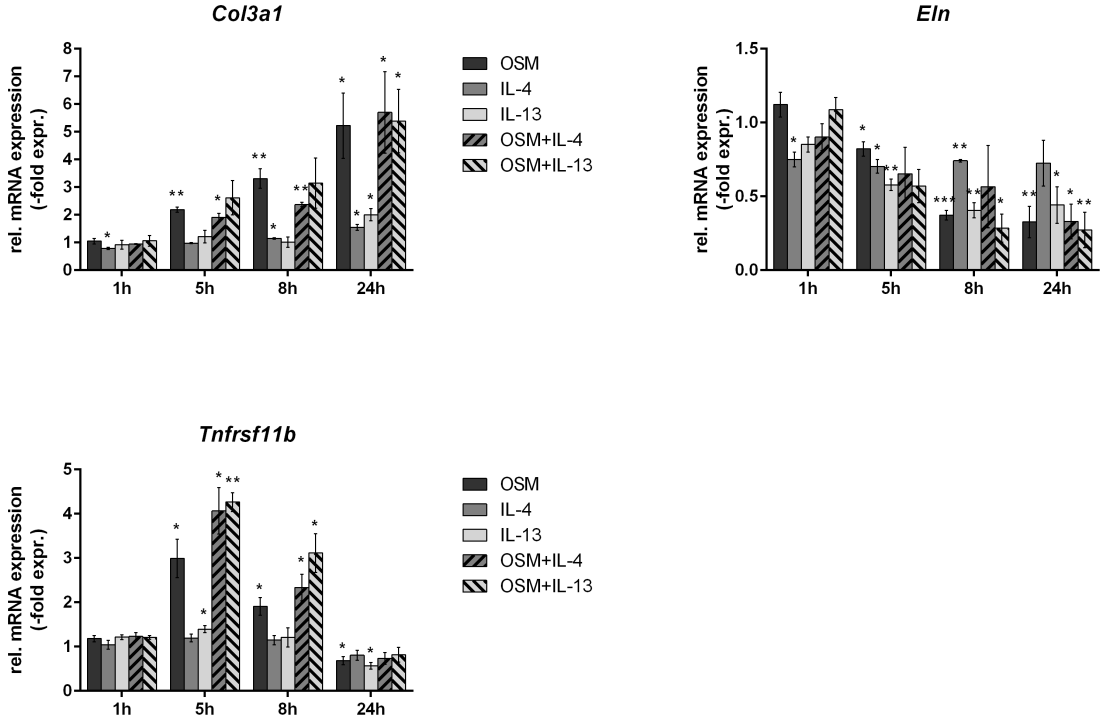

Figure 4.17: **Changes in mRNA expression levels of the atherosclerotic target genes *Col3a1*, *Tnfrsf11b*, and *Eln* in VSMCs in response to OSM, IL-4 and IL-13.** *Wt* VSMCs were stimulated with mOSM, mIL-4, mIL-13, mOSM+mIL-4 or mOSM+mIL-13 (10ng/ml each) for one hour, five, eight and 24 hours. Transcription of *Col3a1*, *Tnfrsf11b* and *Eln* was analysed by qRT-PCR. Data represent mean-fold changes in mRNA levels normalized to untreated cells (not shown) and house-keeping gene *Hprt* (n=3-4) with standard error of the mean (SEM). $^{*}p < 0.05$, $^{**}p < 0.01$, $^{***}p < 0.001$ stimulated vs. unstimulated VSMCs.

4.4.3 Analysis of IL-4/IL-13-activated signalling pathway in VSMCs

In order to find out which signalling pathways were activated, *wt* VSMCs were stimulated with mIL-4, mIL-13 and as a control with mOSM (10ng/ml each) for five, 15, 20 and 30 minutes. Cell lysis was described in subsection 3.4.1. The phosphorylation status of the transcription factors STAT3 (Y705) and STAT6 (Y641) and the mitogen-activated protein kinases (MAPK) ERK1/2 (T202/Y204) and p38 (T180/Y182) were detected via Western blot analysis (Figure 4.18).
Subsection 4.2.3 describes the phosphorylation status of JAK/STAT, Ras-Raf-MAPK and PI3K pathway induced by OSM in *wt* VSMCs. STAT1 was phosphorylated at Y701, STAT3 at Y705 and STAT6 at Y641. Additionally, ERK1/2 was activated through phosphorylation at T202/Y204, p38 at T180/Y182 and Akt at S473. However, Figure 4.18 shows clearly that mIL-4 and mIL-13 were only responsible for the phosphorylation of STAT6 at Y641. No other tested signalling pathways was activated by either IL-4 or IL-13 in *wt* VSMCs.

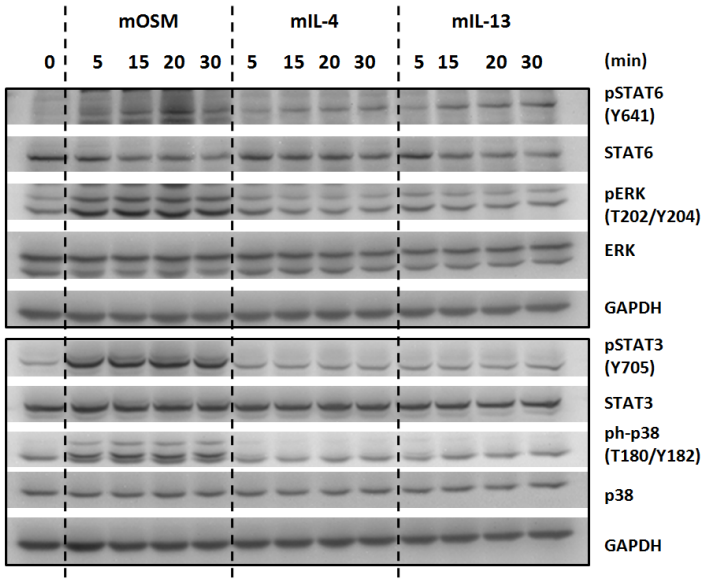

Figure 4.18: **Signalling pathways activated by OSM, IL-4 and IL-13 in VSMCs.** *Wt* VSMCs were stimulated with mOSM, mIL-4 and mIL-13 (10ng/ml each) for five, 15, 20 and 30 minutes. Whole cellular extracts were separated by SDS-Page and specific antibodies against the activatory phosphorylation sites of STAT3, STAT6, ERK and p38 as well as against total proteins were used for Western blot analyses. House-keeping protein GAPDH was used as a loading control. One representative out of two independent experiments is shown.

Fritz et al. postulated that the IL-4 or IL-13 induced STAT6 phosphorylation was enhanced when fibroblasts (NIH3T3) were primed with OSM [158]. To investigate if this effect could also be observed in VSMCs, the experiment was carried out as as described by Fritz et al [158] (Figure 4.19). VSMCs isolated from wild-type mice were pretreated with mOSM (10ng/ml) for 2.5 or six hours. Afterwards, the cells were stimulated with mIL-4 (Figure 4.19 A) or mIL-13 (Figure 4.19 B) in two different suboptimal concentrations (1ng/ml or 2.5ng/ml) for 15 minutes in the presence of the initially applied mOSM. As controls, *wt* VSMCs were either left unstimulated or stimulated with mOSM (10ng/ml), mIL-4 and mIL-13 (1ng/ml or 2.5ng/ml) for 15 minutes without priming.

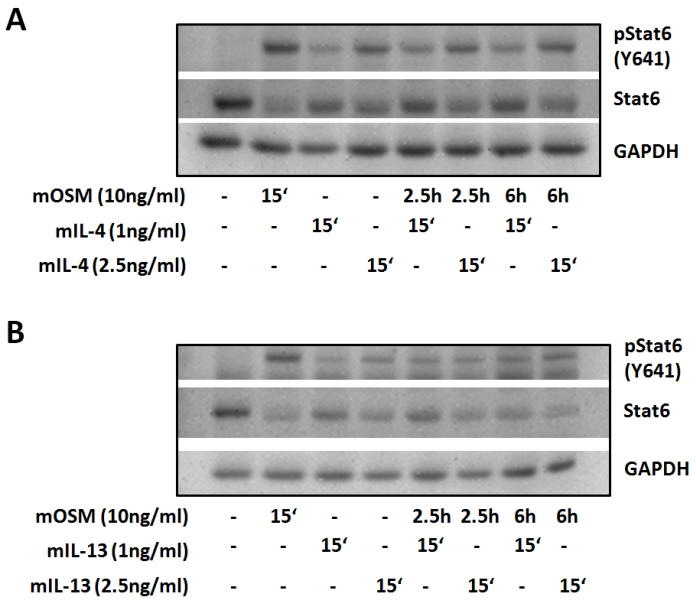

Figure 4.19: **STAT6 phosphorylation induced by IL-4 or IL-13 is not enhanced after priming with OSM in VSMCs.** *Wt* VSMCs were primed with mOSM (10ng/ml) for 2.5 or six hours followed by stimulation with mIL-4 (**A**) and mIL-13 (**B**) for 15 minutes (1ng/ml and 2.5ng/ml) in the presence of the initially applied mOSM. Unstimulated cells and cells stimulated with mOSM, mIL-4 and mIL-13 for 15 minutes without a priming were used as control samples. Specific antibodies against the activatory phosphorylation site of STAT6 as well as against total protein were used for Western blot analyses. House-keeping protein GAPDH was used as a loading control. One representative out of three independent experiments is shown.

All three cytokines induced the tyrosine phosphorylation of STAT6 (Y641) after 15 minutes. In contrast to the results obtained in fibroblasts, the IL-4 or IL-13 mediated STAT6 phosphorylation could not be further enhanced by mIL-4 or mIL-13 stimulation after priming VSMCs with mOSM.

4.4.4 Regulation of the decoy receptor expression by OSM, IL-4 and IL-13

One possible reason for the missing enhanced STAT6 phosphorylation after priming VSMCs with OSM could be that the signalling is negatively regulated over time. In addition to the IL-4R/IL-13Rα1 complex another receptor exists on the cell surface of VSMCs called IL-13Rα2. This receptor is known as a decoy receptor for IL-13 signalling and serves as a target gene of IL-13 as well [165]. When *Il13ra2* is transcribed and transported to the cell surface, it can function as a negative feedback mechanism for IL-13. In order to identify if OSM, IL-4 or IL-13 influence the expression of IL-13Rα2, VSMCs were stimulated with mOSM, mIL-4, mIL-13, mOSM+mIL-4 and mOSM+mIL-13 for one hour, five, eight and 24 hours (10ng/ml each) (Figure 4.20).

The amount of *Il13ra2* was increased continuously after stimulation with all three cytokines. The strongest increase, however, occured after treatment with IL-13 for 24 hours (10-fold upregulated). This effect could be further enhanced when the cells additionally were co-stimulated with OSM and IL-4 or IL-13 (mOSM+mIL-4 or mOSM+mIL-13) (Figure 4.20).
Protein levels of IL-13Rα2 could not be analysed, because no specific antibody for FACS or Western Blot analysis was available within the time frame of this thesis.

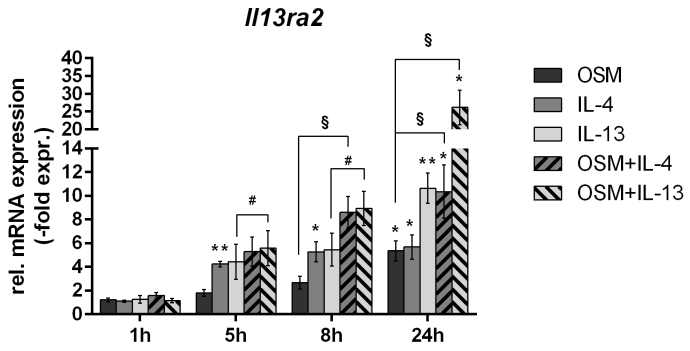

Figure 4.20: **Stimulation of VSMCs with OSM, IL-4 or IL-13 increases the mRNA expression of the decoy receptor *Il13ra2*.** *Wt* VSMCs were stimulated with mOSM, mIL-4, mIL-13, mOSM+mIL-4 and mOSM+mIL-13 (10ng/ml each) for one hour, five, eight and 24 hours. Transcription of *Il13ra2* was analysed by qRT-PCR. Data represent mean-fold changes in mRNA levels normalized to untreated cells (not shown) and house-keeping gene *Hprt* (n=3-4) with standard error of the mean (SEM). $*p < 0.05$, $**p < 0.01$ stimulated vs. unstimulated, $\#p < 0.05$ mIL-4/mIL-13 vs. mOSM+mIL-4/mOSM+mIL-13, $\S p < 0.01$ mOSM vs. mOSM+mIL-4/mOSM+mIL-13.

4.5 Cross-talk between OSM and IL-17

As mentioned in subsection 1.5, IL-17 has been found in atherosclerotic lesions of humans and mice [144, 145]. However, the function of IL-17 in atherosclerosis is still controversial and further investigations are necessary. Some studies showed that IL-17 is protective [147, 148], other studies postulated it is pathogenic [146, 149, 150]. The following experiments investigate the cross-talk between OSM and IL-17 in VSMCs and the possible regulation of receptor and atherosclerotic target gene expression by IL-17.

4.5.1 Analysis of the OSM and IL-4/IL-13 receptor expression in VSMCs

Similar to the results for IL-4 and IL-13, the influence of IL-17 was investigated by determining the mRNA amount of the OSM receptor type II complex and IL-4 receptor type II complex in VSMCs. Therefore, *wt* VSMCs were stimulated with mIL-17A (10ng/ml) for 24 hours. As a control, *wt* VSMCs were also stimulated with mOSM since its regulatory effect on receptor expressions was already determined before. The transcription of *Osmr*, *Il6st*, *Il4r*, and *Il13ra1* was detected by qRT-PCR (Figure 4.21).

The data presented in figure 4.21 confirm that OSM up-regulated the mRNA amount of *Osmr* and *Il6st* as well as *Il4r* and *Il13ra1* which was already shown in subsection 4.4.1. The cytokine mIL-17A, however, played no role in the regulation of both receptor complexes. This corresponded well to the results obtained by Kwofie *et al.* [156]. There, *Osmr*, *Il6st*, and *Il4r* mRNA expression was increased in human airway smooth muscle cells (HASMCs) mainly by OSM and not by IL-4, IL-13, or IL-17.

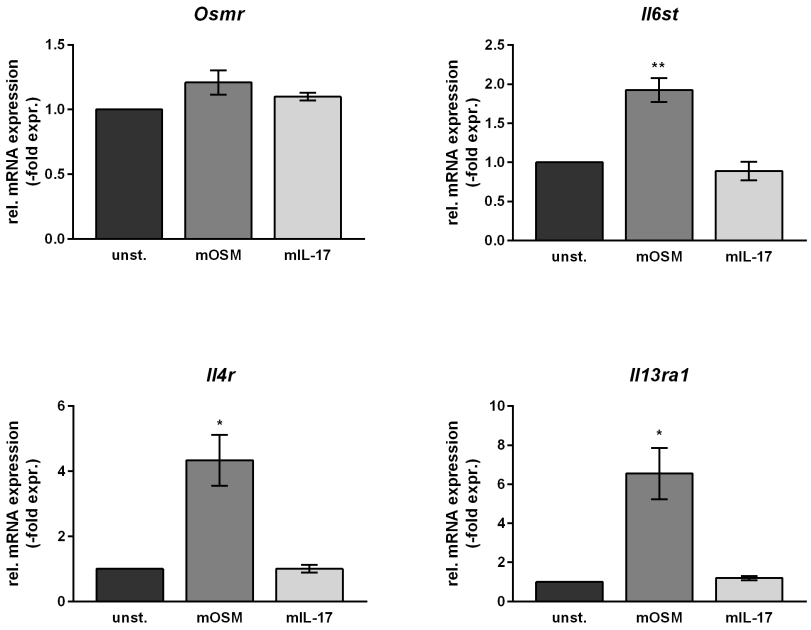

Figure 4.21: **OSM, but not IL-17 regulates the mRNA expression of *Osmr*, *IL6st*, *Il4r*, and *Il13ra1* in VSMCs.** *Wt* VSMCs were stimulated with mOSM and mIL-17A (10ng/ml each) for 24 hours. Transcription of *Osmr*, *IL6st*, *Il4r* and *Il13ra1* was analysed by qRT-PCR. Data represent mean-fold changes in mRNA levels normalized to untreated cells and housekeeping gene *Hprt* (n=4) with standard error of the mean (SEM). $^{*}p < 0.05$, $^{**}p < 0.01$ mOSM stimulated vs. unstimulated VSMCs.

4.5.2 Regulation of atherosclerotic target genes by OSM and IL-17

Since it is not known if IL-17 regulates some of the atherosclerotic target genes investigated here or interferes with their OSM-mediated regulation, *wt* VSMCs were stimulated with mOSM, mIL-17A and mOSM+mIL-17A (10ng/ml each) for 24 hours. The mRNA amount of *Col3a1*, *Tnfrsf11b* and *Eln* was determined by qRT-PCR. Thereby, OSM, the shown regulator of these target genes, functioned again as a control cytokine (Subsection 4.3.2 and 4.4.2).
In contrast to OSM, mIL-17A alone showed no influence on VSMC mRNA expression for *Col3a1*, *Tnfrsf11b* and *Eln*. However, when VSMCs were treated with mOSM+mIL-17A, the mRNA amount of *Eln* decreased significantly stronger compared to mOSM alone (Figure 4.22). Thus, mIL-17 seemed to foster the negative effect of OSM on the target gene *Eln*.

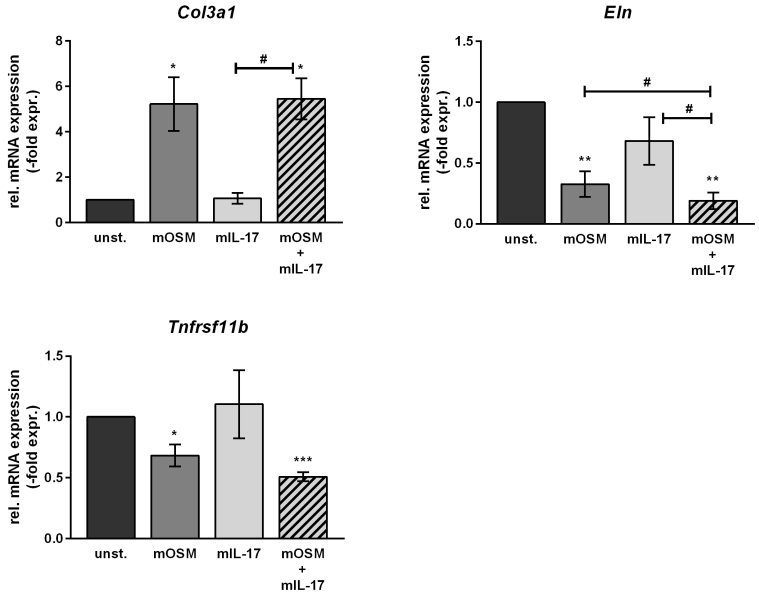

Figure 4.22: **Changes in mRNA expression levels of *Col3a1*, *Tnfrsf11b*, and *Eln* in VSMCs in response to OSM compared to IL-17.** *Wt* VSMCs were stimulated with mOSM, mIL-17A or mOSM+mIL-17A (10ng/ml each) for 24 hours. Transcription of *Col3a1*, *Tnfrsf11b* and *Eln* was analysed by qRT-PCR. Data represent mean-fold changes in mRNA levels normalized to untreated cells and house-keeping gene *Hprt* (n=4) with standard error of the mean (SEM). $*p < 0.05$, $**p < 0.01$, $***p < 0.001$ stimulated vs. unstimulated VSMCs, $\#p < 0.05$ mOSM+mIL-17A vs. mOSM or mIL-17A.

4.5.3 Regulation of the IL-13Ra2 decoy receptor and IL-6 expression by OSM and IL-17

OSM, IL-4 and IL-13 were able to regulate the expression of the decoy receptor *Il13ra2* in VSMCs which could be further enhanced when the cells were co-stimulated with OSM and IL-4 or IL-13 (Subsection 4.4.4). Furthermore, OSM regulates the expression of IL-6 in VSMCs. A similar finding has recently been published for endothelial cells and fibroblasts [93, 229]. In combination with IL-17A, however, the OSM-enhanced expression of IL-6 was further augmented in human airway smooth muscle cells (HASMCs) [156]. To establish whether IL-17 exerts an equal influence in VSMCs, *wt* cells were stimulated with mOSM, mIL-17A or mOSM+mIL-17A (10ng/ml each) for 24 hours. The transcription of *Il13ra2* and *Il6* was detected by qRT-PCR (Figure 4.23).

Besides mOSM, mIL-17A displayed a trend up-regulate the mRNA expression of *Il13ra2* about five-fold (p=0.093). The mRNA expression of *Il6* was also enhanced after mOSM or mIL-17A treatment. An additional increase in the amount of *Il13ra2* and *Il6* mRNA could be obtained when *wt* VSMCs were co-stimulated with both cytokines (mOSM+mIL-17A) (Figure 4.23). A similar synergistic effect for *Il13ra2* was already found for the treatment with mOSM+mIL-4 and mOSM+mIL-13 in subsection 4.4.4 but not for the expression of *Il6* (data not shown). Thus, all tested cytokines - OSM, IL-4, IL-13, and IL-17 - are capable to change the mRNA expression of decoy receptor *Il13ra2*, whereas only mOSM and mIL-17A influences the mRNA amount of *Il6* in VSMCs. The physiological consequence of these findings require further investigations.
The protein amount of the IL-13Rα2 could not be analysed, since no specific antibody for FACS or Western Blot analysis was available within the time frame of this thesis.

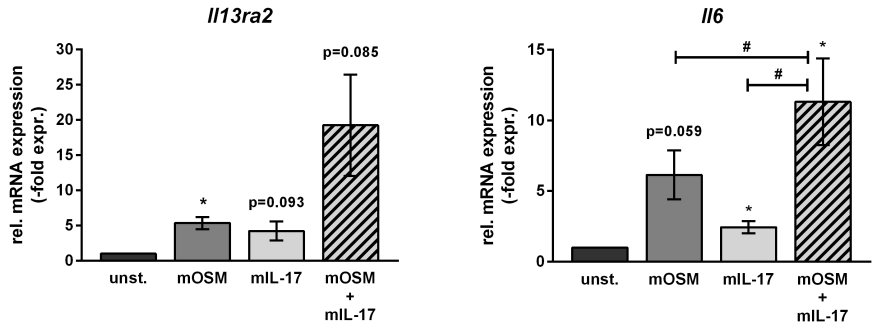

Figure 4.23: **Stimulation of VSMCs with OSM and/or IL-17 increases the mRNA expression of the decoy receptor *Il13ra2* and *Il6*.** *Wt* VSMCs were stimulated with mOSM, mIL-17A or mOSM+mIL-17A (10ng/ml each) for 24 hours. Transcription of *Il13ra2* and *Il6* was analysed by qRT-PCR. Data represent mean-fold changes in mRNA levels normalized to untreated cells and house-keeping gene *Hprt* (n=4) with standard error of the mean (SEM). $^*p < 0.05$ mOSM, mIL-17A, mOSM+mIL-17A vs. unstimulated VSMCs, $\#p < 0.05$ mOSM+mIL-17A vs. mOSM or mIL-17A.

4.6 Characterisation of Ldlr-/-Osmr-/- mice on a high fat/high cholesterol diet (WD)

In order to study OSM and its role for the progression of atherosclerosis *in vivo*, a new mouse model was generated. Therefore, two established transgenic mouse lines were crossed. First, *B6.129S7-Ldlr$^{tm1Her/J}$* (*Ldlr$^{-/-}$*) mice have a deficiency in the low density lipoprotein receptor (*Ldlr*) which leads to a blockade for the clearance of lipoproteins followed by a moderate accumulation of LDL on normal chow diet [78, 85]. When these mice are fed a cholesterol rich diet (Western diet, WD), they develop hyperlipidemia and atherosclerotic lesions [85]. Second, *Osmr$^{-/-}$* mice are not able to respond to OSM but their phenotype and behaviour is normal, albeit slight effects on hematopoiesis [3]. Recent studies could show, that *Osmr$^{-/-}$* mice are developing hepatic steatosis and obesity induced insulin resistance [230]. Both mouse lines have been back-crossed onto the *C57Bl/6* background and were crossed to generate *Ldlr$^{-/-}$Osmr$^{-/-}$* and *Ldlr$^{-/-}$Osmr$^{+/+}$* mice. To characterise their genotype, gDNA from ear marks of *Ldlr$^{-/-}$Osmr$^{+/+}$* and *Ldlr$^{-/-}$Osmr$^{-/-}$* mice was used for the analysis of the transgenic region in the *Ldlr* and *Osmr* gen locus by PCR and agarose gel electrophoresis (subsection 3.1.2 and 3.1.3).

When the mice were 11 weeks old, ten *Ldlr$^{-/-}$Osmr$^{+/+}$* and ten *Ldlr$^{-/-}$Osmr$^{-/-}$* female mice were fed a Western diet (WD) for 12 weeks. The composition of the food was described in section 2.12. Animals were monitored at least once a week to check their health status and the body weight was documented every week. Afterwards, the mice were sacrificed. Blood and organs were collected, liver and spleen were weighed and non-fasted blood glucose level was measured. Furthermore, mRNA from the liver was analysed for receptor and gene expressions regulating cholesterol and bile acid synthesis as well as extracellular matrix (ECM). All experiments were approved by the local authorities (Regierung von Unterfranken; Az 55.2-2531.01-27/14).

4.6.1 Differences in body and liver weight between Ldlr-/-Osmr-/- and Ldlr-/-Osmr+/+ mice after 12 weeks of WD

The body weight of the *Ldlr$^{-/-}$Osmr$^{+/+}$* and *Ldlr$^{-/-}$Osmr$^{-/-}$* mice was measured every week during WD treatment (W 0 to W 12). At the age of 11 weeks before feeding with this diet started, *Ldlr$^{-/-}$Osmr$^{+/+}$* mice weighed about four gram more compared to

Ldlr$^{-/-}$*Osmr*$^{-/-}$ mice (24.6 ± 0.51 g to 20.5 ± 0.18 g). At the end of the WD treatment (W 12), *Ldlr*$^{-/-}$*Osmr*$^{+/+}$ mice gained about 13.3 g, whereas *Ldlr*$^{-/-}$*Osmr*$^{-/-}$ mice gained about 5.8 g (Figure 4.24 A).

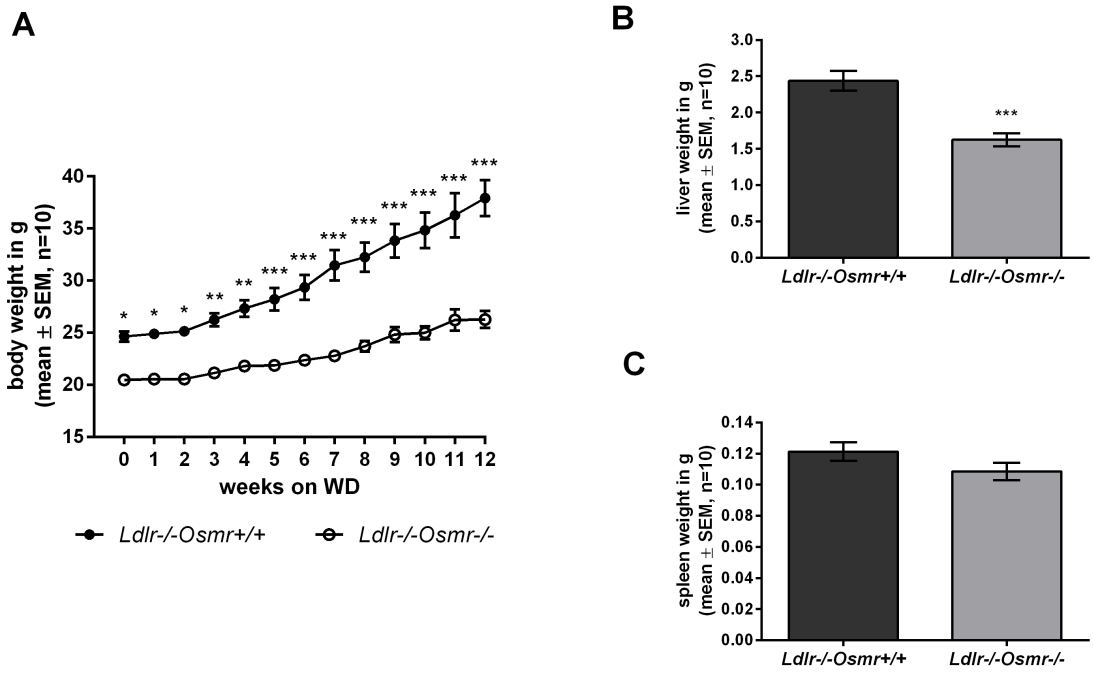

Figure 4.24: **Body, liver and spleen weights from *Ldlr*$^{-/-}$*Osmr*$^{+/+}$ and *Ldlr*$^{-/-}$*Osmr*$^{-/-}$ mice after 12 weeks of WD treatment.** Mean value (± SEM) of body (A), liver (B) and spleen (C) weights are shown (n=10), $^{*}p < 0.05$, $^{**}p < 0.01$, $^{***}p < 0.001$ *Ldlr*$^{-/-}$*Osmr*$^{-/-}$ vs. *Ldlr*$^{-/-}$*Osmr*$^{+/+}$ mice.

The average liver weight from the *Ldlr*$^{-/-}$*Osmr*$^{+/+}$ mice was significantly higher than the average liver weight from *Ldlr*$^{-/-}$*Osmr*$^{-/-}$ mice (2.4 ± 0.136 g to 1.6 ± 0.091 g) (Figure 4.24 B). The average weight of the spleen was similar in both groups (0.12 ± 0.006 g *Ldlr*$^{-/-}$*Osmr*$^{+/+}$ mice and 0.11 ± 0.006 g for *Ldlr*$^{-/-}$*Osmr*$^{-/-}$ mice) (Figure 4.24 C).

4.6.2 Reduced non-fasted blood glucose levels of Ldlr-/-Osmr-/- mice compared to Ldlr-/-Osmr+/+ mice after 12 weeks of WD

For further characterisation, non-fasted blood glucose level was measured from the tail tip immediately after sacrifice using the Contour® glucometer (Bayer) (Figure 4.25). The blood glucose level from *Ldlr*$^{-/-}$*Osmr*$^{-/-}$ mice was less strongly enhanced compared to *Ldlr*$^{-/-}$*Osmr*$^{+/+}$ mice.

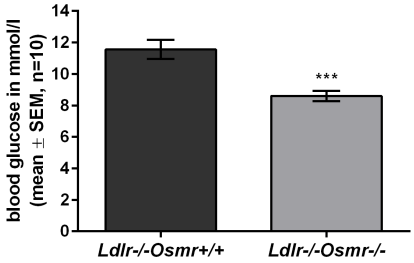

Figure 4.25: **Non-fasted blood glucose level from *Ldlr*$^{-/-}$*Osmr*$^{+/+}$ and *Ldlr*$^{-/-}$*Osmr*$^{-/-}$ mice.** Non-fasted blood glucose levels were analysed from *Ldlr*$^{-/-}$*Osmr*$^{+/+}$ and *Ldlr*$^{-/-}$*Osmr*$^{-/-}$ mice after 12 weeks of WD treatment using a drop of blood that was applied onto the Contour® test strip. Data represent mean glucose concentrations in mmol/l ± SEM (n=10), $***p < 0.001$ *Ldlr*$^{-/-}$*Osmr*$^{-/-}$ vs. *Ldlr*$^{-/-}$*Osmr*$^{+/+}$ mice.

4.6.3 Haematological analysis of whole blood from Ldlr-/-Osmr-/- and Ldlr-/-Osmr+/+ mice after 12 weeks of WD

For differential analysis of blood components, whole blood from *Ldlr*$^{-/-}$*Osmr*$^{+/+}$ and *Ldlr*$^{-/-}$*Osmr*$^{-/-}$ mice was analysed using a Sysmex haematology analyser after 12 weeks of WD treatment (Figure 4.26).
The erythrocyte and thrombocyte counts (Figure 4.26 B and C) were decreased in *Ldlr*$^{-/-}$*Osmr*$^{-/-}$ mice compared to *Ldlr*$^{-/-}$*Osmr*$^{+/+}$ mice, whereas the leukocyte count was the same in both groups (Figure 4.26 A). The mean cell volume (MCV) of erythrocytes, however, was significantly larger in *Ldlr*$^{-/-}$*Osmr*$^{-/-}$ mice compared to *Ldlr*$^{-/-}$*Osmr*$^{+/+}$ mice (Figure 4.26 D).

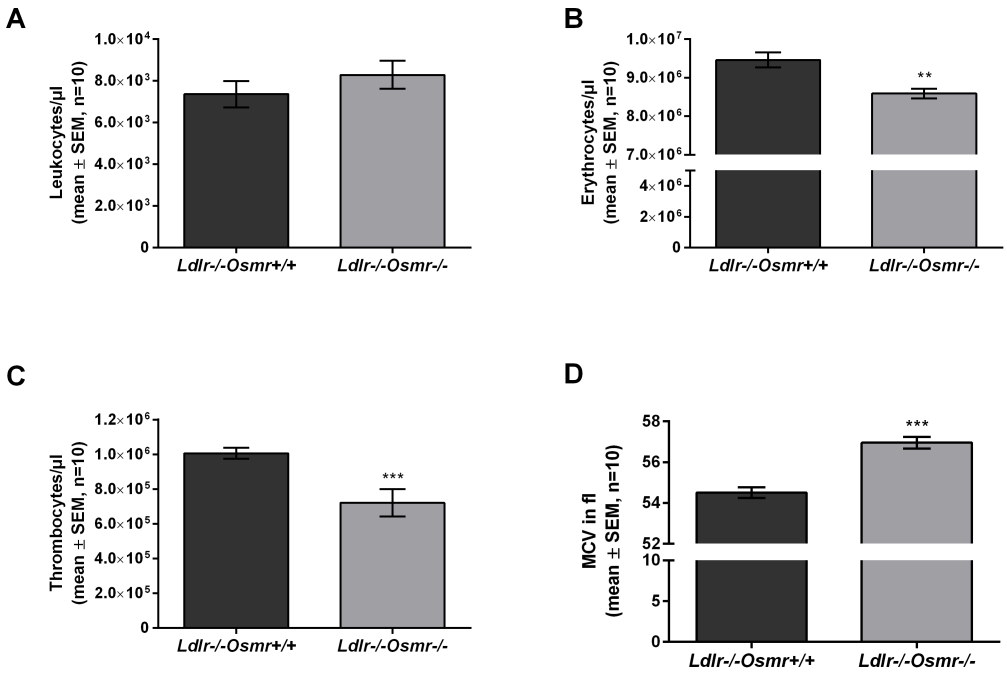

Figure 4.26: **Haematological analysis of whole blood from *Ldlr$^{-/-}$Osmr$^{+/+}$* and *Ldlr$^{-/-}$Osmr$^{-/-}$* mice.** Leukocyte (A), erythrocyte (B), thrombocyte (C) counts and mean cell volume of erythrocytes (MCV, D) was measured in whole blood of *Ldlr$^{-/-}$Osmr$^{+/+}$* and *Ldlr$^{-/-}$Osmr$^{-/-}$* mice after 12 weeks of WD. Data represent mean cell counts or cell volume ± SEM (n=10), $^{**}p < 0.01$, $^{***}p < 0.001$ *Ldlr$^{-/-}$Osmr$^{-/-}$* vs. *Ldlr$^{-/-}$Osmr$^{+/+}$* mice.

4.6.4 Analysis of atherogenesis: En face and aortic root staining

Plaque formation was evaluated by *en face* staining (Figure 4.27) and aortic root sections (Figure 4.28) of *Ldlr$^{-/-}$Osmr$^{+/+}$* and *Ldlr$^{-/-}$Osmr$^{-/-}$* mice after 12 weeks of WD which was kindly performed by Melanie Schott (Institute of Clinical Biochemistry and Pathobiochemistry, University Hospital Würzburg).
Compared to *Ldlr$^{-/-}$Osmr$^{+/+}$* mice, *Ldlr$^{-/-}$Osmr$^{-/-}$* mice displayed a significant reduction in the atherosclerotic lesion area (as percent of total aortic surface area, (Figure 4.27)) as well as in the atherosclerotic plaque growth in the aortic roots (Figure 4.28).

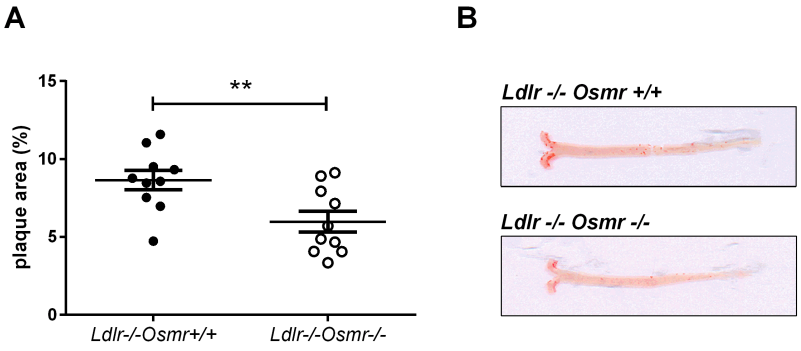

Figure 4.27: **En face staining the aorta of *Ldlr*$^{-/-}$*Osmr*$^{+/+}$ and *Ldlr*$^{-/-}$*Osmr*$^{-/-}$ mice after WD treatment.** **A**, Calculation of the atherosclerotic lesion area as percent of total aortic surface area from *Ldlr*$^{-/-}$*Osmr*$^{+/+}$ and *Ldlr*$^{-/-}$*Osmr*$^{-/-}$ mice. Data represent the plaque area in % ± SEM (n=10), $^{**}p < 0.01$. **B**, Representative pictures of total aortas from *Ldlr*$^{-/-}$*Osmr*$^{+/+}$ and *Ldlr*$^{-/-}$*Osmr*$^{-/-}$ mice stained with Oil-Red-O.

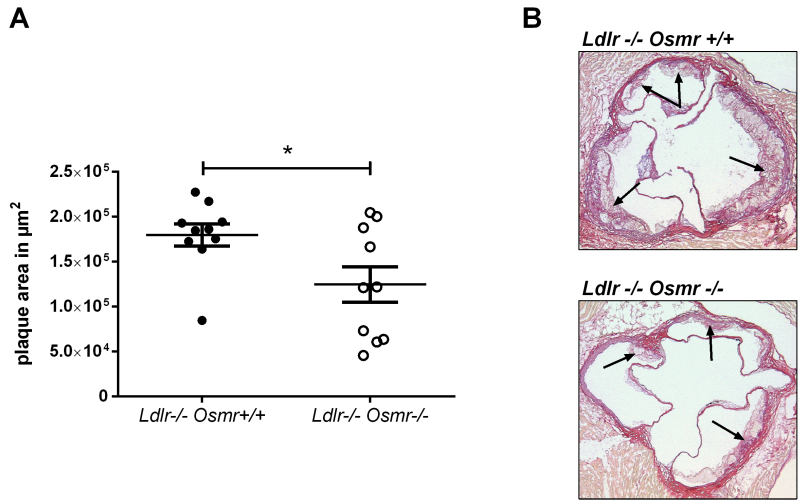

Figure 4.28: **Aortic root staining of *Ldlr*$^{-/-}$*Osmr*$^{+/+}$ and *Ldlr*$^{-/-}$*Osmr*$^{-/-}$ mice after WD treatment.** **A**, Quantification of the plaque area in aortic root sections. Data represent plaque area in µm^2 ± SEM (n=10), $^{*}p < 0.05$. **B**, Representative pictures of aortic roots sections from *Ldlr*$^{-/-}$*Osmr*$^{+/+}$ and *Ldlr*$^{-/-}$*Osmr*$^{-/-}$ mice stained with Aldehyde-Fuchsin solution (collagen and elastin staining). Black arrows indicate plaque areas.

4.6.5 Analysis of the expression of liver enzymes on mRNA level

Based on the results of the difference in liver weight between Ldlr$^{-/-}$ and Ldlr$^{-/-}$Osmr$^{-/-}$ mice after WD treatment (Figure 4.24), mRNA from this organ was extracted and analysed for enzyme (Figure 4.29) and transporter gene expression (Figure 4.30). All named genes are involved in the bile acid or fatty acid synthesis.

Cholesterol 7α-hydroxylase (*Cyp7a1*) is a liver-specific enzyme which catalyses the initial step in the classical bile acid synthetic pathway [231]. Bile acid synthesis is the major pathway responsible for the maintenance of whole body cholesterol homeostasis. The expression of CYP7A1 is controlled in two different ways. Positive regulation occurs by liver X receptor (LXR), while farnesoid X receptor (FXR) negatively regulates the transcription of *Cyp7a1*. The balance between LXR and FXR activity differs between species. Deficiency of CYP7A1 results in a hypercholesterolemic phenotype in humans [232] and it causes the development of atherosclerosis, cholesterol gallstone and fatty liver disease in mice [233].

Elongation of very long chain fatty acids protein 6 (*Elovl6*) belongs to the Elovl family composed of seven distinct fatty acid elongase subtypes (Elovl1-7). It is highly expressed in mice where lipogenesis and steroidogenesis are active like the adrenal gland, liver, white and brown adipose tissue, brain, testis and skin [234]. Elovl6 catalyses the elongation of saturated and monounsaturated fatty acids with 12, 14 and 16 carbons [235]. The expression of Elovl6 is directly regulated by sterol regulatory element-binding protein 1a (SREBP-1a), SREBP-1c and SREBP-2 as well as other lipogenic enzymes such as fatty acid synthase (FASN) and stearoyl coenzyme A desaturase 1 (SCD1) [234, 235, 236, 237, 238]. Saito et al. found out that the absence of Elovl6 in macrophages increases cholesterol efflux. This is associated with suppression of atherosclerosis in Ldlr$^{-/-}$ mice. Therefore, Elovl6 plays a crucial role in the development of both foam cells and atherosclerotic lesions [239].

Fatty acid synthase (*Fasn*) catalyses the last step in fatty acid biosynthesis. It synthesizes long chain fatty acids by using acetyl-CoA as a primer, malonyl-CoA as a carbon donor, and NADPH as a reducing equivalent [240, 241, 242]. FASN expression is regulated by SREBPs. SREBP1 is induced by high insulin levels and feeding a high carbohydrate diet induced hepatic FASN expression in rats [243]. Furthermore, tissue specific inactivation of FASN in macrophages decreases diet induced atherosclerosis in

mice through mechanisms that appear to involve the induction of LXRα. The results suggest that FASN generates lipids involved in feedback inhibition of LXRα [244].

Stearoyl-coenzyme A desaturase 1 (*Scd1*) converts saturated fatty acids (SFAs) to monounsaturated fatty acids (MUFAs). SCD is a highly regulated and conserved enzyme with multiple isoforms (SCD1-4 in the mouse) having overlapping but distinct tissue distribution and substrate specificity [245, 246]. SCD1 has been shown to play a critical part in the development of metabolic diseases, including diet and leptin-deficiency induced obesity, hepatic steatosis, insulin resistance and atherosclerosis [247, 248, 249, 250, 251]. In *Ldlr*$^{-/-}$ mice on high fat diet (HFD), SCD1 deficiency exhibited increased atherosclerosis in the aorta despite the improved metabolic parameters, such as decreased adiposity, reduced liver steatosis and increased insulin sensitivity [252, 253]. This observation might be attributed to an increased inflammation in *Scd1*$^{-/-}$ mice due to an accumulation of SFAs.

Acetyl-CoA carboxylase (*Acc*) catalyses the synthesis of malonyl-CoA, a metabolite that plays a role in the synthesis of fatty acids as the donor of C2 units [254, 255] and in the oxidation of fatty acid as the regulator of the mitochondrial shuttle system [256]. ACC links fatty acid and carbohydrate metabolism through the shared intermediate acetyl-CoA [257]. Two isoforms are identified, ACC1 and ACC2, both endcoded by separate genes (*Acaca* for ACC1 and *Acacb* for ACC2) [257]. ACC1 is highly expressed in liver and adipose tissue, whereas ACC2 is predominantly localized in heart and muscle, and to a lesser extent in liver [255, 258, 259]. Furthermore, ACC1 can be found in the cytosol and ACC2 in the mitochondria [260]. In this study, primer sets for *Acaca* were designed and used for qRT-PCR analysis of liver tissue.

In figure 4.29, most of the liver enzymes displayed the same expression level between *Ldlr*$^{-/-}$*Osmr*$^{-/-}$ and *Ldlr*$^{-/-}$*Osmr*$^{+/+}$ mice. Only the expression of *Cyp7a1* showed a significantly different mRNA level in *Ldlr*$^{-/-}$*Osmr*$^{-/-}$ mice compared to *Ldlr*$^{-/-}$*Osmr*$^{+/+}$ mice after WD treatment. Nevertheless, it is important to note that further controls (*C57Bl/6* or *Osmr*$^{-/-}$ mice) should be added to compare the "normal" mRNA expression from the controls to the one from the *Ldlr*$^{-/-}$*Osmr*$^{+/+}$ and *Ldlr*$^{-/-}$*Osmr*$^{-/-}$ mice in figure 4.29. Thereafter, an interpretation of this result would be possible and plausible.

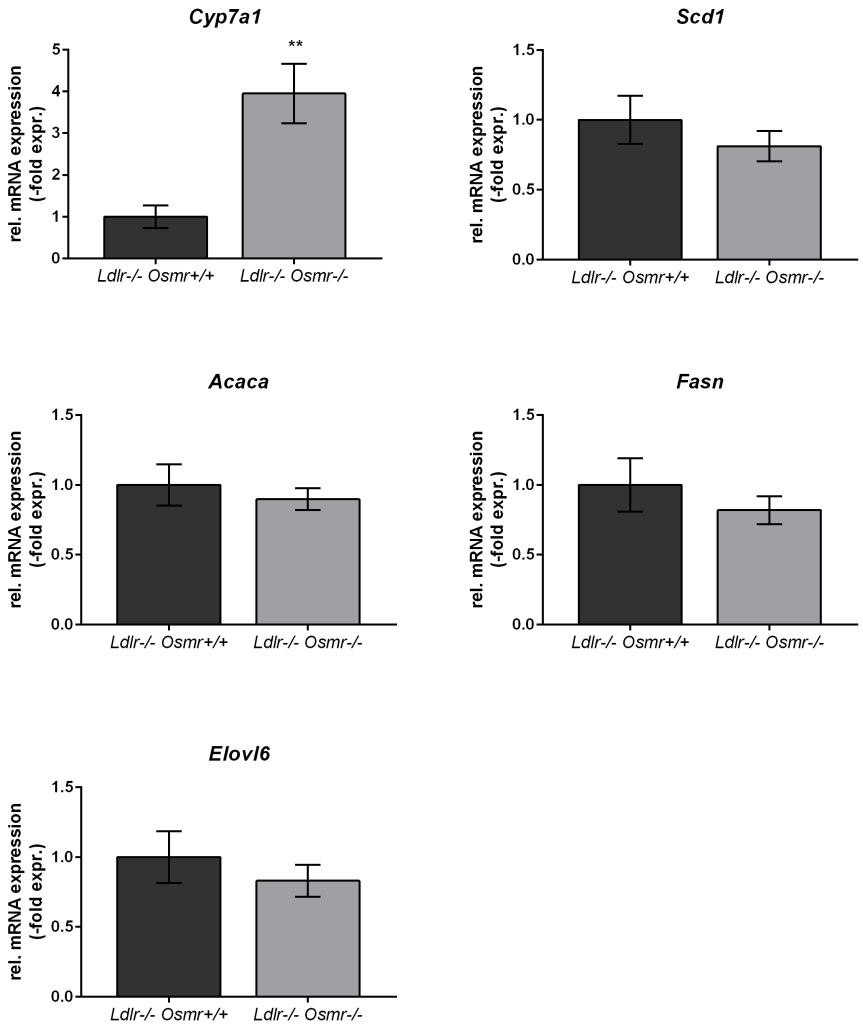

Figure 4.29: **Expression levels of liver enzymes from *Ldlr$^{-/-}$Osmr$^{+/+}$* and *Ldlr$^{-/-}$Osmr$^{-/-}$* mice after WD treatment.** Transcription of *Cyp7a1*, *Scd1*, *Acaca*, *Fasn* and *Elovl6* in liver tissue was analysed by qRT-PCR. Data represent mean-fold changes in mRNA levels normalized to *Ldlr$^{-/-}$Osmr$^{+/+}$* mice and house-keeping gene *Hprt* ± SEM (n=10), $^{**}p < 0.01$ *Ldlr$^{-/-}$Osmr$^{-/-}$* vs. *Ldlr$^{-/-}$Osmr$^{+/+}$* mice.

ATP-binding cassette protein A1 (*Abca1*) belongs to the largest transporter protein family (ABC) with several hundred members. Subfamilies are categorized from ABCA to ABCG. ABCA1 facilitates the efflux of phospholipids and cholesterol onto lipid-poor apolipoproteins, initiating the formation of high density lipoportein (HDL) particles [261]. It is widely expressed in the human body, e.g. in liver, kidney, adrenal gland, intestine and central nervous system [262]. ABCA1 is also prominent in foam cells of atherosclerotic lesions. While basal levels of ABCA1 mRNA and protein in macrophages are low, both are induced with cholesterol loading and this effect can be reversed by HDL-mediated cholesterol efflux [263, 264].

Sodium-taurocholate co-transporting polypeptide (*Ntcp*) and bile salt export pump (*Bsep*) are two key transporters for hepatic bile acid uptake and excretion. Bile acid uptake from blood into liver is mediated mainly by NTCP and efflux from liver into bile by BSEP [265]. BSEP is also known as ABCB11 (ATP Binding Cassette protein B11) and belongs to ATP binding cassette family just as ABCA1.

Farnesoid X receptor (*Fxr*) controls expression of critical genes in bile acid and cholesterol homoeostasis. Among others, FXR inhibits the expression of Cyp7a1 [266, 267, 268] and NTCP [269] and activates the expression of BSEP [270, 271]. Studies that assessed a direct role for FXR in the initiation and progression of atherosclerosis in mice are controversial [272, 273, 274].

Small heterodimer partner (*Shp*, *Nr0b2* for nuclear receptor subfamily 0, group B, member 2) is a member of the mammalian nuclear receptor (NR) superfamily and is classified as an orphan subgroup, as its ligand has not yet been identified [275]. SHP functions as a corepressor through heterodimeric interaction with a wide array of nuclear receptors and repressing their transcriptional activity [276]. This orphan NR has been identified as a key transcriptional regulator of signalling pathways [275, 277] involved in metabolic processes such as cholesterol, bile acid and fatty acid metabolism, glucose and energy homeostasis [278].

As before, for most of these target genes the mRNA expression remained unchanged in $Ldlr^{-/-}Osmr^{-/-}$ and $Ldlr^{-/-}Osmr^{+/+}$ mice (Figure 4.30). Only the expression of *Ntcp* showed a slight but significantly different mRNA level in the double deficient mice compared to $Ldlr^{-/-}Osmr^{+/+}$ mice after WD treatment. Again, further controls (*C57Bl/6* or $Osmr^{-/-}$) have to be analysed for a better interpretation of the results between $Ldlr^{-/-}Osmr^{+/+}$ and $Ldlr^{-/-}Osmr^{-/-}$ mice.

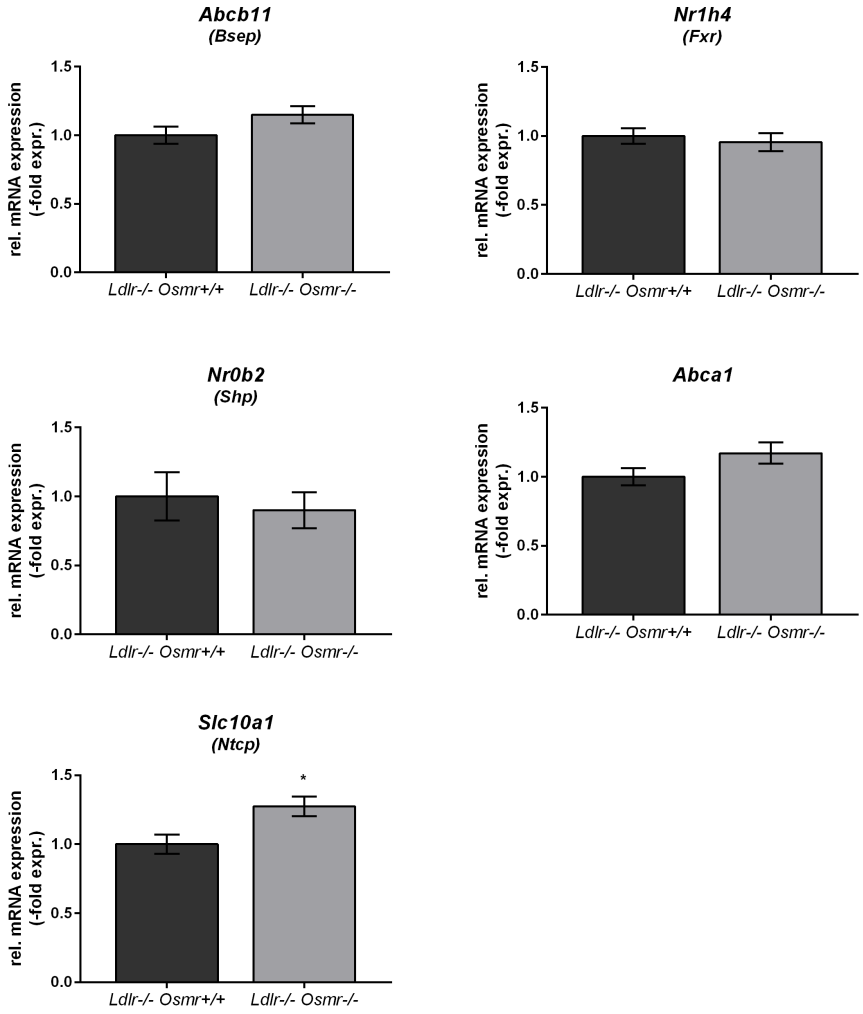

Figure 4.30: **Expression levels of transporter and receptor systems in the liver of *Ldlr*$^{-/-}$*Osmr*$^{+/+}$ and *Ldlr*$^{-/-}$*Osmr*$^{-/-}$ mice after WD treatment.** Transcription of *Bsep*, *Fxr*, *Shp*, *Abca1* and *Ntcp* in liver tissue was analysed by qRT-PCR. Data represent mean-fold changes of mRNA levels normalized to *Ldlr*$^{-/-}$*Osmr*$^{+/+}$ mice and house-keeping gene *Hprt* ± SEM (n=10), $^{*}p < 0.05$ *Ldlr*$^{-/-}$*Osmr*$^{-/-}$ vs. *Ldlr*$^{-/-}$*Osmr*$^{+/+}$ mice.

4.6.6 Analysis of cytokine receptor mRNA expression by quantitative RT-PCR

In order to control the expression of the OSM receptor complex in the livers of *Ldlr*$^{-/-}$*Osmr*$^{+/+}$ and *Ldlr*$^{-/-}$*Osmr*$^{-/-}$ mice, the mRNA expression of *Osmr* and *Il6st* was determined by qRT-PCR.
As expected, the mRNA expression of *Osmr* was decreased in *Ldlr*$^{-/-}$*Osmr*$^{-/-}$ mice compared to *Ldlr*$^{-/-}$*Osmr*$^{+/+}$ mice whereas the mRNA amount of *Il6st* was unaltered in both groups (Figure 4.31).

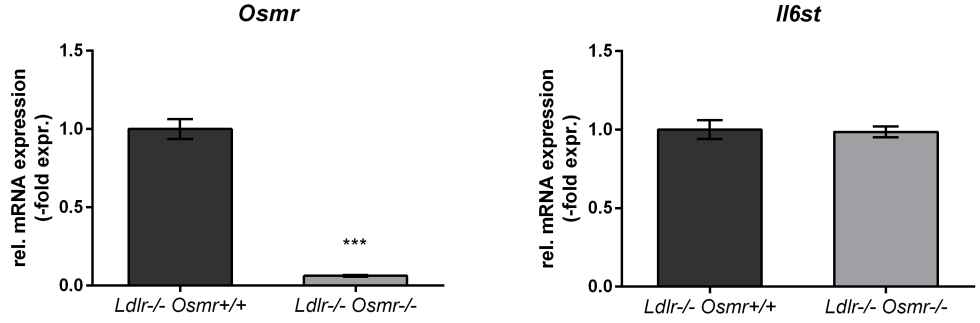

Figure 4.31: **Expression level of the OSM receptor complex type II in *Ldlr*$^{-/-}$*Osmr*$^{+/+}$ and *Ldlr*$^{-/-}$*Osmr*$^{-/-}$ mice.** Transcription of *Osmr* and *Il6st* from liver tissue was analysed by qRT-PCR. Data represent mean-fold changes of mRNA levels normalized to *Ldlr*$^{-/-}$*Osmr*$^{+/+}$ mice and house-keeping gene *Hprt* ± SEM (n=10), $***p < 0.001$ *Ldlr*$^{-/-}$*Osmr*$^{-/-}$ vs. *Ldlr*$^{-/-}$*Osmr*$^{+/+}$ mice.

4.6.7 Analysis of transcriptional regulation of extracellular matrix genes by quantitative RT-PCR

In order to determine whether the transcription of selected genes involved in regulation of the extracellular matrix changes in the liver from *Ldlr*$^{-/-}$*Osmr*$^{+/+}$ and *Ldlr*$^{-/-}$*Osmr*$^{-/-}$ mice after 12 weeks of WD treatment, the mRNA expression of *Col1a1*, *Col1a2*, *Col3a1*, *Eln*, *Tnfrsf11b* and *Spp1* was determined by qRT-PCR (Figure 4.32). The target gene *Thbs-4* is not expressed in the liver.
Similar to *Eln*, the mRNA expression of *Col1a1* and *Col1a2* remained almost unaltered, whereas the mRNA for *Col3a1* and *Tnfrsf11b* was decreased in the *Ldlr*$^{-/-}$*Osmr*$^{-/-}$ mice.

Spp1 was significantly higher expressed in the liver of $Ldlr^{-/-}Osmr^{-/-}$ mice compared to $Ldlr^{-/-}Osmr^{+/+}$ mice (Figure 4.32). If this effect resulted from the treatment with WD or from the knock-out in the *Osmr* gene could not be clarified within the time frame of this thesis. Further investigations by using positive controls (*C57Bl/6* or $Osmr^{-/-}$ mice) under WD or $Ldlr^{-/-}Osmr^{+/+}$ and $Ldlr^{-/-}Osmr^{-/-}$ mice under normal diet would be necessary.

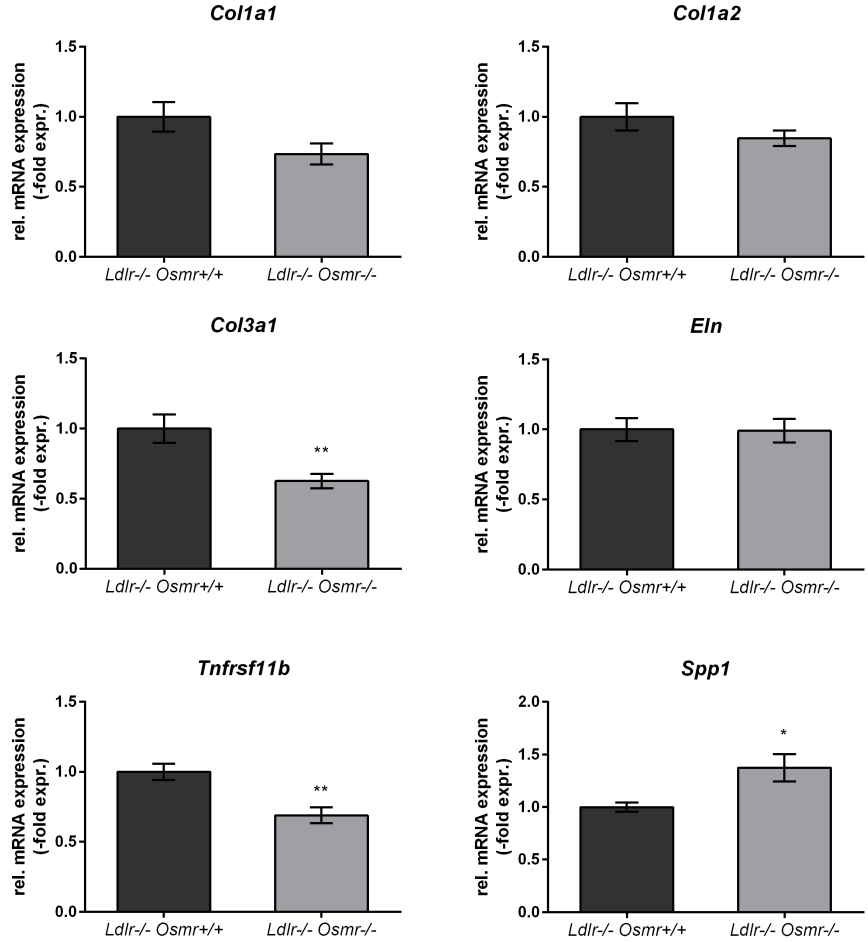

Figure 4.32: **Changes in expression rate of genes involved in the regulation and composition of ECM in $Ldlr^{-/-}Osmr^{-/-}$ compared to $Ldlr^{-/-}Osmr^{+/+}$ mice after WD treatment.** Transcription of *Col1a1*, *Col1a2*, *Col3a1*, *Eln*, *Tnfrsf11b* and *Spp1* from liver tissue was analysed by qRT-PCR. Data represent mean-fold changes of mRNA levels normalized to $Ldlr^{-/-}Osmr^{+/+}$ mice and house-keeping gene *Hprt* ± SEM (n=10), $^{*}p < 0.05$, $^{**}p < 0.01$ $Ldlr^{-/-}Osmr^{-/-}$ vs. $Ldlr^{-/-}Osmr^{+/+}$ mice.

5 Discussion

5.1 Characterisation of VSMCs by smooth muscle marker

Vascular smooth muscle cells (VSMCs) are located in the middle layer (media layer) of vascular vessels and are responsible for maintaining vascular tone [97]. Under normal conditions, these cells exhibit a contractile phenotype without proliferation and stay silent. Unlike other muscle cells they do not terminally differentiate. During plaque formation of atherosclerotic lesions, VSMCs can be induced to change phenotype, from a contractile to a proliferating state, which is also known as a synthetic phenotype [279]. Cultured VSMCs isolated from the aortas of *wt* and *Osmr*$^{-/-}$ mice were able to proliferate. They could be distinguished from endothelial cells or fibroblasts by comparing their cell growth behaviour. VSMCs form overlapping layers whereas endothelial cells display the cobblestone-like morphology and grow in a monolayer (Figure 4.1). Since VSMCs are primary, non-immortalized cells they became senescent and ceased growth after passage seven.

VSMCs can be characterised further by different smooth muscle markers described in the review article from Rensen *et al.* [280]. In this work, smooth muscle actin (SMA) and smooth muscle protein 22-alpha (SM22α) were used for Western Blot analysis and immunofluorescence. The cells did not lose their smooth muscle characteristics from passage 0 to 6 and were not overgrown by other cell types (Figure 4.2 and 4.3). This indicates that no cell contamination occurred during culturing and no other cell type was able to influence the results in this thesis.

5.2 Oncostatin M induces multiple effects on VSMCs

Oncostatin M (OSM) is involved in numerous physiological and pathophysiological processes including inflammation, hematopoiesis, tissue remodeling, development and cell growth. It was also found in vascular diseases. Albasanz-Puig *et al.* described that OSM was expressed in atherosclerotic lesions of human patients. They concluded that OSM may promote smooth muscle cell proliferation, migration and extracellular matrix protein synthesis through the JAK/STAT pathway [15]. OSM is mainly produced by activated T cells, monocytes and macrophages [91]. These cells can be found in atherosclerotic lesions as well. The exact target genes of OSM and the molecular mechanism of induction, however, remained uninvestigated.

5.2.1 OSM regulates receptor expression and activates signalling pathways in VSMCs

OSM binds to two different receptor complexes in the human system: OSM receptor type I (LIFRβ/gp130) and type II (OSMRβ/gp130). In the murine system, OSM signals only through OSMRβ and gp130 [26, 94]. Indeed, VSMCs express particularly high levels of gp130 and OSMRβ, which together form the type II OSM receptor complex (Figure 4.4). Additionally, lower expression levels of LIFRβ were found (Figure 4.4). Therefore, VSMCs represent excellent target cells for OSM. However, the reduction of LIFRβ by OSM on mRNA and protein level indicate an attenuation in the formation of the type I OSM receptor complex (Figure 4.5 and 4.6 A and B). While the expression for *Osmr* and *Il6st* [1] was enhanced transiently in VSMCs, only the protein amount of gp130 was increased during OSM treatment. The cell surface expression of OSMRβ even decreased. One reasonable explanation was described by Blanchard *et al.* [176]. There, internalisation of OSMRβ, LIFRβ, and gp130 was induced after ligand binding. The internalisation of gp130 and LIFRβ is mediated by a di-leucine motif in the cytoplasmatic region of these receptors [177, 178, 179]. Therefore, it is possible that OSM regulates the internalisation of OSMRβ in VSMCs in the same way.

OSM activates several signalling pathways, partially dependent on the investigated cell type. Activated pathways include: the JAK/STAT [26, 281], Ras-Raf-MAPK [26, 282,

[1] *Osmr* and *Il6st* encode OSMRβ and gp130 protein

283, 281], and the PI3K/Akt pathway [26, 283, 284]. In VSMCs, OSM induced the phosphorylation of STAT1 at Y701, STAT3 at Y705, STAT6 at Y641 as well as ERK 1/2 at T202/Y204, p38 at T180/Y182, and Akt at S473 (Figure 4.7). In *Osmr-/-* VSMCs, the basal phosphorylation was slightly enhanced for all proteins and no further increase was detectable after OSM stimulation indicating that OSM-mediated signalling in the absence of OSMRβ was not compensated by LIFRβ (Figure 4.7). Similar experiments were carried out in human airway smooth muscle cells (HASMCs) by Kwofie *et al.* [156]. They described that OSM, but not other IL-6-type cytokines (LIF, IL-11, IL-31 and IL-6), induces signal transduction in these cells. Moreover, the LIFRβ complex (type I) in these cells was minimally functional [156]. Consequently, in HASMCs as well as in murine VSMCs, OSM signals mainly through the OSMR type II complex (OSMRβ/gp130).

5.2.2 OSM induces the expression of genes involved in atherogenesis

OSM influenced the expression of a number of target genes described in literature as being affected in atherogenesis. In this thesis, the focus lay on two groups of genes: the first involved in the regulation and composition of extracellular matrix (ECM) and the second in the innate and adaptive immunity. Thus, all of them influence the de-differentiaton of VSMCs from a contractile to a pro-inflammatory and proliferating phenotype, a process observed during atherogenesis [102].

The strongest up-regulated gene after OSM treatment was *Thbs4* (Figure 4.9) which has been shown to induce VSMC proliferation [190]. Multiple reports have documented a genetic association between Thbs-4 and accelerated atherogenesis [192, 193, 194, 195]. Moreover, *Thbs4* deficient mice show a reduction in the development and inflammation of atherosclerotic lesions [196]. Thereby, it was postulated that Thbs-4 regulates vascular inflammation and atherogenesis by recruiting and interacting with macrophages to increase their adhesion and migration [196]. Taken from the results obtained here, OSM could promote atherosclerotic plaque development by enhancing Thbs-4 expression on mRNA and protein level. Unfortunately, all antibodies tested during the course of this thesis to prove the OSM-mediated increase in Thbs-4 expression on protein level turned out to recognize multiple proteins with none of them displaying the correct molecular

weight. Therefore further investigations are necessary for a better understanding of OSM induced-Thbs-4 in atherosclerotic plaques.

Elastin and collagens secreted by VSMCs are an important stabilizer of any vascular vessel wall. Thereby, the composition of elastic lamellae, collagen fibers, and smooth muscle cells contribute to vascular strength and flexibility [183]. For the formation of elastic lamellae, lysyl oxidase (LOX) cross-linked elastin precursors (tropoelastin) to elastin polymers. Thus, LOX which is expressed in fibroblasts, endothelial cells and smooth muscle cells is an important factor for ECM stability. Additionally, this enzyme controls the epithelial-to-mesenchymal transposition, cell migration, adhesion, transformation, and gene regulation [285, 286]. LOX deficient mice ($Lox^{-/-}$) are characterised by aortic aneurysms and aortic rupture and die soon after birth [287, 288]. Transforming growth factor β (TGFβ) and plateled-derived growth factor (PDGF) induce LOX expression in VSMCs [289, 290, 291]. The mRNA expression of *Lox*, however, was not regulated by OSM in murine smooth muscle cells (data not shown). $Eln^{-/-}$ mice died prematurely in early postnatal life from arterial occlusion due to the excessive subendothelial proliferation and accumulation of VSMCs [292]. Moreover, elastin regulates the phenotypic modulation, proliferation and migration of VSMCs in culture by G-protein-coupled receptor signalling pathways [279], since VSMCs start to proliferate and migrate in absence of elastin [180, 293]. Furthermore, elastin fibers may be degraded by matrix metalloproteinases (MMPs). They are present in latent forms under normal physiologic conditions and become activated following vessel wall injury [294, 293].

OSM decreases *Eln* and increases *Col3a1* mRNA level in VSMCs (Figure 4.9). Col3α1 is one of the main collagens next to collagen type I in fibrous plaques [295]. Similar to elastin, collagens regulate VSMC adhesion, migration, proliferation and cytoskeletal arrangement through multiple receptor pathways including integrins [183]. In contrast to *Col3a1*, *Col1a1* and *Col1a2* mRNA were slightly reduced in VSMCs after OSM stimulation (Figure 4.9). Culture of SMC on polymerized collagen type I inhibits SMC proliferation and mimics many of the properties of medial SMC [296, 297]. Thus, a reduction in collagen type I expression by OSM could promote VSMC proliferation. According to the results in this thesis, it is conceivable that OSM promotes de-differentiation and proliferation of VSMCs in atherosclerotic lesions. This may occur through the reduction of elastin and collagen type I on the one hand, and an increase of the collagen type III on the other hand.

OPG is a soluble decoy receptor for receptor activator of NF-κB ligand (RANKL),

regulator of osteoclast biology [298]. Deficiency of OPG in mice resulted in vascular calcification of the aorta and renal arteries [299]. Furthermore, high OPG expression was detected in VSMCs derived from atherosclerotic plaques of human carotids compared to VSMCs from normal aortas [300]. Additionally, the authors could show that OPG was up-regulated in primary VSMCs by stimuli such as calcium or phosphate ions. When they added OPG in a concentration between 0.1 and 1 ng/ml to cultured VSMCs, calcification of theses cells was significantly reduced. However, higher concentrations of OPG had no inhibitory effect [300]. Other studies show that OPG incudes proliferation of VSMCs [301, 302]. So far, one of the main inducers of OPG is platelet-derived growth factor (PDGF), a known growth factor promoting proliferation of VSMCs [303]. In this study, the gene for OPG protein - *Tnfrsf11b* - was up-regulated by OSM (Figure 4.9). OSM might therefore influence the concentration of OPG in atherosclerotic plaques resulting in a switch of OPG from an inhibitor to a promoter of vascular calcification.

Glycoprotein OPN has been found in atherosclerotic arteries and its elevated serum levels are associated with vascular calcifications [200]. Furthermore, it has been shown to be involved in de-differentiation, proliferation and migration of VSMCs [304, 305]. Pedersen *et al.* showed that loss of osteopontin resulted in reduced de-differentiation of SMC in uraemic atherosclerosis [306]. On the one hand, phosphorylated OPN acts as a calcification inhibitor in VSMCs [201, 202]. On the other hand, cleaved OPN acts as a pro-inflammatory cytokine facilitating vascular mineralization [201, 203, 204]. Similar to Thbs-4 OPN has also been implicated in macrophage adhesion and migration, another important factor in the development of atherosclerosis [307]. In this study, the transcription of the gene *Spp1* [2] was enhanced by OSM indicating that OPN might play an important role for atherogenesis (Figure 4.9).

Furthermore, tenascin C (*Tnc*) is strongly induced by OSM as well (Figure 4.9). This ECM glycoprotein is normally expressed in a variety of embryonic tissues, but its expression in adult tissues is low in healthy individuals. At sites of vascular disease, however, *Tnc* has been shown to be up-regulated and its best described pathophysiological function is its involvement in intimal hyperplasia [197, 308, 309]. It has been suggested that the induction of *Tnc* is related to an altered SMC phenotype [310]. The TnC polypeptide contains following domains: tenascin assembly domain, epidermal growth factor-like domains, fibronectin type III (FN III) domains and a fibrinogen-homology domain. Alternative splicing results in a number of various isoforms which contain one

[2] *Spp1* encodes OPN protein

to six extra FN III domains. These isoforms of TnC appear to have different pathophysiological effects [197]. In this study primer sets were used to amplify *Tnc* mRNA which detect a region in the variably spliced A to D FNIII repeats (exactly AD2 to C). This region is known to bind to annexin II (annexin A2) localized to the extracellular leaflet of the plasma membrane, whereby cell adhesion is inhibited [197, 199]. Annexin II was originally characterised as a cytoplasmic protein [311]. However, it can also be secreted to the extracellular space by an unknown mechanism acting as a receptor for various proteins [312, 313, 314]. Experiments demonstrate that loss of focal adhesions, mitogenesis, and enhanced cell migration result from the interaction of the alternatively spliced segment TNfnA-D with annexin II [314].

Chemokines and their receptors play an important role in the regulation of inflammatory diseases like atherosclerosis [315]. They are expressed by many cells of the vessel wall including endothelial cells [316] and smooth muscle cells [217, 317], but also from emigrating leukocytes. Their functional contribution to atherogenesis is well described in the reviews by Zernecke and Weber [318, 319]. In this study, CCR1 was strongly regulated by OSM (Figure 4.10). This protein acts as receptor for the chemokines CCL3/MIP-1α, CCL4/MIP-1β, and CCL5/RANTES. Therefore, OSM could have an important function in the early activation of VSMCs from a quiescent to a proliferating status. Initially considered as important receptors expressed in monocytes and T lymphocytes to allow their transendothelial migration, chemokine receptors have been shown to be expressed on VSMCs where they play an important role in the proliferation and migration of VSMCs from the media to the intima [218]. *Ccr1* deficiency was shown to exacerbate plaque formation [320]. However, studies using *Ccr1* deficient mice indicated that the effect of this chemokine receptor on plaque development appears to be highly stage-dependent. Compared to control mice, atherosclerotic lesions in *Ccr1*$^{-/-}$ *Apoe*$^{-/-}$ mice are smaller after one month, comparable at two months and larger at three months of high-fat diet [321]. The initial protective effect of *Ccr1* deficiency might be a direct result of its role in leukocyte recruitment, particularly of neutrophils and Ly6C^{hi} inflammatory monocytes. Interestingly, in these studies no changes in cell-surface expression levels could be detected for CCR1 on Ly6C^{hi} monocytes [321] or neutrophils [322] in *Apoe*$^{-/-}$ mice. In contrast to these finding the results presented in this thesis showed an increased cell surface expression of CCR1 in VSMCs (Figure 4.11). Since CCR1 is expressed in VSMCs [218] its function in these cells might contribute substantially to atherogenesis [217, 323]. *In vivo* application of Met-RANTES, a known antagonist of CCR1, reduces progression of atherosclerosis in hypercholesterolemic mice [323]. Here, the authors do

not only observe a decrease in leukocyte infiltration, but also an increase of collagen-rich atheroma, features associated with plaque stability. A recent study investigating intima thickening in graft arterial disease elucidated that the invading smooth muscle-like cells dominating the intima differed from medial aortic SMC particularly in the expression of CCR1 [217].

The principle role of SerpinB2 [3] and PAI-1 is the inhibition of urokinase plasminogen activator (uPA) and tissue plasminogen activator (tPA). The binding of uPA or tPA to PAI-1 or PAI-2 may alter cell-associated proteolytic activity, degradation of ECM, and neointimal formation after vascular injury [324]. Both plasminogen activators, uPA and tPA, produced by monocytes/macrophages activate plasminogen triggering a proteolysis cascade. SerpinB2 is expressed by many different cell types including monocytes/macrophages, fibroblasts, and endothelial cells in connection with inflammatory processes [209] as well as smooth muscle cells [210, 211, 212]. Due to intracellular binding partners, SerpinB2 is not necessarily secreted [213]. Next to angiotensin II, which stimulates PAI-1 and -2 expression in vascular endothelial and smooth muscle cells [210], also OSM induces *Pai2* mRNA expression in VSMCs (Figure 4.10). It was already described that PAI-1 was induced by OSM in human VSMCs [325] and by IL-6 and OSM in human adipose tissue [326]. Furthermore, the authors speculated that OSM may contribute to plaque progression, plaque destabilization, and thrombus formation, since OSM enhanced the proliferation of smooth muscle cells via the induction of PAI-1 [325]. Similar results may be true between OSM and SerpinB2 in VSMCs, but further investigations are necessary.

5.2.3 Blockade of ERK1/2 or p38 activity affects OSM-mediated transcription of Thbs4, Ccr1, Col3a1, and Eln

OSM is a strong activator of different signalling pathways. In order to characterise the involvement of MAPK signalling pathways in the transcription of OSM-regulated target genes, VSMC were pre-incubated with the MEK1/2 inhibitor III or the p38 MAPK inhibitor SB203580 prior to stimulation with OSM. Earlier studies showed that expressions and functional activities of CCR1 and CCR2 were reduced upon inhibition of p38 MAPK and ERK activity in 9-cis retinoic acid treated human monocytic THP-1 cells indicating that both pathways are involved in CCR1 and CCR2 expression in these cells

[3] SerpinB2 = PAI-2 (Plasminogen activator inhibitor-2)

[327]. OSM-mediated *Ccr1* as well as *Thbs4* mRNA expression in VSMCs is ERK1/2 dependent, since inhibition of their upstream kinase MEK1/2 abrogates the enhanced transcription of both genes (Figure 4.13). Inhibition of p38 MAPK, however, led to a further increase in OSM-mediated *Ccr1* expression indicating that other pathways - which are able to enhance the *Ccr1* mRNA level as well - may be negatively regulated by the p38 MAPK pathway (Figure 4.14). Böing *et al.* nicely showed that the OSM induced phosphorylation of ERK1/2 was prolonged from 30 to 60 minutes when MCF-7 breast carcinoma cells were treated with p38 inhibitor SB202190 [328]. Although the phosphorylation of ERK1/2 after treatment with p38 inhibitor SB203580 and OSM was not investigated in this thesis, ERK1/2 itself might be negatively regulated by p38 MAPK. While gene transcription of *Thbs4* and *Ccr1* was completely blocked after treatment with MEK1/2 inhibitor III, the amount of OSM-mediated *Col3a1* mRNA was enhanced (Figure 4.13) indicating a suppressive activity of ERK1/2 pathway on collagen type III expression. Experiments on rat pulmonary arterial smooth muscle cells (PASMCs) showed that urotensin II induced proliferation and collagen synthesis seems to be ERK1/2 dependent [329]. Thus, several mechanisms for the synthesis of collagens are possible due to the environment of SMCs. Moreover, the transcription of *Col3a1* was not influenced by p38 MAPK pathway (Figure 4.14). On the one hand, basal *Eln* mRNA expression was slightly increased when treated with MEK1/2 inhibitor III. This suggests a suppressive effect of ERK1/2 (Figure 4.13). On the other hand, basal transcription decreased upon inhibition of SB203580 activity indicating that p38 MAPK pathway may prevent to a certain degree the loss of *Eln* transcription in VSMCs (Figure 4.14). Thus, the regulation of *Eln* transcription seems to be balanced by different signalling pathways and is only interrupted after OSM stimulation.
In conclusion, up-regulation of *Thbs4* and *Ccr1* mRNA in VSMCs is ERK1/2 dependent. Furthermore, ERK1/2 functions as a suppressor for the transcription of *Col3a1*. Balance between different pathways may protect *Eln* mRNA level against accelerated degradation. In order to get more insights in this field, further experiments with other inhibitors and more detailed analysis of biochemical changes in OSM-induced signalling pathways are required.

Taken together, OSM might influence de-differentiation, proliferation, and calcification of VSMCs through the regulation of certain target genes promoting atherogenesis. With exception of CCR1, all results in these subsections were carried out on mRNA level. As a future prospect, OSM-induced changes in the protein expression level of these genes have to be accomplished by cell culture (*in vitro*) or by an atherosclerotic mouse model

(*in vivo*) to confirm the obtained mRNA data.

5.3 Influence of the Th2 cytokines IL-4/IL-13 and the Th17 cytokine IL-17 on VSMCs compared to OSM

Although macrophages and Th1 cells are the predominant immune cell types in atherosclerotic lesions, IL-4/IL-13 producing Th2 and Th17 cells, which secrete IL-17, are present as well. However, the function of their released cytokines in atherogenesis is still not fully understood. IL-4 deficiency in the *Apoe*$^{-/-}$ model reduces atherosclerotic lesions [129]. Another study showed that IL-4 does not significantly influence the development of atherosclerotic lesions in *Apoe*$^{-/-}$ mice of either gender or in female *Ldlr*$^{-/-}$ mice, irrespective of the mode of induction of atherosclerosis [135]. Administration of IL-13 in *Ldlr*$^{-/-}$ model promotes favourable plaque morphology by increasing lesional collagen content, decreasing VCAM-dependent monocyte recruitment and inducing M2 macrophage phenotype [137]. Deficiency of IL-13 accelerates atherosclerosis [137]. Similarly to IL-4, there is still a controversial discussion about the influence of IL-17. Some studies assumed that IL-17 is protective [147, 148], while others postulate it is pathogenic [146, 149, 150] or has even no effect on the alteration of plaque burden [151, 152]. A summary of the role of cytokines in atherosclerosis together with therapeutic approaches is reviewed by Ramji *et al.* [227].
In the study summarized here, VSMCs isolated from murine aortas were treated with OSM, IL-4, IL-13, and IL-17A to investigate changes in receptor and target gene expressions as well as in the signalling pathways.

5.3.1 Receptor expression regulated by OSM, but not by IL-4, IL-13 or IL-17

As seen before in this study, smooth muscle cells express the OSM receptor type I (LIFRβ/gp130) and II (OSMRβ/gp130), but also the IL-4/IL-13 receptor type II (IL-4R/IL-13Rα1), and the IL-17 receptor (IL-17RA/IL-17RC) [156, 330]. As shown and discussed earlier OSM stimulation of VSMCs enhances OSMRβ and gp130 and reduces LIFRβ expression (Figure 4.5 and 4.6, Subsection 5.2.1). None of the investigated Th2 cytokines - IL-4 or IL-13 - influenced the transcription of the signal transducing

IL-6-type cytokine receptors (gp130, OSMRβ, LIFRβ) in VSMCs. The influence of IL-17A was not analysed here. Besides the regulation of its own signalling receptor complex, OSM stimulation of VSMCs resulted in an increased amount of mRNA for the IL-4/IL-13 receptor type II (Figure 4.15). For the IL-4Rα increased expression was confirmed on protein level, shown by an enhanced fluorescence intensity of OSM-stimulated VSMCs labelled with anti-IL-4Rα antibodies (Figure 4.16). Studies with HASMCs and fibroblasts confirmed these results nicely [156, 158]. Another study showed that on several haematopoietic cell lines, the Th2 cytokine IL-4 itself was able to regulate the expression of IL-4Rα [331, 332]. This offered the possibility that OSM induces the enhanced transcription of IL-4Rα indirectly via induction of IL-4 production and release from VSMCs. However, direct stimulation of VSMCs with either IL-4 or IL-13 did not increase the amount of detectable mRNA for IL-4Rα or IL-13Rα (Figure 4.15). Therefore, it seems likely that OSM directly induces the enhanced transcription of the IL-4/IL-13 receptor type II complex. Promising transcription factor candidates to be involved in the increase in IL-4Rα mRNA levels are OSM-activated STAT3 and STAT6. In T cells, the IL-4 induced *Il4r* gene transcription was STAT6 dependent [333]. Kwofie *et al.* showed that transcription of the genes encoding *Il17ra* and *Il17rc* was not changed after OSM treatment [156]. In this thesis, the expression level of the IL-17 receptor complex was not investigated in VSMCs. IL-17A treatment had no impact on the expression of *Il6st*, *Osmr*, *Il4ra* or *Il13ra1* in VSMCs (Figure 4.21) and in human airway smooth muscle cells (HASMCs) [156].
In summary, OSM, but not IL-4, IL-13 or IL-17A stimulates the transcription of various cytokine receptor genes in VSMCs, namely the OSMR type I and type II as well as the receptor type II complex for Th2 cytokines IL-4/IL-13. At least for the IL-4Rα an increase in protein expression in response to OSM could be confirmed.

5.3.2 Expression of Col3a1, Eln, and OPG mainly regulated by OSM

Three out of the ten atherosclerotic target genes regulated by OSM (Subsection 4.3.2) were chosen to elaborate cross-talk effects in response to OSM, IL-4, IL-13 or IL-17A treatment. *Col3a1*, *Eln*, and *Tnfrsf11b* [4] are involved in the regulation and composition of extracellular matrix (ECM) and were regulated by OSM (Figure 4.9). Hofbauer *et al.* postulated that IL-4 influences the OPG expression in human coronary artery

[4] *Tnfrsf11b* encodes protein OPG

smooth muscle cells (CASMCs) [228]. Indeed, they showed that short-term exposure of IL-4 enhances the OPG production through a STAT6-dependent mechanism, while long-term exposure causes an osteogenic transformation and a decreased production of OPG. Furthermore, IL-4 and IL-13 decreased *Rankl* and *Rank* mRNA and increased *Tnfrsf11b* mRNA in calvariae which was also STAT6 dependent [334]. Further evidence came from Stein *et al.* who demonstrated that IL-4 and IL-13 induced OPG expression through activation of STAT6 in endothelial cells [335].

In contrast, IL-17 enhances the expression of RANKL and inhibits the expression of OPG in human periodontal ligament cells (hPDLCs) [336]. However, no regulation of the *Tnfrsf11b* mRNA level was detectable in VSMCS in response to IL-4, IL-13 or IL-17 stimulation (Figure 4.17 and 4.22). In the study by Lin *et al.* a concentration of 50ng/ml IL-17 was used for the stimulation of hPDLCs [336], whereas a five time lower concentration was used for all three cytokines in this study indicating that an increase in the concentration may also influence the gene transcription in VSMCs. However, future experiments need to corroborate this hypothesis.

Similar to the findings that IL-13 reduces the transcription level of *Eln* in VSMCs (Figure 4.17), IL-13 suppresses elastin gene expression in airway fibroblasts as well which is mediated by matrix metalloproteinases-1 and -2 (MMP1 and MMP2) [337]. Although it is described that IL-4 regulates the expression of collagen genes and ECM proteins in human fibroblasts [338, 339, 340], this result could not be verified in murine VSMCs (Figure 4.17). Only the *Col3a1* mRNA was slightly increased after IL-4 or IL-13 stimulation for 24 hours. In addition, a synergistic or additive effect for gene transcription after OSM+IL-4 or OSM+IL13 treatment was not seen in VSMCs (Figure 4.17). Furthermore, it was shown that the expression of elastin was decreased in IL-17 deficient (*Il17-/-*) mice [341]. However, the function of IL-17 in atherosclerosis is still disputed. In this study, IL-17A showed no effect on the regulation of *Col3a1*, *Eln* or *Tnfrsf11b* mRNA expression in VSMCs (Figure 4.22). In general, an inactivity of this Th17 cytokine can be excluded, since the mRNA expression of *Il13ra2* and *Il6* was regulated by IL-17A on VSMCs (Figure 4.23, Subsection 5.3.4 and 5.3.5). For future studies, a dose-response experiment for IL-17A on VSMCs will be helpful. However, the transcription of *Eln* was significantly less pronounced when cells were stimulated with OSM+IL-17A compared to OSM treatment alone (Figure 4.22).
To conclude, the mRNA level of all three genes was less strongly influenced by Th2 or Th17 cytokines compared to the IL-6-type cytokine OSM.

5.3.3 Signal transduction of IL-4 and IL-13 appears to be limited to STAT6 phosphorylation in VSMCs

Upon binding of OSM to its receptor complex, changes in gene transcription require the activation of several signalling pathways (JAK/STAT, Ras-Raf-MAPK, PI3K/Akt). Thereby, the activation of different transcription factors of the STAT family or downstream of the kinases ERK1/2, p38, and Akt is achieved mainly through phosphorylation of specific activatory sites by OSM in VSMCs (Figure 4.7). In contrast to all other IL-6-type cytokines, OSM is a potent inducer of STAT6 phosphorylation at Y641 in VSMCs (Figure 4.18) and fibroblasts [158]. The activation of this transcription factor has so far mainly been attributed to IL-4 and IL-13 which also induce a phosphorylation of STAT6 (Y641) in VSMCs, but no other tested signalling pathway (Figure 4.18). Fritz *et al.* showed further that STAT6 phosphorylation can be increased when fibroblasts were primed with OSM before IL-4 or IL-13 stimulation [158]. According to their results this experiment was repeated here for smooth muscle cells. However, despite the fact that OSM increased the expression of the IL-4/IL-13 receptor complex, the priming effect could not be verified in VSMCs (Figure 4.19). One possible explanation for the missing priming effect could be the enhanced expression of the decoy receptor IL-13Rα2 by OSM. As known so far, IL-13Rα2 is a target gene of and a negative feedback mechanism for IL-13. The activation of STAT6 mediated by IL-13 is decelerated when the decoy receptor is expressed on the cell surface [342]. Indeed, OSM stimulation leads to a pronounced increase in the *Il13ra2* mRNA expression level (Figure 4.20). However, this explanation does not necessarily hold true for the cytokine IL-4, since at least it is not bound by IL-13Rα2 and therefore possibly not negatively regulated in the same way as IL-13. Therefore, it remains currently unclear why OSM priming did not increase the IL-4 mediated STAT6 phosphorylation in VSMCs in a similar manner as described for fibroblasts [158].

5.3.4 The decoy receptor for IL-13 (IL-13Ra2) is synergistically regulated by OSM, IL-4, IL-13, and IL-17

The decoy receptor IL-13Rα2 is a target gene of IL-13. Once located at the cell surface, it binds IL-13 with a higher affinity than the IL-4/IL-13 receptor type II. The cytoplasmic part of IL-13Rα2 is very short without any binding sites for JAKs, an indication that no

signalling occurs downstream of this receptor subunit. Therefore, it is postulated that IL-13Rα2 acts as a negative feedback mechanism for IL-13 [165, 166, 167]. However, studies carried out by Fichtner-Feigl *et al.* indicate that IL-13 signals through IL-13Rα2; thereby it induces TGFβ1 production in macrophages in a STAT6-independent pathway leading to collagen deposition *in vivo* [168]. The up-regulation of IL-13Rα2 by both IL-4 and IL-13 has been described in different cell types [167, 343, 344]. Moreover, treatment of epithelial cells with IFN-γ increases surface expression of IL-13Rα2 through mobilisation from intracellular stores [169]. This indicates that different cytokines are involved in the regulation of IL-13Rα2 expression and that this receptor subunit might regulate the Th1 and Th2 cell balance and their responses. Indeed, all tested cytokines in this study - OSM, IL-4, IL-13, and IL-17A - induce increased mRNA expression for *Il13ra2* in VSMCs (Figure 4.20 and 4.23). Gene transcription is even more enhanced when cells were simultaneously stimulated with OSM in combination with IL-4, IL-13 or IL-17A. While combination with IL-4 resulted in an additive effect, simultaneous stimulation of OSM with IL-13 or IL-17 appeared to mediate even a synergistic increase in *Il13ra2* transcription. This indicates that more IL-13Rα2 could be expressed on the cell surface resulting in a more pronounced negative regulation of IL-13 signalling (Figure 4.20 and 4.23). However, protein expression for IL-13Rα2 could not be tested since no specific antibody for Western blot or FACS analysis was available within the time frame of this thesis. Next to the membrane bound form, a soluble form of IL-13Rα2 (sIL-13Rα2) was found in mice [169, 170, 171] but not in humans [173]. It is postulated that these two alternatively spliced variants of IL-13Rα2 may have a distinct biological function *in vivo* [172]. However, the mechanism of how this decoy receptor regulates IL-13 signalling is still in the focus of new investigations.

5.3.5 IL-6 transcription is synergistically regulated by OSM and IL-17

OSM and IL-6 are secreted by macrophages [94] - cells which can be found in early and in ruptured plaques [89, 90]. Earlier studies already described that OSM induced the production of IL-6 in endothelial cells or fibroblasts [93, 229]. Furthermore, a synergistically regulated expression of IL-6 was mediated by simultaneous OSM and IL-17A stimulation in HASMCs [156]. Similar results were obtained in VSMCs (Figure 4.23). Thereby, cells treated with OSM together with IL-17A showed a higher *Il6* mRNA ex-

pression (12-fold) compared to OSM or IL-17A alone (7-fold and 3-fold respectively). Neither IL-4 nor IL-13 was able to regulate the mRNA level of *Il6* (data not shown). So far, the role of IL-6 in atherogenesis is discussed controversially. Huber *et al.* described that fatty lesion development in *Apoe* deficient mice on a high-cholesterol diet was enhanced by weekly injections of recombinant mouse IL-6 compared to non-obese diabetic (NOD) mice [87]. However, $Apoe^{+/-}$ $Il6^{-/-}$ mice on a cholesterol rich diet developed unstable plaques, since macrophage infiltration, apoptosis, and lipid content were increased and SMC mass was decreased indicating an athero-protective role for IL-6 [88]. Indeed, an enhanced formation of atherosclerotic lesions, reduced collagen metabolism, and elevated levels of serum cholesterol was measured in *Il6* deficient $Apoe^{-/-}$ ($Apoe^{-/-}$ $Il6^{-/-}$) mice [345].
Taken together, the cross-talk of OSM with other cytokines seems to be an important factor to understand its role in atherogenesis. Therefore, further investigations on this topic are helpful and relevant.

5.4 Characterisation of Ldr-/- Osmr-/- mice compared to Ldlr-/- Osmr +/+ mice on WD

B6.129S7-Ldlr$^{tm1Her/J}$ ($Ldlr^{-/-}$) mice are deficient for the low density lipoprotein receptor (*Ldlr*) leading to a blockade for the clearance of lipoproteins followed by a moderate accumulation of LDL on normal chow diet [78, 85]. When these mice are fed a cholesterol rich diet (Western diet, WD), they develop hyperlipidemia and atherosclerotic lesions [85].
$Osmr^{-/-}$ mice are not able to respond to OSM but their phenotype and behaviour is normal, albeit slight differences in haematopoiesis [3]. Further analysis demonstrated that the numbers of peripheral erythrocytes and platelets were reduced compared to wild-type mice [3]. Moreover, progenitors of erythroid and megakaryocyte lineages were reduced in the bone marrow (BM) of $Osmr^{-/-}$ mice indicating that OSM might be required for the maintenance of erythroid and megakaryocyte progenitor pools in BM [3]. New studies could show that $Osmr^{-/-}$ mice develop hepatic steatosis and obesity induced insulin resistance with age [230].

Both mouse lines - $Ldlr^{-/-}$ and $Osmr^{-/-}$ - have the same *C57Bl/6* background and were crossed to generate $Ldlr^{-/-}Osmr^{-/-}$ and $Ldlr^{-/-}Osmr^{+/+}$ mice. In order to induce an

atherosclerotic situation, 11 weeks old *Ldlr*$^{-/-}$*Osmr*$^{+/+}$ and *Ldlr*$^{-/-}$*Osmr*$^{-/-}$ female mice were fed a Western diet (WD) for 12 weeks. At 23 weeks of age, the mice were sacrificed and characterised for differences in plaque development and physical conditions as well as changes in glucose level, blood components and gene expression. For a better interpretation and discussion, results from the controls *C57Bl/6* and *Osmr*$^{-/-}$ mice under the same conditions were used partially although their treatment was not completed until the end of this study.

Before and during WD treatment, the body weight of *Ldlr*$^{-/-}$*Osmr*$^{+/+}$ and *Ldlr*$^{-/-}$*Osmr*$^{-/-}$ mice was measured. At 11 weeks of age and the beginning of WD treatment, the body weight of *Ldlr*$^{-/-}$*Osmr*$^{+/+}$ mice increased by four gram in comparison to *Ldlr*$^{-/-}$*Osmr*$^{-/-}$ mice. At the end of WD treatment, *Ldlr*$^{-/-}$*Osmr*$^{+/+}$ mice also gained more weight compared to *Ldlr*$^{-/-}$*Osmr*$^{-/-}$ mice (Figure 4.24 A). Komori *et al.* showed that the body weight of *Osmr*$^{-/-}$ already increases when getting older compared to wild-type mice under standard chow [230] as well as under high fat diet (HFD) conditions [346] at eight weeks of age. Interestingly, *Osmr* deficient *Ldlr*$^{-/-}$ mice, when compared with *Osmr*$^{-/-}$ mice under the same feeding conditions, showed the opposite effect (Data not shown). Similar results were obtained for the liver. *Osmr*$^{-/-}$ and *Ldlr*$^{-/-}$*Osmr*$^{+/+}$ mice had an increased liver weight (Data not shown) whereas the liver weight from *Ldlr*$^{-/-}$*Osmr*$^{-/-}$ mice decreased (Figure 4.24 B). The deficiency of Ldlr seems to reduce body and liver weight gain in *Osmr*$^{-/-}$ mice.

Komori *et al.* showed further that *Osmr* deficient mice exhibit higher glucose and serum insulin levels in fed and fasted conditions at 32 weeks of age and already higher serum insulin levels at 16 weeks of age [230]. These results suggest that *Osmr*$^{-/-}$ mice exhibit systemic inflammation and disturbance of glucose metabolism preceding obesity [230]. Furthermore, the blood glucose level raised in *Osmr*$^{-/-}$ mice compared to wild-type mice when fed a high fat diet [230]. In this study, the blood glucose level of *Osmr*$^{-/-}$ under standard chow and WD conditions at 23 weeks of age did not change compared to *C57Bl/6* mice (Data not shown). In contrast, the blood glucose level from both *Ldlr*$^{-/-}$*Osmr*$^{+/+}$ and *Ldlr*$^{-/-}$*Osmr*$^{-/-}$ mice was increased compared to *Osmr*$^{-/-}$ mice after 12 weeks of WD treatment. However, blood glucose level of *Ldlr*$^{-/-}$*Osmr*$^{-/-}$ mice was less strong enhanced in comparison to *Ldlr*$^{-/-}$*Osmr*$^{+/+}$ mice (Figure 4.25) indicating that missing OSMRβ reduces the blood glucose level in mice.

Additionally, the erythrocyte and thrombocyte counts decreased in *Ldlr*$^{-/-}$*Osmr*$^{-/-}$ mice compared to *Ldlr*$^{-/-}$*Osmr*$^{+/+}$ mice, whereas the leukocyte count was the same in both groups. The mean cell volume (MCV) of erythrocytes, however, was significantly larger

in *Ldlr*$^{-/-}$*Osmr*$^{-/-}$ mice than in *Ldlr*$^{-/-}$*Osmr*$^{+/+}$ mice (Figure 4.26).
Moreover, the loss of OSMRβ seems to reduce atherosclerosis in mice, since plaque size of the atherosclerotic lesion area as well as in the total plaque area of aortic roots was decreased in *Ldlr*$^{-/-}$*Osmr*$^{-/-}$ mice in comparison to *Ldlr*$^{-/-}$*Osmr*$^{+/+}$ mice (Figure 4.27 and 4.28).

Another point of this thesis included the analysis of liver mRNA of *Ldlr*$^{-/-}$*Osmr*$^{+/+}$ and *Ldlr*$^{-/-}$*Osmr*$^{-/-}$ mice after 12 weeks of WD. Thereby, liver enzymes and transporter as well as proteins regulating ECM compositions and of course receptor expressions were detected via qRT-PCR. It was shown before that deficiency of CYP7A1 results in a hypercholesterolemic phenotype in humans [232] and it causes the development of atherosclerosis, cholesterol gallstone and fatty liver disease in mice [233]. In this study, *Ldlr*$^{-/-}$*Osmr*$^{-/-}$ mice expressed higher levels of *Cyp7a1* mRNA compared to *Ldlr*$^{-/-}$*Osmr*$^{+/+}$ mice when fed a WD (Figure 4.29). Together with lower liver weight (Figure 4.24 B) this indicates that there might be a prevention for *Ldlr*$^{-/-}$*Osmr*$^{-/-}$ mice developing a fatty liver disease compared to *Ldlr*$^{-/-}$*Osmr*$^{+/+}$ mice. Most of the other tested liver enzymes remained unchanged in both mouse groups. However for a better interpretation of these results, this mRNA levels have to be compared with wild-type (*C57Bl/6*) or *Osmr*$^{-/-}$ mice under the same WD condition.
Only the expression of liver transporter *Ntcp* showed a slightly but significantly different mRNA level in the double deficient mice compared to *Ldlr*$^{-/-}$*Osmr*$^{+/+}$ mice after feeding with WD for 12 weeks (Figure 4.30). Former studies examined the hypothesis that bile acids which are FXR ligands mediate negative feedback regulation of *Ntcp* via activation of the FXR target gene *Shp* [347, 268, 269]. However, *Shp* up-regulation and thus *Ntcp* mRNA down-regulation could not be verified without comparison of the mRNA expression level from *C57Bl/6* or *Osmr*$^{-/-}$ with those of *Ldlr*$^{-/-}$*Osmr*$^{+/+}$ and *Ldlr*$^{-/-}$*Osmr*$^{-/-}$ mice.

As expected, the transcription amount of *Osmr* was decreased in *Ldlr*$^{-/-}$*Osmr*$^{-/-}$ mice compared to *Ldlr*$^{-/-}$*Osmr*$^{+/+}$ mice. The *Ldlr* mRNA level did not change, since both groups do not express LDLR (Figure 4.31). Interestingly, *Osmr*$^{-/-}$ showed only 50% of *Ldlr* expression compared to *C57Bl/6* due to the fact that *Ldlr* is a target gene of OSM (Data not shown).
The mRNA level of *Col3a1* and *Tnfrsf11b* [5] was decreased, whereas *Spp1* [6] was signifi-

[5] *Tnfrsf11b* encodes for OPG protein
[6] *Spp1* encodes for OPN protein

cantly higher expressed in the liver of *Ldlr*$^{-/-}$*Osmr*$^{-/-}$ mice in comparison to *Ldlr*$^{-/-}$*Osmr*$^{+/+}$ mice (Figure 4.32). If this effect resulted from the treatment with WD or from the knock-out in the *Osmr* gene could not be clarified. Further investigations by using positive controls (*C57Bl/6* or *Osmr*$^{-/-}$ mice) under WD or *Ldlr*$^{-/-}$*Osmr*$^{+/+}$ and *Ldlr*$^{-/-}$*Osmr*$^{-/-}$ mice under normal diet would be useful.

All in all, *Ldlr*$^{-/-}$*Osmr*$^{-/-}$ mice seem to be less affected by atherosclerosis or by the development of fatty liver disease compared to Ldlr$^{-/-}$ mice. However, further investigations are necessary to discover the role of OSM during the development of atherosclerotic lesions in mice.

5.5 Concluding remarks

This thesis shows that the interleukin-6-type cytokine OSM is a strong inducer of an array of target genes involved in de-differentiation, proliferation, and calcification of VSMCs, a process known to contribute substantially to atherogenesis. As underlying mechanism, the OSM-mediated regulation of two genes - *Thbs4* and *Ccr1* - is shown to be ERK-dependent. On protein level, however, only the upregulation of CCR1 could be confirmed. For the other identified target genes these findings still need to be verified when appropriate antibodies will become available. Furthermore, OSM regulates the mRNA and protein expression of its own receptor complex (OSMRβ, gp130) and the IL-4 receptor type II complex consisting of IL-4R and IL-13Rα1. The gene for decoy receptor IL-13Rα2 (*Il13ra2*) was not only regulated by OSM, but also by IL-4, IL-13, and IL-17A alone or synergistically with OSM (Figure 5.1).
Our new mouse model - the double deficient *Ldlr*$^{-/-}$*Osmr*$^{-/-}$ mouse - gave new insights on the role of OSM for the development of atherosclerosis when fed a Western diet (WD). Nevertheless, further studies are required to determine the relevance of these findings and the potential role of OSM antagonists as therapeutic agents in atherosclerosis *in vivo* and *in vitro*.

5.6 Perspective

The *in vitro* study on vascular smooth muscle cells gave first insights into the role of OSM for the pathophysiology and differentiation of these cells. With the help of the RT^2 Profiler PCR™ Array, several protein target genes of OSM were identified which are involved in the regulation and composition of extracellular matrix (ECM), required for cell adhesion or the immune response. However, it is still not clear if OSM influences the migration of VSMCs into the intima of atherosclerotic lesions or if co-stimulation with cytokines other than IL-4, IL-13 or IL-17A has any effect on VSMCs. Furthermore, only 10 out of 18 genes regulated by OSM were used for further experiments in VSMCs. According to these findings, however, other genes recognised by this array could be of interest as well. Since OSM shows a multifunctional character, many possibilities are conceivable. Additionally, the results for atherosclerotic target genes were obtained on mRNA level. With the exception of CCR1, the regulation by OSM on protein level could not be tested without specific antibodies during the time frame of this thesis. Therefore, future experiments will be needed to confirm these mRNA results when further antibodies will be available.

The *in vivo* studies carried out in this thesis gave new insights on the complex biology of OSM in the organism. After *Ldlr*$^{-/-}$*Osmr*$^{+/+}$ and *Ldlr*$^{-/-}$*Osmr*$^{-/-}$ mice were fed a WD for 12 weeks, atherosclerosis was induced in these animals and analysed. It was clearly shown that the development of atherosclerotic lesions was reduced in *Ldlr*$^{-/-}$*Osmr*$^{-/-}$ mice compared to *Ldlr*$^{-/-}$*Osmr*$^{+/+}$ mice. With respect to the findings by Komori *et al.* who showed that *Osmr*$^{-/-}$ mice are prone to develop insulin resistance and liver steatosis [230], this result was rather surprising. However it fits to observations made by Kubin *et al.* who investigated OSM activity in the context of cardiomyopathies. They could clearly show that OSM can carry out beneficial as well as detrimental activities depending on the model used to induce the cardiomyopathy [348]. Since these experiments were still at the beginning when this thesis was concluded further investigations are needed to determine the underlying molecular mechanism. Furthermore, shorter or longer feeding times (e.g. six or 18 weeks of WD) will complement these findings.

With the *Ldlr*$^{-/-}$*Osmr*$^{-/-}$ mouse, a new atherosclerotic mouse model was generated studying the role of OSM in one of the most common diseases in the western world and a major cause of deaths.

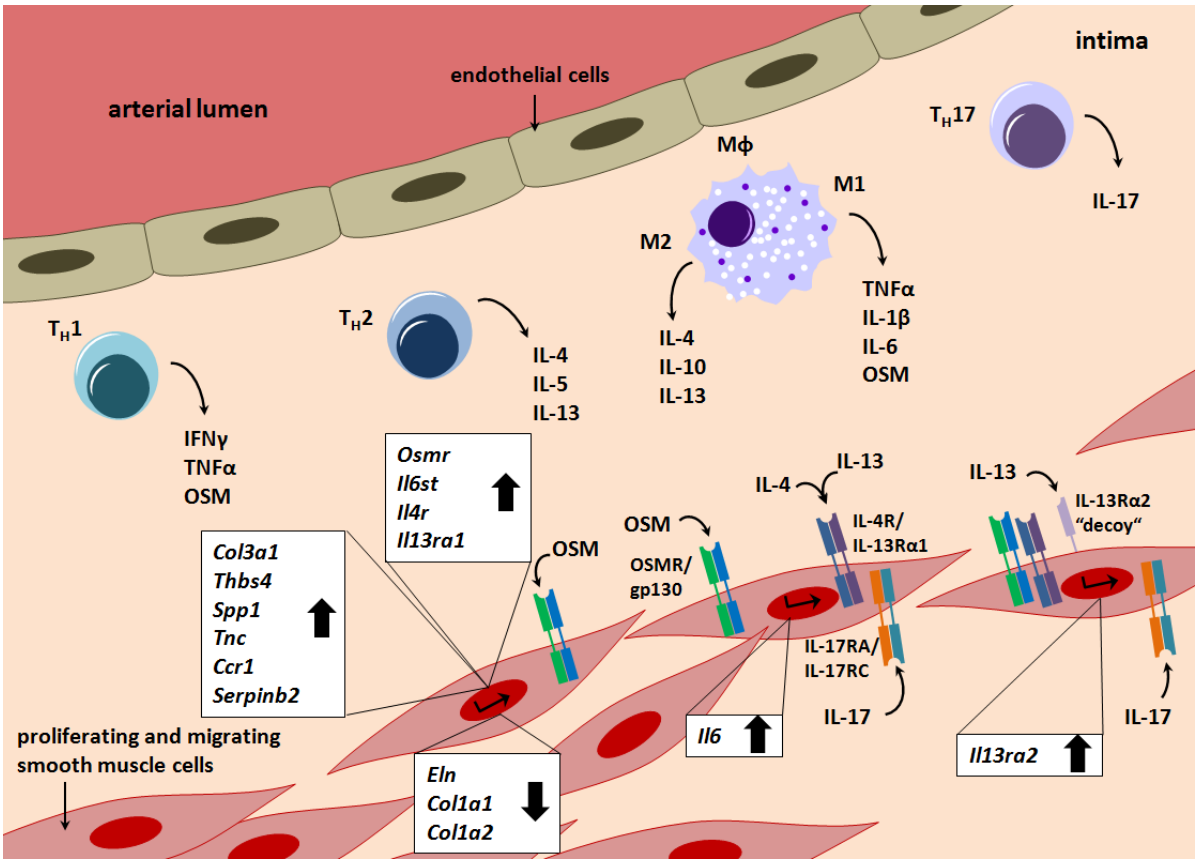

Figure 5.1: **Summarising the influence of OSM on murine VSMCs.** Within the intima of an atherosclerotic lesion, several immune cells including T helper cells (Th1, Th2, Th17), macrophages (MΦ), and dendritic cells (not shown) can be found. Th cells and MΦ secrete different cytokines which are able to bind to receptors on the cell surface of VSMCs. OSM activates different signalling pathways leading to changes in gene transcription. OSM induced the up-regulation of atherosclerotic target genes (*Col3a1*, *Thbs4*, *Spp1*, *Tnc*, *Ccr1*, *Serpinb2*) as well as genes for several cytokine receptors (*Osmr*, *Il6st*, *Il4r*, and *Il13ra1*). Down-regulated genes by OSM are *Eln*, *Col1a1*, and *Col1a2*. Additionally, OSM, IL-4, IL-13, and IL-17 are responsible for the regulation of the decoy receptor *Il13ra2* mRNA. Enhanced *Il6* mRNA level is induced by OSM and IL-17, particularly strong by a combination of both cytokines.

Bibliography

[1] J. M. Zarling, M. Shoyab, H. Marquardt, M. B. Hanson, M. N. Lioubin, and G. J. Todaro. Oncostatin M: a growth regulator produced by differentiated histiocytic lymphoma cells. *Proc. Natl. Acad. Sci. U.S.A.*, 83(24):9739–9743, Dec 1986.

[2] H. E. Broxmeyer, H. A. Bruns, S. Zhang, S. Cooper, G. Hangoc, A. N. McKenzie, A. L. Dent, U. Schindler, L. K. Naeger, T. Hoey, and M. H. Kaplan. Th1 cells regulate hematopoietic progenitor cell homeostasis by production of oncostatin M. *Immunity*, 16(6):815–825, Jun 2002.

[3] M. Tanaka, Y. Hirabayashi, T. Sekiguchi, T. Inoue, M. Katsuki, and A. Miyajima. Targeted disruption of oncostatin M receptor results in altered hematopoiesis. *Blood*, 102(9):3154–3162, Nov 2003.

[4] T. Kinoshita, K. Nagata, N. Sorimachi, H. Karasuyama, T. Sekiguchi, and A. Miyajima. Oncostatin M suppresses generation of lymphoid progenitors in fetal liver by inhibiting the hepatic microenvironment. *Exp. Hematol.*, 29(9):1091–1097, Sep 2001.

[5] T. Kinoshita, T. Sekiguchi, M. J. Xu, Y. Ito, A. Kamiya, K. Tsuji, T. Nakahata, and A. Miyajima. Hepatic differentiation induced by oncostatin M attenuates fetal liver hematopoiesis. *Proc. Natl. Acad. Sci. U.S.A.*, 96(13):7265–7270, Jun 1999.

[6] A. Kamiya, T. Kinoshita, Y. Ito, T. Matsui, Y. Morikawa, E. Senba, K. Nakashima, T. Taga, K. Yoshida, T. Kishimoto, and A. Miyajima. Fetal liver development requires a paracrine action of oncostatin M through the gp130 signal transducer. *EMBO J.*, 18(8):2127–2136, Apr 1999.

[7] A. Okaya, J. Kitanaka, N. Kitanaka, M. Satake, Y. Kim, K. Terada, T. Sugiyama, M. Takemura, J. Fujimoto, N. Terada, A. Miyajima, and T. Tsujimura. Oncostatin

M inhibits proliferation of rat oval cells, OC15-5, inducing differentiation into hepatocytes. *Am. J. Pathol.*, 166(3):709–719, Mar 2005.

[8] K. Nakamura, H. Nonaka, H. Saito, M. Tanaka, and A. Miyajima. Hepatocyte proliferation and tissue remodeling is impaired after liver injury in oncostatin M receptor knockout mice. *Hepatology*, 39(3):635–644, Mar 2004.

[9] C. H. Clegg, J. T. Rulffes, P. M. Wallace, and H. S. Haugen. Regulation of an extrathymic T-cell development pathway by oncostatin M. *Nature*, 384(6606):261–263, Nov 1996.

[10] C. Boileau, M. Houde, G. Dulude, C. H. Clegg, and C. Perreault. Regulation of extrathymic T cell development and turnover by oncostatin M. *J. Immunol.*, 164(11):5713–5720, Jun 2000.

[11] M. Vasse, J. Pourtau, V. Trochon, M. Muraine, J. P. Vannier, H. Lu, J. Soria, and C. Soria. Oncostatin M induces angiogenesis in vitro and in vivo. *Arterioscler. Thromb. Vasc. Biol.*, 19(8):1835–1842, Aug 1999.

[12] W. Hui, M. Bell, and G. Carroll. Detection of oncostatin M in synovial fluid from patients with rheumatoid arthritis. *Ann. Rheum. Dis.*, 56(3):184–187, Mar 1997.

[13] C. Bonifati, A. Mussi, L. D'Auria, M. Carducci, E. Trento, P. Cordiali-Fei, and F. Ameglio. Spontaneous release of leukemia inhibitory factor and oncostatin-M is increased in supernatants of short-term organ cultures from lesional psoriatic skin. *Arch. Dermatol. Res.*, 290(1-2):9–13, 1998.

[14] A. Gazel, M. Rosdy, B. Bertino, C. Tornier, F. Sahuc, and M. Blumenberg. A characteristic subset of psoriasis-associated genes is induced by oncostatin-M in reconstituted epidermis. *J. Invest. Dermatol.*, 126(12):2647–2657, Dec 2006.

[15] A. Albasanz-Puig, J. , M. Preusch, D. Coan, M. Namekata, Y. Patel, Z. M. Dong, M. E. Rosenfeld, and E. S. Wijelath. Oncostatin M is expressed in atherosclerotic lesions: a role for Oncostatin M in the pathogenesis of atherosclerosis. *Atherosclerosis*, 216(2):292–298, Jun 2011.

[16] A. Grenier, D. Combaux, J. Chastre, M. A. Gougerot-Pocidalo, C. Gibert, M. Dehoux, and S. Chollet-Martin. Oncostatin M production by blood and alveolar neutrophils during acute lung injury. *Lab. Invest.*, 81(2):133–141, Feb 2001.

[17] T. J. Brown, M. N. Lioubin, and H. Marquardt. Purification and characterization of cytostatic lymphokines produced by activated human T lymphocytes. Synergistic antiproliferative activity of transforming growth factor beta 1, interferon-gamma, and oncostatin M for human melanoma cells. *J. Immunol.*, 139(9):2977–2983, Nov 1987.

[18] T. Suda, K. Chida, A. Todate, K. Ide, K. Asada, Y. Nakamura, K. Suzuki, H. Kuwata, and H. Nakamura. Oncostatin M production by human dendritic cells in response to bacterial products. *Cytokine*, 17(6):335–340, Mar 2002.

[19] T. M. Rose and A. G. Bruce. Oncostatin M is a member of a cytokine family that includes leukemia-inhibitory factor, granulocyte colony-stimulating factor, and interleukin 6. *Proc. Natl. Acad. Sci. U.S.A.*, 88(19):8641–8645, Oct 1991.

[20] P. C. Heinrich, I. Behrmann, G. Muller-Newen, F. Schaper, and L. Graeve. Interleukin-6-type cytokine signalling through the gp130/Jak/STAT pathway. *Biochem. J.*, 334 (Pt 2):297–314, Sep 1998.

[21] D. Derouet, F. Rousseau, F. Alfonsi, J. Froger, J. Hermann, F. Barbier, D. Perret, C. Diveu, C. Guillet, L. Preisser, A. Dumont, M. Barbado, A. Morel, O. deLapeyriere, H. Gascan, and S. Chevalier. Neuropoietin, a new IL-6-related cytokine signaling through the ciliary neurotrophic factor receptor. *Proc. Natl. Acad. Sci. U.S.A.*, 101(14):4827–4832, Apr 2004.

[22] S. Pflanz, J. C. Timans, J. Cheung, R. Rosales, H. Kanzler, J. Gilbert, L. Hibbert, T. Churakova, M. Travis, E. Vaisberg, W. M. Blumenschein, J. D. Mattson, J. L. Wagner, W. To, S. Zurawski, T. K. McClanahan, D. M. Gorman, J. F. Bazan, R. de Waal Malefyt, D. Rennick, and R. A. Kastelein. IL-27, a heterodimeric cytokine composed of EBI3 and p28 protein, induces proliferation of naive CD4+ T cells. *Immunity*, 16(6):779–790, Jun 2002.

[23] G. Senaldi, B. C. Varnum, U. Sarmiento, C. Starnes, J. Lile, S. Scully, J. Guo, G. Elliott, J. McNinch, C. L. Shaklee, D. Freeman, F. Manu, W. S. Simonet, T. Boone, and M. S. Chang. Novel neurotrophin-1/B cell-stimulating factor-3: a cytokine of the IL-6 family. *Proc. Natl. Acad. Sci. U.S.A.*, 96(20):11458–11463, Sep 1999.

[24] U. A. White and J. M. Stephens. The gp130 receptor cytokine family: regulators of adipocyte development and function. *Curr. Pharm. Des.*, 17(4):340–346, 2011.

[25] J. V. Castell, M. J. Gomez-Lechon, M. David, R. Fabra, R. Trullenque, and P. C. Heinrich. Acute-phase response of human hepatocytes: regulation of acute-phase protein synthesis by interleukin-6. *Hepatology*, 12(5):1179–1186, Nov 1990.

[26] P. C. Heinrich, I. Behrmann, S. Haan, H. M. Hermanns, G. Muller-Newen, and F. Schaper. Principles of interleukin (IL)-6-type cytokine signalling and its regulation. *Biochem. J.*, 374(Pt 1):1–20, Aug 2003.

[27] L. W. Collison, G. M. Delgoffe, C. S. Guy, K. M. Vignali, V. Chaturvedi, D. Fairweather, A. R. Satoskar, K. C. Garcia, C. A. Hunter, C. G. Drake, P. J. Murray, and D. A. Vignali. The composition and signaling of the IL-35 receptor are unconventional. *Nat. Immunol.*, 13(3):290–299, Mar 2012.

[28] S. R. Dillon, C. Sprecher, A. Hammond, J. Bilsborough, M. Rosenfeld-Franklin, S. R. Presnell, H. S. Haugen, M. Maurer, B. Harder, J. Johnston, S. Bort, S. Mudri, J. L. Kuijper, T. Bukowski, P. Shea, D. L. Dong, M. Dasovich, F. J. Grant, L. Lockwood, S. D. Levin, C. LeCiel, K. Waggie, H. Day, S. Topouzis, J. Kramer, R. Kuestner, Z. Chen, D. Foster, J. Parrish-Novak, and J. A. Gross. Interleukin 31, a cytokine produced by activated T cells, induces dermatitis in mice. *Nat. Immunol.*, 5(7):752–760, Jul 2004.

[29] N. Ghilardi, J. Li, J. A. Hongo, S. Yi, A. Gurney, and F. J. de Sauvage. A novel type I cytokine receptor is expressed on monocytes, signals proliferation, and activates STAT-3 and STAT-5. *J. Biol. Chem.*, 277(19):16831–16836, May 2002.

[30] T. Kishimoto, S. Akira, M. Narazaki, and T. Taga. Interleukin-6 family of cytokines and gp130. *Blood*, 86(4):1243–1254, Aug 1995.

[31] S. Chevalier, M. Fourcin, O. Robledo, J. Wijdenes, A. Pouplard-Barthelaix, and H. Gascan. Interleukin-6 family of cytokines induced activation of different functional sites expressed by gp130 transducing protein. *J. Biol. Chem.*, 271(25):14764–14772, Jun 1996.

[32] H. M. Hermanns. Oncostatin M and interleukin-31: Cytokines, receptors, signal transduction and physiology. *Cytokine Growth Factor Rev.*, 26(5):545–558, Oct 2015.

[33] N. Malik, H. S. Haugen, B. Modrell, M. Shoyab, and C. H. Clegg. Developmental abnormalities in mice transgenic for bovine oncostatin M. *Mol. Cell. Biol.*, 15(5):2349–2358, May 1995.

[34] T. Hara, M. Ichihara, A. Yoshimura, and A. Miyajima. Cloning and biological activity of murine oncostatin M. *Leukemia*, 11 Suppl 3:449–450, Apr 1997.

[35] D. P. Gearing, M. R. Comeau, D. J. Friend, S. D. Gimpel, C. J. Thut, J. McGourty, K. K. Brasher, J. A. King, S. Gillis, and B. Mosley. The IL-6 signal transducer, gp130: an oncostatin M receptor and affinity converter for the LIF receptor. *Science*, 255(5050):1434–1437, Mar 1992.

[36] M. Ichihara, T. Hara, H. Kim, T. Murate, and A. Miyajima. Oncostatin M and leukemia inhibitory factor do not use the same functional receptor in mice. *Blood*, 90(1):165–173, Jul 1997.

[37] B. Mosley, C. De Imus, D. Friend, N. Boiani, B. Thoma, L. S. Park, and D. Cosman. Dual oncostatin M (OSM) receptors. Cloning and characterization of an alternative signaling subunit conferring OSM-specific receptor activation. *J. Biol. Chem.*, 271(51):32635–32643, Dec 1996.

[38] R. A. Lindberg, T. S. Juan, A. A. Welcher, Y. Sun, R. Cupples, B. Guthrie, and F. A. Fletcher. Cloning and characterization of a specific receptor for mouse oncostatin M. *Mol. Cell. Biol.*, 18(6):3357–3367, Jun 1998.

[39] M. Tanaka, T. Hara, N. G. Copeland, D. J. Gilbert, N. A. Jenkins, and A. Miyajima. Reconstitution of the functional mouse oncostatin M (OSM) receptor: molecular cloning of the mouse OSM receptor beta subunit. *Blood*, 93(3):804–815, Feb 1999.

[40] J. Drechsler, J. Grotzinger, and H. M. Hermanns. Characterization of the rat oncostatin M receptor complex which resembles the human, but differs from the murine cytokine receptor. *PLoS ONE*, 7(8):e43155, 2012.

[41] D. Metcalf. The unsolved enigmas of leukemia inhibitory factor. *Stem Cells*, 21(1):5–14, 2003.

[42] D. P. Gearing, T. VandenBos, M. P. Beckmann, C. J. Thut, M. R. Comeau, B. Mosley, and S. F. Ziegler. Reconstitution of high affinity leukaemia inhibitory

factor (LIF) receptors in haemopoietic cells transfected with the cloned human LIF receptor. *Ciba Found. Symp.*, 167:245–255, 1992.

[43] J. G. Zhang, C. M. Owczarek, L. D. Ward, G. J. Howlett, L. J. Fabri, B. A. Roberts, and N. A. Nicola. Evidence for the formation of a heterotrimeric complex of leukaemia inhibitory factor with its receptor subunits in solution. *Biochem. J.*, 325 (Pt 3):693–700, Aug 1997.

[44] D. J. Hilton and N. A. Nicola. Kinetic analyses of the binding of leukemia inhibitory factor to receptor on cells and membranes and in detergent solution. *J. Biol. Chem.*, 267(15):10238–10247, May 1992.

[45] C. M. Owczarek, Y. Zhang, M. J. Layton, D. Metcalf, B. Roberts, and N. A. Nicola. The unusual species cross-reactivity of the leukemia inhibitory factor receptor alpha-chain is determined primarily by the immunoglobulin-like domain. *J. Biol. Chem.*, 272(38):23976–23985, Sep 1997.

[46] A. F. Wilks, A. G. Harpur, R. R. Kurban, S. J. Ralph, G. Zurcher, and A. Ziemiecki. Two novel protein-tyrosine kinases, each with a second phosphotransferase-related catalytic domain, define a new class of protein kinase. *Mol. Cell. Biol.*, 11(4):2057–2065, Apr 1991.

[47] A. G. Harpur, A. C. Andres, A. Ziemiecki, R. R. Aston, and A. F. Wilks. JAK2, a third member of the JAK family of protein tyrosine kinases. *Oncogene*, 7(7):1347–1353, Jul 1992.

[48] T. Takahashi and T. Shirasawa. Molecular cloning of rat JAK3, a novel member of the JAK family of protein tyrosine kinases. *FEBS Lett.*, 342(2):124–128, Apr 1994.

[49] I. Firmbach-Kraft, M. Byers, T. Shows, R. Dalla-Favera, and J. J. Krolewski. tyk2, prototype of a novel class of non-receptor tyrosine kinase genes. *Oncogene*, 5(9):1329–1336, Sep 1990.

[50] K. Ghoreschi, A. Laurence, and J. J. O'Shea. Janus kinases in immune cell signaling. *Immunol. Rev.*, 228(1):273–287, Mar 2009.

[51] S. G. Rane and E. P. Reddy. JAK3: a novel JAK kinase associated with terminal differentiation of hematopoietic cells. *Oncogene*, 9(8):2415–2423, Aug 1994.

[52] R. J. Duhe and W. L. Farrar. Structural and mechanistic aspects of Janus kinases: how the two-faced god wields a double-edged sword. *J. Interferon Cytokine Res.*, 18(1):1–15, Jan 1998.

[53] C. Haan, H. Is'harc, H. M. Hermanns, H. Schmitz-Van De Leur, I. M. Kerr, P. C. Heinrich, J. Grotzinger, and I. Behrmann. Mapping of a region within the N terminus of Jak1 involved in cytokine receptor interaction. *J. Biol. Chem.*, 276(40):37451–37458, Oct 2001.

[54] J. E. Darnell, I. M. Kerr, and G. R. Stark. Jak-STAT pathways and transcriptional activation in response to IFNs and other extracellular signaling proteins. *Science*, 264(5164):1415–1421, Jun 1994.

[55] H. M. Hermanns, S. Radtke, F. Schaper, P. C. Heinrich, and I. Behrmann. Non-redundant signal transduction of interleukin-6-type cytokines. The adapter protein Shc is specifically recruited to rhe oncostatin M receptor. *J. Biol. Chem.*, 275(52):40742–40748, Dec 2000.

[56] C. F. Lai, J. Ripperger, K. K. Morella, Y. Wang, D. P. Gearing, G. H. Fey, and H. Baumann. Separate signaling mechanisms are involved in the control of STAT protein activation and gene regulation via the interleukin 6 response element by the box 3 motif of gp130. *J. Biol. Chem.*, 270(25):14847–14850, Jun 1995.

[57] D. K. Fritz, C. Kerr, R. Fattouh, A. Llop-Guevara, W. I. Khan, M. Jordana, and C. D. Richards. A mouse model of airway disease: oncostatin M-induced pulmonary eosinophilia, goblet cell hyperplasia, and airway hyperresponsiveness are STAT6 dependent, and interstitial pulmonary fibrosis is STAT6 independent. *J. Immunol.*, 186(2):1107–1118, Jan 2011.

[58] D. K. Fritz, C. Kerr, L. Tong, D. Smyth, and C. D. Richards. Oncostatin-M up-regulates VCAM-1 and synergizes with IL-4 in eotaxin expression: involvement of STAT6. *J. Immunol.*, 176(7):4352–4360, Apr 2006.

[59] T. Fukada, M. Hibi, Y. Yamanaka, M. Takahashi-Tezuka, Y. Fujitani, T. Yamaguchi, K. Nakajima, and T. Hirano. Two signals are necessary for cell proliferation induced by a cytokine receptor gp130: involvement of STAT3 in anti-apoptosis. *Immunity*, 5(5):449–460, Nov 1996.

[60] M. Takahashi-Tezuka, Y. Yoshida, T. Fukada, T. Ohtani, Y. Yamanaka, K. Nishida, K. Nakajima, M. Hibi, and T. Hirano. Gab1 acts as an adapter molecule linking the cytokine receptor gp130 to ERK mitogen-activated protein kinase. *Mol. Cell. Biol.*, 18(7):4109–4117, Jul 1998.

[61] N. Stahl, T. J. Farruggella, T. G. Boulton, Z. Zhong, J. E. Darnell, and G. D. Yancopoulos. Choice of STATs and other substrates specified by modular tyrosine-based motifs in cytokine receptors. *Science*, 267(5202):1349–1353, Mar 1995.

[62] G. Pearson, F. Robinson, T. Beers Gibson, B. E. Xu, M. Karandikar, K. Berman, and M. H. Cobb. Mitogen-activated protein (MAP) kinase pathways: regulation and physiological functions. *Endocr. Rev.*, 22(2):153–183, Apr 2001.

[63] S. H. Jee, H. C. Chiu, T. F. Tsai, W. L. Tsai, Y. H. Liao, C. Y. Chu, and M. L. Kuo. The phosphotidyl inositol 3-kinase/Akt signal pathway is involved in interleukin-6-mediated Mcl-1 upregulation and anti-apoptosis activity in basal cell carcinoma cells. *J. Invest. Dermatol.*, 119(5):1121–1127, Nov 2002.

[64] M. Kortylewski, F. Feld, K. D. Kruger, G. Bahrenberg, R. A. Roth, H. G. Joost, P. C. Heinrich, I. Behrmann, and A. Barthel. Akt modulates STAT3-mediated gene expression through a FKHR (FOXO1a)-dependent mechanism. *J. Biol. Chem.*, 278(7):5242–5249, Feb 2003.

[65] R. Eulenfeld and F. Schaper. A new mechanism for the regulation of Gab1 recruitment to the plasma membrane. *J. Cell. Sci.*, 122(Pt 1):55–64, Jan 2009.

[66] P. Libby, P. M. Ridker, and G. K. Hansson. Progress and challenges in translating the biology of atherosclerosis. *Nature*, 473(7347):317–325, May 2011.

[67] G. K. Hansson and A. Hermansson. The immune system in atherosclerosis. *Nat. Immunol.*, 12(3):204–212, Mar 2011.

[68] R. Ross. Atherosclerosis–an inflammatory disease. *N. Engl. J. Med.*, 340(2):115–126, Jan 1999.

[69] C. Weber and H. Noels. Atherosclerosis: current pathogenesis and therapeutic options. *Nat. Med.*, 17(11):1410–1422, 2011.

[70] A. C. van der Wal and A. E. Becker. Atherosclerotic plaque rupture–pathologic basis of plaque stability and instability. *Cardiovasc. Res.*, 41(2):334–344, Feb 1999.

[71] K. Skalen, M. Gustafsson, E. K. Rydberg, L. M. Hulten, O. Wiklund, T. L. Innerarity, and J. Boren. Subendothelial retention of atherogenic lipoproteins in early atherosclerosis. *Nature*, 417(6890):750–754, Jun 2002.

[72] I. Tabas, K. J. Williams, and J. Boren. Subendothelial lipoprotein retention as the initiating process in atherosclerosis: update and therapeutic implications. *Circulation*, 116(16):1832–1844, Oct 2007.

[73] E. Matsuura, K. Kobayashi, M. Tabuchi, and L. R. Lopez. Oxidative modification of low-density lipoprotein and immune regulation of atherosclerosis. *Prog. Lipid Res.*, 45(6):466–486, Nov 2006.

[74] G. K. Hansson and P. Libby. The immune response in atherosclerosis: a double-edged sword. *Nat. Rev. Immunol.*, 6(7):508–519, Jul 2006.

[75] B. Halvorsen, K. Otterdal, T. B. Dahl, M. Skjelland, L. Gullestad, E. ?ie, and P. Aukrust. Atherosclerotic plaque stability–what determines the fate of a plaque? *Prog Cardiovasc Dis*, 51(3):183–194, 2008.

[76] G. K. Hansson, A. K. Robertson, and C. Soderberg-Naucler. Inflammation and atherosclerosis. *Annu Rev Pathol*, 1:297–329, 2006.

[77] G. S. Getz and C. A. Reardon. Animal models of atherosclerosis. *Arterioscler. Thromb. Vasc. Biol.*, 32(5):1104–1115, May 2012.

[78] J. F. Bentzon and E. Falk. Atherosclerotic lesions in mouse and man: is it the same disease? *Curr. Opin. Lipidol.*, 21(5):434–440, Oct 2010.

[79] S. H. Zhang, R. L. Reddick, J. A. Piedrahita, and N. Maeda. Spontaneous hypercholesterolemia and arterial lesions in mice lacking apolipoprotein E. *Science*, 258(5081):468–471, Oct 1992.

[80] A. S. Plump, J. D. Smith, T. Hayek, K. Aalto-Setala, A. Walsh, J. G. Verstuyft, E. M. Rubin, and J. L. Breslow. Severe hypercholesterolemia and atherosclerosis in apolipoprotein E-deficient mice created by homologous recombination in ES cells. *Cell*, 71(2):343–353, Oct 1992.

[81] Y. Nakashima, A. S. Plump, E. W. Raines, J. L. Breslow, and R. Ross. ApoE-deficient mice develop lesions of all phases of atherosclerosis throughout the arterial tree. *Arterioscler. Thromb.*, 14(1):133–140, Jan 1994.

[82] G. S. Getz and C. A. Reardon. Apoprotein E as a lipid transport and signaling protein in the blood, liver, and artery wall. *J. Lipid Res.*, 50 Suppl:S156–161, Apr 2009.

[83] S. Fazio, V. R. Babaev, A. B. Murray, A. H. Hasty, K. J. Carter, L. A. Gleaves, J. B. Atkinson, and M. F. Linton. Increased atherosclerosis in mice reconstituted with apolipoprotein E null macrophages. *Proc. Natl. Acad. Sci. U.S.A.*, 94(9):4647–4652, Apr 1997.

[84] M. Van Eck, N. Herijgers, M. Vidgeon-Hart, N. J. Pearce, P. M. Hoogerbrugge, P. H. Groot, and T. J. Van Berkel. Accelerated atherosclerosis in C57Bl/6 mice transplanted with ApoE-deficient bone marrow. *Atherosclerosis*, 150(1):71–80, May 2000.

[85] S. Ishibashi, M. S. Brown, J. L. Goldstein, R. D. Gerard, R. E. Hammer, and J. Herz. Hypercholesterolemia in low density lipoprotein receptor knockout mice and its reversal by adenovirus-mediated gene delivery. *J. Clin. Invest.*, 92(2):883–893, Aug 1993.

[86] L. K. Curtiss, N. Kubo, N. K. Schiller, and W. A. Boisvert. Participation of innate and acquired immunity in atherosclerosis. *Immunol. Res.*, 21(2-3):167–176, 2000.

[87] S. A. Huber, P. Sakkinen, D. Conze, N. Hardin, and R. Tracy. Interleukin-6 exacerbates early atherosclerosis in mice. *Arterioscler. Thromb. Vasc. Biol.*, 19(10):2364–2367, Oct 1999.

[88] M. Madan, B. Bishayi, M. Hoge, and S. Amar. Atheroprotective role of interleukin-6 in diet- and/or pathogen-associated atherosclerosis using an ApoE heterozygote murine model. *Atherosclerosis*, 197(2):504–514, Apr 2008.

[89] J. J. Boyle. Macrophage activation in atherosclerosis: pathogenesis and pharmacology of plaque rupture. *Curr Vasc Pharmacol*, 3(1):63–68, Jan 2005.

[90] J. J. Boyle, P. L. Weissberg, and M. R. Bennett. Tumor necrosis factor-alpha promotes macrophage-induced vascular smooth muscle cell apoptosis by direct and autocrine mechanisms. *Arterioscler. Thromb. Vasc. Biol.*, 23(9):1553–1558, Sep 2003.

[91] J. P. Pelletier and J. Martel-Pelletier. Oncostatin M: foe or friend? *Arthritis Rheum.*, 48(12):3301–3303, Dec 2003.

[92] S. P. Kastl, W. S. Speidl, K. M. Katsaros, C. Kaun, G. Rega, A. Assadian, G. W. Hagmueller, M. Hoeth, R. de Martin, Y. Ma, G. Maurer, K. Huber, and J. Wojta. Thrombin induces the expression of oncostatin M via AP-1 activation in human macrophages: a link between coagulation and inflammation. *Blood*, 114(13):2812–2818, Sep 2009.

[93] T. J. Brown, J. M. Rowe, J. W. Liu, and M. Shoyab. Regulation of IL-6 expression by oncostatin M. *J. Immunol.*, 147(7):2175–2180, Oct 1991.

[94] C. D. Richards. The Enigmatic Cytokine Oncostatin M and Roles in Disease. *ISRN Inflamm*, 2013:512103, 2013.

[95] R. I. Grove, C. Eberhardt, S. Abid, C. Mazzucco, J. Liu, P. Kiener, G. Todaro, and M. Shoyab. Oncostatin M is a mitogen for rabbit vascular smooth muscle cells. *Proc. Natl. Acad. Sci. U.S.A.*, 90(3):823–827, Feb 1993.

[96] V. Modur, M. J. Feldhaus, A. S. Weyrich, D. L. Jicha, S. M. Prescott, G. A. Zimmerman, and T. M. McIntyre. Oncostatin M is a proinflammatory mediator. In vivo effects correlate with endothelial cell expression of inflammatory cytokines and adhesion molecules. *J. Clin. Invest.*, 100(1):158–168, Jul 1997.

[97] V. P. Iyemere, D. Proudfoot, P. L. Weissberg, and C. M. Shanahan. Vascular smooth muscle cell phenotypic plasticity and the regulation of vascular calcification. *J. Intern. Med.*, 260(3):192–210, Sep 2006.

[98] M. J. Barnes and R. W. Farndale. Collagens and atherosclerosis. *Exp. Gerontol.*, 34(4):513–525, Jul 1999.

[99] C. M. Shanahan, N. R. Cary, J. C. Metcalfe, and P. L. Weissberg. High expression of genes for calcification-regulating proteins in human atherosclerotic plaques. *J. Clin. Invest.*, 93(6):2393–2402, Jun 1994.

[100] C. M. Shanahan and P. L. Weissberg. Smooth muscle cell heterogeneity: patterns of gene expression in vascular smooth muscle cells in vitro and in vivo. *Arterioscler. Thromb. Vasc. Biol.*, 18(3):333–338, Mar 1998.

[101] P. L. Weissberg, G. J. Clesham, and M. R. Bennett. Is vascular smooth muscle cell proliferation beneficial? *Lancet*, 347(8997):305–307, Feb 1996.

[102] D. A. Chistiakov, A. N. Orekhov, and Y. V. Bobryshev. Vascular smooth muscle cell in atherosclerosis. *Acta Physiol (Oxf)*, 214(1):33–50, May 2015.

[103] W. Karwowski, B. Naumnik, M. Szczepa?ski, and M. My?liwiec. The mechanism of vascular calcification - a systematic review. *Med. Sci. Monit.*, 18(1):1–11, Jan 2012.

[104] M. J. Butcher and E. V. Galkina. Phenotypic and functional heterogeneity of macrophages and dendritic cell subsets in the healthy and atherosclerosis-prone aorta. *Front Physiol*, 3:44, 2012.

[105] J. H. Qiao, J. Tripathi, N. K. Mishra, Y. Cai, S. Tripathi, X. P. Wang, S. Imes, M. C. Fishbein, S. K. Clinton, P. Libby, A. J. Lusis, and T. B. Rajavashisth. Role of macrophage colony-stimulating factor in atherosclerosis: studies of osteopetrotic mice. *Am. J. Pathol.*, 150(5):1687–1699, May 1997.

[106] K. J. Moore and I. Tabas. Macrophages in the pathogenesis of atherosclerosis. *Cell*, 145(3):341–355, Apr 2011.

[107] V. Andres, O. M. Pello, and C. Silvestre-Roig. Macrophage proliferation and apoptosis in atherosclerosis. *Curr. Opin. Lipidol.*, 23(5):429–438, Oct 2012.

[108] J. Khallou-Laschet, A. Varthaman, G. Fornasa, C. Compain, A. T. Gaston, M. Clement, M. Dussiot, O. Levillain, S. Graff-Dubois, A. Nicoletti, and G. Caligiuri. Macrophage plasticity in experimental atherosclerosis. *PLoS ONE*, 5(1):e8852, 2010.

[109] A. Kadl, A. K. Meher, P. R. Sharma, M. Y. Lee, A. C. Doran, S. R. Johnstone, M. R. Elliott, F. Gruber, J. Han, W. Chen, T. Kensler, K. S. Ravichandran, B. E. Isakson, B. R. Wamhoff, and N. Leitinger. Identification of a novel macrophage phenotype that develops in response to atherogenic phospholipids via Nrf2. *Circ. Res.*, 107(6):737–746, Sep 2010.

[110] R. Kleemann, S. Zadelaar, and T. Kooistra. Cytokines and atherosclerosis: a comprehensive review of studies in mice. *Cardiovasc. Res.*, 79(3):360–376, Aug 2008.

[111] R. M. Steinman. Linking innate to adaptive immunity through dendritic cells. *Novartis Found. Symp.*, 279:101–109, 2006.

[112] W. E. Paul, R. Steinman, B. Beutler, and J. Hoffmann. Bridging innate and adaptive immunity. *Cell*, 147(6):1212–1215, Dec 2011.

[113] C. Erbel, K. Sato, F. B. Meyer, S. L. Kopecky, R. L. Frye, J. J. Goronzy, and C. M. Weyand. Functional profile of activated dendritic cells in unstable atherosclerotic plaque. *Basic Res. Cardiol.*, 102(2):123–132, Mar 2007.

[114] Y. V. Bobryshev, T. Taksir, R. S. Lord, and M. W. Freeman. Evidence that dendritic cells infiltrate atherosclerotic lesions in apolipoprotein E-deficient mice. *Histol. Histopathol.*, 16(3):801–808, Jul 2001.

[115] F. Geissmann, S. Jung, and D. R. Littman. Blood monocytes consist of two principal subsets with distinct migratory properties. *Immunity*, 19(1):71–82, Jul 2003.

[116] K. E. Paulson, S. N. Zhu, M. Chen, S. Nurmohamed, J. Jongstra-Bilen, and M. I. Cybulsky. Resident intimal dendritic cells accumulate lipid and contribute to the initiation of atherosclerosis. *Circ. Res.*, 106(2):383–390, Feb 2010.

[117] E. K. Koltsova and K. Ley. How dendritic cells shape atherosclerosis. *Trends Immunol.*, 32(11):540–547, Nov 2011.

[118] C. Buono, H. Pang, Y. Uchida, P. Libby, A. H. Sharpe, and A. H. Lichtman. B7-1/B7-2 costimulation regulates plaque antigen-specific T-cell responses and atherogenesis in low-density lipoprotein receptor-deficient mice. *Circulation*, 109(16):2009–2015, Apr 2004.

[119] J. Sun, K. Hartvigsen, M. Y. Chou, Y. Zhang, G. K. Sukhova, J. Zhang, M. Lopez-Ilasaca, C. J. Diehl, N. Yakov, D. Harats, J. George, J. L. Witztum, P. Libby, H. Ploegh, and G. P. Shi. Deficiency of antigen-presenting cell invariant chain reduces atherosclerosis in mice. *Circulation*, 122(8):808–820, Aug 2010.

[120] E. C. de Jong, H. H. Smits, and M. L. Kapsenberg. Dendritic cell-mediated T cell polarization. *Springer Semin. Immunopathol.*, 26(3):289–307, Jan 2005.

[121] H. H. Smits, A. J. van Beelen, C. Hessle, R. Westland, E. de Jong, E. Soeteman, A. Wold, E. A. Wierenga, and M. L. Kapsenberg. Commensal Gram-negative bacteria prime human dendritic cells for enhanced IL-23 and IL-27 expression and enhanced Th1 development. *Eur. J. Immunol.*, 34(5):1371–1380, May 2004.

[122] M. Benagiano, A. Azzurri, A. Ciervo, A. Amedei, C. Tamburini, M. Ferrari, J. L. Telford, C. T. Baldari, S. Romagnani, A. Cassone, M. M. D'Elios, and G. Del Prete. T helper type 1 lymphocytes drive inflammation in human atherosclerotic lesions. *Proc. Natl. Acad. Sci. U.S.A.*, 100(11):6658–6663, May 2003.

[123] A. Tedgui and Z. Mallat. Cytokines in atherosclerosis: pathogenic and regulatory pathways. *Physiol. Rev.*, 86(2):515–581, Apr 2006.

[124] J. Frostegard, A. K. Ulfgren, P. Nyberg, U. Hedin, J. Swedenborg, U. Andersson, and G. K. Hansson. Cytokine expression in advanced human atherosclerotic plaques: dominance of pro-inflammatory (Th1) and macrophage-stimulating cytokines. *Atherosclerosis*, 145(1):33–43, Jul 1999.

[125] L. Rogge, E. Bianchi, M. Biffi, E. Bono, S. Y. Chang, H. Alexander, C. Santini, G. Ferrari, L. Sinigaglia, M. Seiler, M. Neeb, J. Mous, F. Sinigaglia, and U. Certa. Transcript imaging of the development of human T helper cells using oligonucleotide arrays. *Nat. Genet.*, 25(1):96–101, May 2000.

[126] G. Paulsson, X. Zhou, E. Tornquist, and G. K. Hansson. Oligoclonal T cell expansions in atherosclerotic lesions of apolipoprotein E-deficient mice. *Arterioscler. Thromb. Vasc. Biol.*, 20(1):10–17, Jan 2000.

[127] G. Liuzzo, J. J. Goronzy, H. Yang, S. L. Kopecky, D. R. Holmes, R. L. Frye, and C. M. Weyand. Monoclonal T-cell proliferation and plaque instability in acute coronary syndromes. *Circulation*, 101(25):2883–2888, Jun 2000.

[128] R. Elhage, J. Jawien, M. Rudling, H. G. Ljunggren, K. Takeda, S. Akira, F. Bayard, and G. K. Hansson. Reduced atherosclerosis in interleukin-18 deficient apolipoprotein E-knockout mice. *Cardiovasc. Res.*, 59(1):234–240, Jul 2003.

[129] P. Davenport and P. G. Tipping. The role of interleukin-4 and interleukin-12 in the progression of atherosclerosis in apolipoprotein E-deficient mice. *Am. J. Pathol.*, 163(3):1117–1125, Sep 2003.

[130] C. Buono, C. J. Binder, G. Stavrakis, J. L. Witztum, L. H. Glimcher, and A. H. Lichtman. T-bet deficiency reduces atherosclerosis and alters plaque antigen-specific immune responses. *Proc. Natl. Acad. Sci. U.S.A.*, 102(5):1596–1601, Feb 2005.

[131] T. S. Lee, H. C. Yen, C. C. Pan, and L. Y. Chau. The role of interleukin 12 in the development of atherosclerosis in ApoE-deficient mice. *Arterioscler. Thromb. Vasc. Biol.*, 19(3):734–742, Mar 1999.

[132] S. Gupta, A. M. Pablo, X. c. Jiang, N. Wang, A. R. Tall, and C. Schindler. IFN-gamma potentiates atherosclerosis in ApoE knock-out mice. *J. Clin. Invest.*, 99(11):2752–2761, Jun 1997.

[133] S. C. Whitman, P. Ravisankar, and A. Daugherty. Interleukin-18 enhances atherosclerosis in apolipoprotein E(-/-) mice through release of interferon-gamma. *Circ. Res.*, 90(2):E34–38, Feb 2002.

[134] A. H. Lichtman. Adaptive immunity and atherosclerosis: mouse tales in the AJP. *Am. J. Pathol.*, 182(1):5–9, Jan 2013.

[135] V. L. King, L. A. Cassis, and A. Daugherty. Interleukin-4 does not influence development of hypercholesterolemia or angiotensin II-induced atherosclerotic lesions in mice. *Am. J. Pathol.*, 171(6):2040–2047, Dec 2007.

[136] C. J. Binder, K. Hartvigsen, M. K. Chang, M. Miller, D. Broide, W. Palinski, L. K. Curtiss, M. Corr, and J. L. Witztum. IL-5 links adaptive and natural immunity specific for epitopes of oxidized LDL and protects from atherosclerosis. *J. Clin. Invest.*, 114(3):427–437, Aug 2004.

[137] L. Cardilo-Reis, S. Gruber, S. M. Schreier, M. Drechsler, N. Papac-Milicevic, C. Weber, O. Wagner, H. Stangl, O. Soehnlein, and C. J. Binder. Interleukin-13 protects from atherosclerosis and modulates plaque composition by skewing the macrophage phenotype. *EMBO Mol Med*, 4(10):1072–1086, Oct 2012.

[138] L. A. Tesmer, S. K. Lundy, S. Sarkar, and D. A. Fox. Th17 cells in human disease. *Immunol. Rev.*, 223:87–113, Jun 2008.

[139] H. Hamada, M. d. e. L. Garcia-Hernandez, J. B. Reome, S. K. Misra, T. M. Strutt, K. K. McKinstry, A. M. Cooper, S. L. Swain, and R. W. Dutton. Tc17, a unique subset of CD8 T cells that can protect against lethal influenza challenge. *J. Immunol.*, 182(6):3469–3481, Mar 2009.

[140] S. Taleb, A. Tedgui, and Z. Mallat. Adaptive T cell immune responses and atherogenesis. *Curr Opin Pharmacol*, 10(2):197–202, Apr 2010.

[141] L. Li, L. Huang, A. L. Vergis, H. Ye, A. Bajwa, V. Narayan, R. M. Strieter, D. L. Rosin, and M. D. Okusa. IL-17 produced by neutrophils regulates IFN-gamma-mediated neutrophil migration in mouse kidney ischemia-reperfusion injury. *J. Clin. Invest.*, 120(1):331–342, Jan 2010.

[142] P. Miossec. IL-17 and Th17 cells in human inflammatory diseases. *Microbes Infect.*, 11(5):625–630, Apr 2009.

[143] S. Chen, T. R. Crother, and M. Arditi. Emerging role of IL-17 in atherosclerosis. *J Innate Immun*, 2(4):325–333, 2010.

[144] O. J. de Boer, J. J. van der Meer, P. Teeling, C. M. van der Loos, M. M. Idu, F. van Maldegem, J. Aten, and A. C. van der Wal. Differential expression of interleukin-17 family cytokines in intact and complicated human atherosclerotic plaques. *J. Pathol.*, 220(4):499–508, Mar 2010.

[145] C. Erbel, M. Akhavanpoor, D. Okuyucu, S. Wangler, A. Dietz, L. Zhao, K. Stellos, K. M. Little, F. Lasitschka, A. Doesch, M. Hakimi, T. J. Dengler, T. Giese, E. Blessing, H. A. Katus, and C. A. Gleissner. IL-17A influences essential functions of the monocyte/macrophage lineage and is involved in advanced murine and human atherosclerosis. *J. Immunol.*, 193(9):4344–4355, Nov 2014.

[146] R. E. Eid, D. A. Rao, J. Zhou, S. F. Lo, H. Ranjbaran, A. Gallo, S. I. Sokol, S. Pfau, J. S. Pober, and G. Tellides. Interleukin-17 and interferon-gamma are produced concomitantly by human coronary artery-infiltrating T cells and act synergistically on vascular smooth muscle cells. *Circulation*, 119(10):1424–1432, Mar 2009.

[147] S. Taleb, M. Romain, B. Ramkhelawon, C. Uyttenhove, G. Pasterkamp, O. Herbin, B. Esposito, N. Perez, H. Yasukawa, J. Van Snick, A. Yoshimura, A. Tedgui, and Z. Mallat. Loss of SOCS3 expression in T cells reveals a regulatory role for interleukin-17 in atherosclerosis. *J. Exp. Med.*, 206(10):2067–2077, Sep 2009.

[148] K. Danzaki, Y. Matsui, M. Ikesue, D. Ohta, K. Ito, M. Kanayama, D. Kurotaki, J. Morimoto, Y. Iwakura, H. Yagita, H. Tsutsui, and T. Uede. Interleukin-17A deficiency accelerates unstable atherosclerotic plaque formation in apolipoprotein E-deficient mice. *Arterioscler. Thromb. Vasc. Biol.*, 32(2):273–280, Feb 2012.

[149] C. Erbel, L. Chen, F. Bea, S. Wangler, S. Celik, F. Lasitschka, Y. Wang, D. Bockler, H. A. Katus, and T. J. Dengler. Inhibition of IL-17A attenuates atherosclerotic lesion development in apoE-deficient mice. *J. Immunol.*, 183(12):8167–8175, Dec 2009.

[150] E. Smith, K. M. Prasad, M. Butcher, A. Dobrian, J. K. Kolls, K. Ley, and E. Galkina. Blockade of interleukin-17A results in reduced atherosclerosis in apolipoprotein E-deficient mice. *Circulation*, 121(15):1746–1755, Apr 2010.

[151] M. S. Madhur, S. A. Funt, L. Li, A. Vinh, W. Chen, H. E. Lob, Y. Iwakura, Y. Blinder, A. Rahman, A. A. Quyyumi, and D. G. Harrison. Role of interleukin 17 in inflammation, atherosclerosis, and vascular function in apolipoprotein e-deficient mice. *Arterioscler. Thromb. Vasc. Biol.*, 31(7):1565–1572, Jul 2011.

[152] X. Cheng, S. Taleb, J. Wang, T. T. Tang, J. Chen, X. L. Gao, R. Yao, J. J. Xie, X. Yu, N. Xia, X. X. Yan, S. F. Nie, M. Y. Liao, Y. Cheng, Z. Mallat, and Y. H. Liao. Inhibition of IL-17A in atherosclerosis. *Atherosclerosis*, 215(2):471–474, Apr 2011.

[153] S. Demyanets, C. Kaun, K. Rychli, S. Pfaffenberger, S. P. Kastl, P. J. Hohensinner, G. Rega, K. M. Katsaros, T. Afonyushkin, V. N. Bochkov, M. Paireder, I. Huk, G. Maurer, K. Huber, and J. Wojta. Oncostatin M-enhanced vascular endothelial growth factor expression in human vascular smooth muscle cells involves PI3K-, p38 MAPK-, Erk1/2- and STAT1/STAT3-dependent pathways and is attenuated by interferon-. *Basic Res. Cardiol.*, 106(2):217–231, Mar 2011.

[154] M. N. Kirchmer, A. Franco, A. Albasanz-Puig, J. Murray, M. Yagi, L. Gao, Z. M. Dong, and E. S. Wijelath. Modulation of vascular smooth muscle cell phenotype by STAT-1 and STAT-3. *Atherosclerosis*, 234(1):169–175, May 2014.

[155] Y. Kakutani, A. Shioi, T. Shoji, H. Okazaki, H. Koyama, M. Emoto, and M. Inaba. Oncostatin M Promotes Osteoblastic Differentiation of Human Vascular Smooth Muscle Cells Through JAK3-STAT3 Pathway. *J. Cell. Biochem.*, 116(7):1325–1333, Jul 2015.

[156] K. Kwofie, M. Scott, R. Rodrigues, J. Guerette, K. Radford, P. Nair, and C. D. Richards. Regulation of IL-17A responses in human airway smooth muscle cells by Oncostatin M. *Respir. Res.*, 16:14, 2015.

[157] C. T. Weaver, R. D. Hatton, P. R. Mangan, and L. E. Harrington. IL-17 family cytokines and the expanding diversity of effector T cell lineages. *Annu. Rev. Immunol.*, 25:821–852, 2007.

[158] D. K. Fritz, C. Kerr, F. Botelho, M. Stampfli, and C. D. Richards. Oncostatin M (OSM) primes IL-13- and IL-4-induced eotaxin responses in fibroblasts: regulation of the type-II IL-4 receptor chains IL-4Ralpha and IL-13Ralpha1. *Exp. Cell Res.*, 315(20):3486–3499, Dec 2009.

[159] D. S. Faffe, L. Flynt, M. Mellema, P. E. Moore, E. S. Silverman, V. Subramaniam, M. R. Jones, J. P. Mizgerd, T. Whitehead, A. Imrich, R. A. Panettieri, and S. A. Shore. Oncostatin M causes eotaxin-1 release from airway smooth muscle: synergy with IL-4 and IL-13. *J. Allergy Clin. Immunol.*, 115(3):514–520, Mar 2005.

[160] S. L. LaPorte, Z. S. Juo, J. Vaclavikova, L. A. Colf, X. Qi, N. M. Heller, A. D. Keegan, and K. C. Garcia. Molecular and structural basis of cytokine receptor pleiotropy in the interleukin-4/13 system. *Cell*, 132(2):259–272, Jan 2008.

[161] D. J. Hilton, J. G. Zhang, D. Metcalf, W. S. Alexander, N. A. Nicola, and T. A. Willson. Cloning and characterization of a binding subunit of the interleukin 13 receptor that is also a component of the interleukin 4 receptor. *Proc. Natl. Acad. Sci. U.S.A.*, 93(1):497–501, Jan 1996.

[162] N. I. Obiri, W. Debinski, W. J. Leonard, and R. K. Puri. Receptor for interleukin 13. Interaction with interleukin 4 by a mechanism that does not involve the common gamma chain shared by receptors for interleukins 2, 4, 7, 9, and 15. *J. Biol. Chem.*, 270(15):8797–8804, Apr 1995.

[163] D. Caput, P. Laurent, M. Kaghad, J. M. Lelias, S. Lefort, N. Vita, and P. Ferrara. Cloning and characterization of a specific interleukin (IL)-13 binding protein structurally related to the IL-5 receptor alpha chain. *J. Biol. Chem.*, 271(28):16921–16926, Jul 1996.

[164] D. D. Donaldson, M. J. Whitters, L. J. Fitz, T. Y. Neben, H. Finnerty, S. L. Henderson, R. M. O'Hara, D. R. Beier, K. J. Turner, C. R. Wood, and M. Collins. The murine IL-13 receptor alpha 2: molecular cloning, characterization, and comparison with murine IL-13 receptor alpha 1. *J. Immunol.*, 161(5):2317–2324, Sep 1998.

[165] K. Arima, K. Sato, G. Tanaka, S. Kanaji, T. Terada, E. Honjo, R. Kuroki, Y. Matsuo, and K. Izuhara. Characterization of the interaction between interleukin-13 and interleukin-13 receptors. *J. Biol. Chem.*, 280(26):24915–24922, Jul 2005.

[166] J. Bernard, D. Treton, C. Vermot-Desroches, C. Boden, P. Horellou, E. Angevin, P. Galanaud, J. Wijdenes, and Y. Richard. Expression of interleukin 13 receptor in glioma and renal cell carcinoma: IL13Ralpha2 as a decoy receptor for IL13. *Lab. Invest.*, 81(9):1223–1231, Sep 2001.

[167] S. Yasunaga, N. Yuyama, K. Arima, H. Tanaka, S. Toda, M. Maeda, K. Matsui, C. Goda, Q. Yang, Y. Sugita, H. Nagai, and K. Izuhara. The negative-feedback regulation of the IL-13 signal by the IL-13 receptor alpha2 chain in bronchial epithelial cells. *Cytokine*, 24(6):293–303, Dec 2003.

[168] S. Fichtner-Feigl, W. Strober, K. Kawakami, R. K. Puri, and A. Kitani. IL-13 signaling through the IL-13alpha2 receptor is involved in induction of TGF-beta1 production and fibrosis. *Nat. Med.*, 12(1):99–106, Jan 2006.

[169] M. O. Daines and G. K. Hershey. A novel mechanism by which interferon-gamma can regulate interleukin (IL)-13 responses. Evidence for intracellular stores of IL-13 receptor alpha -2 and their rapid mobilization by interferon-gamma. *J. Biol. Chem.*, 277(12):10387–10393, Mar 2002.

[170] M. O. Daines, Y. Tabata, B. A. Walker, W. Chen, M. R. Warrier, S. Basu, and G. K. Hershey. Level of expression of IL-13R alpha 2 impacts receptor distribution and IL-13 signaling. *J. Immunol.*, 176(12):7495–7501, Jun 2006.

[171] P. J. Lupardus, M. E. Birnbaum, and K. C. Garcia. Molecular basis for shared cytokine recognition revealed in the structure of an unusually high affinity complex between IL-13 and IL-13Ralpha2. *Structure*, 18(3):332–342, Mar 2010.

[172] Y. Tabata, W. Chen, M. R. Warrier, A. M. Gibson, M. O. Daines, and G. K. Hershey. Allergy-driven alternative splicing of IL-13 receptor alpha2 yields distinct membrane and soluble forms. *J. Immunol.*, 177(11):7905–7912, Dec 2006.

[173] M. O'Toole, H. Legault, R. Ramsey, T. A. Wynn, and M. T. Kasaian. A novel and sensitive ELISA reveals that the soluble form of IL-13R-alpha2 is not expressed in plasma of healthy or asthmatic subjects. *Clin. Exp. Allergy*, 38(4):594–601, Apr 2008.

[174] M. W. Pfaffl. A new mathematical model for relative quantification in real-time RT-PCR. *Nucleic Acids Res.*, 29(9):e45, May 2001.

[175] U. K. Laemmli. Cleavage of structural proteins during the assembly of the head of bacteriophage T4. *Nature*, 227(5259):680–685, Aug 1970.

[176] F. Blanchard, Y. Wang, E. Kinzie, L. Duplomb, A. Godard, and H. Baumann. Oncostatin M regulates the synthesis and turnover of gp130, leukemia inhibitory factor receptor alpha, and oncostatin M receptor beta by distinct mechanisms. *J. Biol. Chem.*, 276(50):47038–47045, Dec 2001.

[177] S. Radtke, A. Jorissen, H. S. de Leur, P. C. Heinrich, and I. Behrmann. Three dileucine-like motifs within the interbox1/2 region of the human oncostatin M receptor prevent efficient surface expression in the absence of an associated Janus kinase. *J. Biol. Chem.*, 281(7):4024–4034, Feb 2006.

[178] E. Dittrich, C. R. Haft, L. Muys, P. C. Heinrich, and L. Graeve. A di-leucine motif and an upstream serine in the interleukin-6 (IL-6) signal transducer gp130 mediate ligand-induced endocytosis and down-regulation of the IL-6 receptor. *J. Biol. Chem.*, 271(10):5487–5494, Mar 1996.

[179] S. Thiel, I. Behrmann, A. Timmermann, H. Dahmen, G. Muller-Newen, F. Schaper, J. Tavernier, V. Pitard, P. C. Heinrich, and L. Graeve. Identification of a Leu-lle internalization motif within the cytoplasmic domain of the leukaemia inhibitory factor receptor. *Biochem. J.*, 339 (Pt 1):15–19, Apr 1999.

[180] B. S. Brooke, A. Bayes-Genis, and D. Y. Li. New insights into elastin and vascular disease. *Trends Cardiovasc. Med.*, 13(5):176–181, Jul 2003.

[181] M. J. Fazio, M. G. Mattei, E. Passage, M. L. Chu, D. Black, E. Solomon, J. M. Davidson, and J. Uitto. Human elastin gene: new evidence for localization to the long arm of chromosome 7. *Am. J. Hum. Genet.*, 48(4):696–703, Apr 1991.

[182] H. Wolinsky and S. Glagov. A lamellar unit of aortic medial structure and function in mammals. *Circ. Res.*, 20(1):99–111, Jan 1967.

[183] B. S. Brooke, S. K. Karnik, and D. Y. Li. Extracellular matrix in vascular morphogenesis and disease: structure versus signal. *Trends Cell Biol.*, 13(1):51–56, Jan 2003.

[184] E. W. Raines. The extracellular matrix can regulate vascular cell migration, proliferation, and survival: relationships to vascular disease. *Int J Exp Pathol*, 81(3):173–182, Jun 2000.

[185] D. J. Prockop and K. I. Kivirikko. Collagens: molecular biology, diseases, and potentials for therapy. *Annu. Rev. Biochem.*, 64:403–434, 1995.

[186] X. Liu, H. Wu, M. Byrne, S. Krane, and R. Jaenisch. Type III collagen is crucial for collagen I fibrillogenesis and for normal cardiovascular development. *Proc. Natl. Acad. Sci. U.S.A.*, 94(5):1852–1856, Mar 1997.

[187] S. Ricard-Blum. The collagen family. *Cold Spring Harb Perspect Biol*, 3(1):a004978, Jan 2011.

[188] J. C. Adams and J. Lawler. The thrombospondins. *Cold Spring Harb Perspect Biol*, 3(10):a009712, Oct 2011.

[189] E. Mustonen, H. Ruskoaho, and J. Rysa. Thrombospondins, potential drug targets for cardiovascular diseases. *Basic Clin. Pharmacol. Toxicol.*, 112(1):4–12, Jan 2013.

[190] O. I. Stenina, S. Y. Desai, I. Krukovets, K. Kight, D. Janigro, E. J. Topol, and E. F. Plow. Thrombospondin-4 and its variants: expression and differential effects on endothelial cells. *Circulation*, 108(12):1514–1519, Sep 2003.

[191] J. Lawler, M. Duquette, C. A. Whittaker, J. C. Adams, K. McHenry, and D. W. DeSimone. Identification and characterization of thrombospondin-4, a new member of the thrombospondin gene family. *J. Cell Biol.*, 120(4):1059–1067, Feb 1993.

[192] E. J. Topol, J. McCarthy, S. Gabriel, D. J. Moliterno, W. J. Rogers, L. K. Newby, M. Freedman, J. Metivier, R. Cannata, C. J. O'Donnell, K. Kottke-Marchant, G. Murugesan, E. F. Plow, O. Stenina, and G. Q. Daley. Single nucleotide polymorphisms in multiple novel thrombospondin genes may be associated with familial premature myocardial infarction. *Circulation*, 104(22):2641–2644, Nov 2001.

[193] Y. Yamada, H. Izawa, S. Ichihara, F. Takatsu, H. Ishihara, H. Hirayama, T. Sone, M. Tanaka, and M. Yokota. Prediction of the risk of myocardial infarction from polymorphisms in candidate genes. *N. Engl. J. Med.*, 347(24):1916–1923, Dec 2002.

[194] J. Wessel, E. J. Topol, M. Ji, J. Meyer, and J. J. McCarthy. Replication of the association between the thrombospondin-4 A387P polymorphism and myocardial infarction. *Am. Heart J.*, 147(5):905–909, May 2004.

[195] J. Cui, E. Randell, J. Renouf, G. Sun, R. Green, F. Y. Han, and Y. G. Xie. Thrombospondin-4 1186G¿C (A387P) is a sex-dependent risk factor for myocardial infarction: a large replication study with increased sample size from the same population. *Am. Heart J.*, 152(3):1–5, Sep 2006.

[196] E. G. Frolova, E. Pluskota, I. Krukovets, T. Burke, C. Drumm, J. D. Smith, L. Blech, M. Febbraio, P. Bornstein, E. F. Plow, and O. I. Stenina. Thrombospondin-4 regulates vascular inflammation and atherogenesis. *Circ. Res.*, 107(11):1313–1325, Nov 2010.

[197] J. Golledge, P. Clancy, J. Maguire, L. Lincz, and S. Koblar. The role of tenascin C in cardiovascular disease. *Cardiovasc. Res.*, 92(1):19–28, Oct 2011.

[198] K. Trescher, B. Thometich, S. Demyanets, H. Kassal, R. Sedivy, R. Bittner, C. Holzinger, and B. K. Podesser. Type A dissection and chronic dilatation: tenascin-C as a key factor in destabilization of the aortic wall. *Interact Cardiovasc Thorac Surg*, 17(2):365–370, Aug 2013.

[199] K. S. Midwood and G. Orend. The role of tenascin-C in tissue injury and tumorigenesis. *J Cell Commun Signal*, 3(3-4):287–310, Dec 2009.

[200] D. Sprini, G. B. Rini, L. Di Stefano, L. Cianferotti, and N. Napoli. Correlation between osteoporosis and cardiovascular disease. *Clin Cases Miner Bone Metab*, 11(2):117–119, May 2014.

[201] S. Evrard, P. Delanaye, S. Kamel, J. P. Cristol, E. Cavalier, J. Arnaud, P. Zaoui, M. C. Carlier, M. Laville, D. Fouque, E. Cavalier, P. Delanaye, J. P. Cristol, A. S. Bargnoux, S. Kamel, Z. Massy, D. Prie, P. Urena-Torres, J. C. Souberbielle, A. Boutten, A. Guerin, T. Hannedouche, G. Jean, M. H. Lafage-Proust, G. London, L. Mercadal, and L. Pieroni. Vascular calcification: from pathophysiology to biomarkers. *Clin. Chim. Acta*, 438:401–414, Jan 2015.

[202] S. Jono, C. Peinado, and C. M. Giachelli. Phosphorylation of osteopontin is required for inhibition of vascular smooth muscle cell calcification. *J. Biol. Chem.*, 275(26):20197–20203, Jun 2000.

[203] M. Scatena, L. Liaw, and C. M. Giachelli. Osteopontin: a multifunctional molecule regulating chronic inflammation and vascular disease. *Arterioscler. Thromb. Vasc. Biol.*, 27(11):2302–2309, Nov 2007.

[204] X. Qin, M. A. Corriere, L. M. Matrisian, and R. J. Guzman. Matrix metalloproteinase inhibition attenuates aortic calcification. *Arterioscler. Thromb. Vasc. Biol.*, 26(7):1510–1516, Jul 2006.

[205] F. W. Kiefer, M. Zeyda, K. Gollinger, B. Pfau, A. Neuhofer, T. Weichhart, M. D. Saemann, R. Geyeregger, M. Schlederer, L. Kenner, and T. M. Stulnig. Neutralization of osteopontin inhibits obesity-induced inflammation and insulin resistance. *Diabetes*, 59(4):935–946, Apr 2010.

[206] Y. Zheng, Z. Wang, L. Deng, X. Yuan, Y. Ma, G. Zhang, M. P. Gantier, J. P. Liu, L. Shen, and D. Xu. Osteopontin promotes inflammation in patients with acute coronary syndrome through its activity on IL-17 producing cells. *Eur. J. Immunol.*, 42(10):2803–2814, Oct 2012.

[207] L. Bazzichi, L. Ghiadoni, A. Rossi, M. Bernardini, M. Lanza, F. De Feo, C. Giacomelli, I. Mencaroni, K. Raimo, M. Rossi, A. M. Mazzone, S. Taddei, and S. Bombardieri. Osteopontin is associated with increased arterial stiffness in rheumatoid arthritis. *Mol. Med.*, 15(11-12):402–406, 2009.

[208] M. Baud'huin, L. Duplomb, S. Teletchea, F. Lamoureux, C. Ruiz-Velasco, M. Maillasson, F. Redini, M. F. Heymann, and D. Heymann. Osteoprotegerin: multiple partners for multiple functions. *Cytokine Growth Factor Rev.*, 24(5):401–409, Oct 2013.

[209] J. A. Lee, J. J. Yerbury, N. Farrawell, R. F. Shearer, P. Constantinescu, D. M. Hatters, W. A. Schroder, A. Suhrbier, M. R. Wilson, D. N. Saunders, and M. Ranson. SerpinB2 (PAI-2) Modulates Proteostasis via Binding Misfolded Proteins and Promotion of Cytoprotective Inclusion Formation. *PLoS ONE*, 10(6):e0130136, 2015.

[210] E. P. Feener, J. M. Northrup, L. P. Aiello, and G. L. King. Angiotensin II induces plasminogen activator inhibitor-1 and -2 expression in vascular endothelial and smooth muscle cells. *J. Clin. Invest.*, 95(3):1353–1362, Mar 1995.

[211] N. J. Beauchamp, T. A. van Achterberg, M. A. Engelse, H. Pannekoek, and C. J. de Vries. Gene expression profiling of resting and activated vascular smooth muscle cells by serial analysis of gene expression and clustering analysis. *Genomics*, 82(3):288–299, Sep 2003.

[212] W. E. Laug, R. Aebersold, A. Jong, W. Rideout, B. L. Bergman, and J. Baker. Isolation of multiple types of plasminogen activator inhibitors from vascular smooth muscle cells. *Thromb. Haemost.*, 61(3):517–521, Jun 1989.

[213] J. A. Lee, B. J. Cochran, S. Lobov, and M. Ranson. Forty years later and the role of plasminogen activator inhibitor type 2/SERPINB2 is still an enigma. *Semin. Thromb. Hemost.*, 37(4):395–407, Jun 2011.

[214] I. F. Charo and R. M. Ransohoff. The many roles of chemokines and chemokine receptors in inflammation. *N. Engl. J. Med.*, 354(6):610–621, Feb 2006.

[215] P. M. Murphy, M. Baggiolini, I. F. Charo, C. A. Hebert, R. Horuk, K. Matsushima, L. H. Miller, J. J. Oppenheim, and C. A. Power. International union of pharmacology. XXII. Nomenclature for chemokine receptors. *Pharmacol. Rev.*, 52(1):145–176, Mar 2000.

[216] D. Rossi and A. Zlotnik. The biology of chemokines and their receptors. *Annu. Rev. Immunol.*, 18:217–242, 2000.

[217] K. Shimizu, M. Minami, R. Shubiki, M. Lopez-Ilasaca, L. MacFarlane, Y. Asami, Y. Li, R. N. Mitchell, and P. Libby. CC chemokine receptor-1 activates intimal smooth muscle-like cells in graft arterial disease. *Circulation*, 120(18):1800–1813, Nov 2009.

[218] I. M. Hayes, N. J. Jordan, S. Towers, G. Smith, J. R. Paterson, J. J. Earnshaw, A. G. Roach, J. Westwick, and R. J. Williams. Human vascular smooth muscle cells express receptors for CC chemokines. *Arterioscler. Thromb. Vasc. Biol.*, 18(3):397–403, Mar 1998.

[219] M. Hibi, M. Murakami, M. Saito, T. Hirano, T. Taga, and T. Kishimoto. Molecular cloning and expression of an IL-6 signal transducer, gp130. *Cell*, 63(6):1149–1157, Dec 1990.

[220] K. Yamasaki, T. Taga, Y. Hirata, H. Yawata, Y. Kawanishi, B. Seed, T. Taniguchi, T. Hirano, and T. Kishimoto. Cloning and expression of the human interleukin-6 (BSF-2/IFN beta 2) receptor. *Science*, 241(4867):825–828, Aug 1988.

[221] M. Murakami, M. Hibi, N. Nakagawa, T. Nakagawa, K. Yasukawa, K. Yamanishi, T. Taga, and T. Kishimoto. IL-6-induced homodimerization of gp130 and associated activation of a tyrosine kinase. *Science*, 260(5115):1808–1810, Jun 1993.

[222] L. D. Ward, G. J. Howlett, G. Discolo, K. Yasukawa, A. Hammacher, R. L. Moritz, and R. J. Simpson. High affinity interleukin-6 receptor is a hexameric complex consisting of two molecules each of interleukin-6, interleukin-6 receptor, and gp-130. *J. Biol. Chem.*, 269(37):23286–23289, Sep 1994.

[223] G. Paonessa, R. Graziani, A. De Serio, R. Savino, L. Ciapponi, A. Lahm, A. L. Salvati, C. Toniatti, and G. Ciliberto. Two distinct and independent sites on IL-6 trigger gp 130 dimer formation and signalling. *EMBO J.*, 14(9):1942–1951, May 1995.

[224] T. Taga, M. Hibi, Y. Hirata, K. Yamasaki, K. Yasukawa, T. Matsuda, T. Hirano, and T. Kishimoto. Interleukin-6 triggers the association of its receptor with a possible signal transducer, gp130. *Cell*, 58(3):573–581, Aug 1989.

[225] A. Mackiewicz, H. Schooltink, P. C. Heinrich, and S. Rose-John. Complex of soluble human IL-6-receptor/IL-6 up-regulates expression of acute-phase proteins. *J. Immunol.*, 149(6):2021–2027, Sep 1992.

[226] M. Fischer, J. Goldschmitt, C. Peschel, J. P. Brakenhoff, K. J. Kallen, A. Wollmer, J. Grotzinger, and S. Rose-John. I. A bioactive designer cytokine for human hematopoietic progenitor cell expansion. *Nat. Biotechnol.*, 15(2):142–145, Feb 1997.

[227] D. P. Ramji and T. S. Davies. Cytokines in atherosclerosis: Key players in all stages of disease and promising therapeutic targets. *Cytokine Growth Factor Rev.*, May 2015.

[228] L. C. Hofbauer, J. Schrader, U. Niebergall, V. Viereck, A. Burchert, D. Horsch, K. T. Preissner, and M. Schoppet. Interleukin-4 differentially regulates osteoprotegerin expression and induces calcification in vascular smooth muscle cells. *Thromb. Haemost.*, 95(4):708–714, Apr 2006.

[229] D. C. Smyth, C. Kerr, and C. D. Richards. Oncostatin M-induced IL-6 expression in murine fibroblasts requires the activation of protein kinase Cdelta. *J. Immunol.*, 177(12):8740–8747, Dec 2006.

[230] T. Komori, M. Tanaka, E. Senba, A. Miyajima, and Y. Morikawa. Lack of oncostatin M receptor leads to adipose tissue inflammation and insulin resistance by switching macrophage phenotype. *J. Biol. Chem.*, 288(30):21861–21875, Jul 2013.

[231] J. Y. Chiang. Bile acid regulation of gene expression: roles of nuclear hormone receptors. *Endocr. Rev.*, 23(4):443–463, Aug 2002.

[232] C. R. Pullinger, C. Eng, G. Salen, S. Shefer, A. K. Batta, S. K. Erickson, A. Verhagen, C. R. Rivera, S. J. Mulvihill, M. J. Malloy, and J. P. Kane. Human cholesterol 7alpha-hydroxylase (CYP7A1) deficiency has a hypercholesterolemic phenotype. *J. Clin. Invest.*, 110(1):109–117, Jul 2002.

[233] S. K. Erickson, S. R. Lear, S. Deane, S. Dubrac, S. L. Huling, L. Nguyen, J. S. Bollineni, S. Shefer, H. Hyogo, D. E. Cohen, B. Shneider, E. Sehayek, M. Ananthanarayanan, N. Balasubramaniyan, F. J. Suchy, A. K. Batta, and G. Salen. Hypercholesterolemia and changes in lipid and bile acid metabolism in male and female cyp7A1-deficient mice. *J. Lipid Res.*, 44(5):1001–1009, May 2003.

[234] Y. A. Moon, N. A. Shah, S. Mohapatra, J. A. Warrington, and J. D. Horton. Identification of a mammalian long chain fatty acyl elongase regulated by sterol regulatory element-binding proteins. *J. Biol. Chem.*, 276(48):45358–45366, Nov 2001.

[235] T. Matsuzaka, H. Shimano, N. Yahagi, T. Yoshikawa, M. Amemiya-Kudo, A. H. Hasty, H. Okazaki, Y. Tamura, Y. Iizuka, K. Ohashi, J. Osuga, A. Takahashi, S. Yato, H. Sone, S. Ishibashi, and N. Yamada. Cloning and characterization of a mammalian fatty acyl-CoA elongase as a lipogenic enzyme regulated by SREBPs. *J. Lipid Res.*, 43(6):911–920, Jun 2002.

[236] J. D. Horton, I. Shimomura, M. S. Brown, R. E. Hammer, J. L. Goldstein, and H. Shimano. Activation of cholesterol synthesis in preference to fatty acid synthesis in liver and adipose tissue of transgenic mice overproducing sterol regulatory element-binding protein-2. *J. Clin. Invest.*, 101(11):2331–2339, Jun 1998.

[237] H. Shimano, J. D. Horton, R. E. Hammer, I. Shimomura, M. S. Brown, and J. L. Goldstein. Overproduction of cholesterol and fatty acids causes massive liver enlargement in transgenic mice expressing truncated SREBP-1a. *J. Clin. Invest.*, 98(7):1575–1584, Oct 1996.

[238] H. Shimano, J. D. Horton, I. Shimomura, R. E. Hammer, M. S. Brown, and J. L. Goldstein. Isoform 1c of sterol regulatory element binding protein is less active than isoform 1a in livers of transgenic mice and in cultured cells. *J. Clin. Invest.*, 99(5):846–854, Mar 1997.

[239] R. Saito, T. Matsuzaka, T. Karasawa, M. Sekiya, N. Okada, M. Igarashi, R. Matsumori, K. Ishii, Y. Nakagawa, H. Iwasaki, K. Kobayashi, S. Yatoh, A. Takahashi, H. Sone, H. Suzuki, N. Yahagi, N. Yamada, and H. Shimano. Macrophage Elovl6 deficiency ameliorates foam cell formation and reduces atherosclerosis in low-density lipoprotein receptor-deficient mice. *Arterioscler. Thromb. Vasc. Biol.*, 31(9):1973–1979, Sep 2011.

[240] J. A. Menendez and R. Lupu. Fatty acid synthase and the lipogenic phenotype in cancer pathogenesis. *Nat. Rev. Cancer*, 7(10):763–777, Oct 2007.

[241] F. J. Asturias, J. Z. Chadick, I. K. Cheung, H. Stark, A. Witkowski, A. K. Joshi, and S. Smith. Structure and molecular organization of mammalian fatty acid synthase. *Nat. Struct. Mol. Biol.*, 12(3):225–232, Mar 2005.

[242] S. S. Chirala and S. J. Wakil. Structure and function of animal fatty acid synthase. *Lipids*, 39(11):1045–1053, Nov 2004.

[243] A. Katsurada, N. Iritani, H. Fukuda, Y. Matsumura, N. Nishimoto, T. Noguchi, and T. Tanaka. Effects of nutrients and hormones on transcriptional and post-transcriptional regulation of fatty acid synthase in rat liver. *Eur. J. Biochem.*, 190(2):427–433, Jun 1990.

[244] J. G. Schneider, Z. Yang, M. V. Chakravarthy, I. J. Lodhi, X. Wei, J. Turk, and C. F. Semenkovich. Macrophage fatty-acid synthase deficiency decreases diet-induced atherosclerosis. *J. Biol. Chem.*, 285(30):23398–23409, Jul 2010.

[245] M. T. Nakamura and T. Y. Nara. Structure, function, and dietary regulation of delta6, delta5, and delta9 desaturases. *Annu. Rev. Nutr.*, 24:345–376, 2004.

[246] H. Sampath and J. M. Ntambi. Stearoyl-coenzyme A desaturase 1, sterol regulatory element binding protein-1c and peroxisome proliferator-activated receptor-alpha: independent and interactive roles in the regulation of lipid metabolism. *Curr Opin Clin Nutr Metab Care*, 9(2):84–88, Mar 2006.

[247] J. M. Ntambi, M. Miyazaki, J. P. Stoehr, H. Lan, C. M. Kendziorski, B. S. Yandell, Y. Song, P. Cohen, J. M. Friedman, and A. D. Attie. Loss of stearoyl-CoA desaturase-1 function protects mice against adiposity. *Proc. Natl. Acad. Sci. U.S.A.*, 99(17):11482–11486, Aug 2002.

[248] P. Dobrzyn, H. Sampath, A. Dobrzyn, M. Miyazaki, and J. M. Ntambi. Loss of stearoyl-CoA desaturase 1 inhibits fatty acid oxidation and increases glucose utilization in the heart. *Am. J. Physiol. Endocrinol. Metab.*, 294(2):E357–364, Feb 2008.

[249] M. Miyazaki, M. T. Flowers, H. Sampath, K. Chu, C. Otzelberger, X. Liu, and J. M. Ntambi. Hepatic stearoyl-CoA desaturase-1 deficiency protects mice from carbohydrate-induced adiposity and hepatic steatosis. *Cell Metab.*, 6(6):484–496, Dec 2007.

[250] H. Sampath, M. T. Flowers, X. Liu, C. M. Paton, R. Sullivan, K. Chu, M. Zhao, and J. M. Ntambi. Skin-specific deletion of stearoyl-CoA desaturase-1 alters skin lipid composition and protects mice from high fat diet-induced obesity. *J. Biol. Chem.*, 284(30):19961–19973, Jul 2009.

[251] J. M. Brown, S. Chung, J. K. Sawyer, C. Degirolamo, H. M. Alger, T. Nguyen, X. Zhu, M. N. Duong, A. L. Wibley, R. Shah, M. A. Davis, K. Kelley, M. D. Wilson, C. Kent, J. S. Parks, and L. L. Rudel. Inhibition of stearoyl-coenzyme A desaturase 1 dissociates insulin resistance and obesity from atherosclerosis. *Circulation*, 118(14):1467–1475, Sep 2008.

[252] M. L. MacDonald, M. van Eck, R. B. Hildebrand, B. W. Wong, N. Bissada, P. Ruddle, A. Kontush, H. Hussein, M. A. Pouladi, M. J. Chapman, C. Fievet, T. J. van Berkel, B. Staels, B. M. McManus, and M. R. Hayden. Despite antiatherogenic metabolic characteristics, SCD1-deficient mice have increased inflammation and atherosclerosis. *Arterioscler. Thromb. Vasc. Biol.*, 29(3):341–347, Mar 2009.

[253] M. L. MacDonald, R. R. Singaraja, N. Bissada, P. Ruddle, R. Watts, J. M. Karasinska, W. T. Gibson, C. Fievet, J. E. Vance, B. Staels, and M. R. Hayden. Absence of stearoyl-CoA desaturase-1 ameliorates features of the metabolic syndrome in LDLR-deficient mice. *J. Lipid Res.*, 49(1):217–229, Jan 2008.

[254] S. J. Wakil, J. K. Stoops, and V. C. Joshi. Fatty acid synthesis and its regulation. *Annu. Rev. Biochem.*, 52:537–579, 1983.

[255] K. G. Thampy. Formation of malonyl coenzyme A in rat heart. Identification and purification of an isozyme of A carboxylase from rat heart. *J. Biol. Chem.*, 264(30):17631–17634, Oct 1989.

[256] J. D. McGarry and N. F. Brown. The mitochondrial carnitine palmitoyltransferase system. From concept to molecular analysis. *Eur. J. Biochem.*, 244(1):1–14, Feb 1997.

[257] L. Abu-Elheiga, M. M. Matzuk, K. A. Abo-Hashema, and S. J. Wakil. Continuous fatty acid oxidation and reduced fat storage in mice lacking acetyl-CoA carboxylase 2. *Science*, 291(5513):2613–2616, Mar 2001.

[258] A. Bianchi, J. L. Evans, A. J. Iverson, A. C. Nordlund, T. D. Watts, and L. A. Witters. Identification of an isozymic form of acetyl-CoA carboxylase. *J. Biol. Chem.*, 265(3):1502–1509, Jan 1990.

[259] A. J. Iverson, A. Bianchi, A. C. Nordlund, and L. A. Witters. Immunological analysis of acetyl-CoA carboxylase mass, tissue distribution and subunit composition. *Biochem. J.*, 269(2):365–371, Jul 1990.

[260] L. Abu-Elheiga, W. R. Brinkley, L. Zhong, S. S. Chirala, G. Woldegiorgis, and S. J. Wakil. The subcellular localization of acetyl-CoA carboxylase 2. *Proc. Natl. Acad. Sci. U.S.A.*, 97(4):1444–1449, Feb 2000.

[261] A. R. Tall, P. Costet, and N. Wang. Regulation and mechanisms of macrophage cholesterol efflux. *J. Clin. Invest.*, 110(7):899–904, Oct 2002.

[262] R. M. Lawn, D. P. Wade, T. L. Couse, and J. N. Wilcox. Localization of human ATP-binding cassette transporter 1 (ABC1) in normal and atherosclerotic tissues. *Arterioscler. Thromb. Vasc. Biol.*, 21(3):378–385, Mar 2001.

[263] T. Langmann, J. Klucken, M. Reil, G. Liebisch, M. F. Luciani, G. Chimini, W. E. Kaminski, and G. Schmitz. Molecular cloning of the human ATP-binding cassette transporter 1 (hABC1): evidence for sterol-dependent regulation in macrophages. *Biochem. Biophys. Res. Commun.*, 257(1):29–33, Apr 1999.

[264] L. Yvan-Charvet, M. Ranalletta, N. Wang, S. Han, N. Terasaka, R. Li, C. Welch, and A. R. Tall. Combined deficiency of ABCA1 and ABCG1 promotes foam cell accumulation and accelerates atherosclerosis in mice. *J. Clin. Invest.*, 117(12):3900–3908, Dec 2007.

[265] X. Cheng, D. Buckley, and C. D. Klaassen. Regulation of hepatic bile acid transporters Ntcp and Bsep expression. *Biochem. Pharmacol.*, 74(11):1665–1676, Dec 2007.

[266] J. Y. Chiang, R. Kimmel, C. Weinberger, and D. Stroup. Farnesoid X receptor responds to bile acids and represses cholesterol 7alpha-hydroxylase gene (CYP7A1) transcription. *J. Biol. Chem.*, 275(15):10918–10924, Apr 2000.

[267] B. Goodwin, S. A. Jones, R. R. Price, M. A. Watson, D. D. McKee, L. B. Moore, C. Galardi, J. G. Wilson, M. C. Lewis, M. E. Roth, P. R. Maloney, T. M. Willson, and S. A. Kliewer. A regulatory cascade of the nuclear receptors FXR, SHP-1, and LRH-1 represses bile acid biosynthesis. *Mol. Cell*, 6(3):517–526, Sep 2000.

[268] T. T. Lu, M. Makishima, J. J. Repa, K. Schoonjans, T. A. Kerr, J. Auwerx, and D. J. Mangelsdorf. Molecular basis for feedback regulation of bile acid synthesis by nuclear receptors. *Mol. Cell*, 6(3):507–515, Sep 2000.

[269] L. A. Denson, E. Sturm, W. Echevarria, T. L. Zimmerman, M. Makishima, D. J. Mangelsdorf, and S. J. Karpen. The orphan nuclear receptor, shp, mediates bile acid-induced inhibition of the rat bile acid transporter, ntcp. *Gastroenterology*, 121(1):140–147, Jul 2001.

[270] M. Ananthanarayanan, N. Balasubramanian, M. Makishima, D. J. Mangelsdorf, and F. J. Suchy. Human bile salt export pump promoter is transactivated by the farnesoid X receptor/bile acid receptor. *J. Biol. Chem.*, 276(31):28857–28865, Aug 2001.

[271] J. Yu, J. L. Lo, L. Huang, A. Zhao, E. Metzger, A. Adams, P. T. Meinke, S. D. Wright, and J. Cui. Lithocholic acid decreases expression of bile salt export pump

through farnesoid X receptor antagonist activity. *J. Biol. Chem.*, 277(35):31441–31447, Aug 2002.

[272] Y. Zhang, X. Wang, C. Vales, F. Y. Lee, H. Lee, A. J. Lusis, and P. A. Edwards. FXR deficiency causes reduced atherosclerosis in Ldlr-/- mice. *Arterioscler. Thromb. Vasc. Biol.*, 26(10):2316–2321, Oct 2006.

[273] G. L. Guo, S. Santamarina-Fojo, T. E. Akiyama, M. J. Amar, B. J. Paigen, B. Brewer, and F. J. Gonzalez. Effects of FXR in foam-cell formation and atherosclerosis development. *Biochim. Biophys. Acta*, 1761(12):1401–1409, Dec 2006.

[274] E. A. Hanniman, G. Lambert, T. C. McCarthy, and C. J. Sinal. Loss of functional farnesoid X receptor increases atherosclerotic lesions in apolipoprotein E-deficient mice. *J. Lipid Res.*, 46(12):2595–2604, Dec 2005.

[275] Y. S. Lee, D. Chanda, J. Sim, Y. Y. Park, and H. S. Choi. Structure and function of the atypical orphan nuclear receptor small heterodimer partner. *Int. Rev. Cytol.*, 261:117–158, 2007.

[276] G. Garruti, H. H. Wang, L. Bonfrate, O. de Bari, D. Q. Wang, and P. Portincasa. A pleiotropic role for the orphan nuclear receptor small heterodimer partner in lipid homeostasis and metabolic pathways. *J Lipids*, 2012:304292, 2012.

[277] V. Giguere. Orphan nuclear receptors: from gene to function. *Endocr. Rev.*, 20(5):689–725, Oct 1999.

[278] Y. Zhang, C. H. Hagedorn, and L. Wang. Role of nuclear receptor SHP in metabolism and cancer. *Biochim. Biophys. Acta*, 1812(8):893–908, Aug 2011.

[279] S. K. Karnik, B. S. Brooke, A. Bayes-Genis, L. Sorensen, J. D. Wythe, R. S. Schwartz, M. T. Keating, and D. Y. Li. A critical role for elastin signaling in vascular morphogenesis and disease. *Development*, 130(2):411–423, Jan 2003.

[280] S. S. Rensen, P. A. Doevendans, and G. J. van Eys. Regulation and characteristics of vascular smooth muscle cell phenotypic diversity. *Neth Heart J*, 15(3):100–108, 2007.

[281] E. Korzus, H. Nagase, R. Rydell, and J. Travis. The mitogen-activated protein kinase and JAK-STAT signaling pathways are required for an oncostatin M-responsive element-mediated activation of matrix metalloproteinase 1 gene expression. *J. Biol. Chem.*, 272(2):1188–1196, Jan 1997.

[282] M. J. Gomez-Lechon. Oncostatin M: signal transduction and biological activity. *Life Sci.*, 65(20):2019–2030, 1999.

[283] L. Tong, D. Smyth, C. Kerr, J. Catterall, and C. D. Richards. Mitogen-activated protein kinases Erk1/2 and p38 are required for maximal regulation of TIMP-1 by oncostatin M in murine fibroblasts. *Cell. Signal.*, 16(10):1123–1132, Oct 2004.

[284] Y. Wang, O. Robledo, E. Kinzie, F. Blanchard, C. Richards, A. Miyajima, and H. Baumann. Receptor subunit-specific action of oncostatin M in hepatic cells and its modulation by leukemia inhibitory factor. *J. Biol. Chem.*, 275(33):25273–25285, Aug 2000.

[285] H. M. Kagan and W. Li. Lysyl oxidase: properties, specificity, and biological roles inside and outside of the cell. *J. Cell. Biochem.*, 88(4):660–672, Mar 2003.

[286] D. F. Higgins, K. Kimura, W. M. Bernhardt, N. Shrimanker, Y. Akai, B. Hohenstein, Y. Saito, R. S. Johnson, M. Kretzler, C. D. Cohen, K. U. Eckardt, M. Iwano, and V. H. Haase. Hypoxia promotes fibrogenesis in vivo via HIF-1 stimulation of epithelial-to-mesenchymal transition. *J. Clin. Invest.*, 117(12):3810–3820, Dec 2007.

[287] J. M. Maki, J. Rasanen, H. Tikkanen, R. Sormunen, K. Makikallio, K. I. Kivirikko, and R. Soininen. Inactivation of the lysyl oxidase gene Lox leads to aortic aneurysms, cardiovascular dysfunction, and perinatal death in mice. *Circulation*, 106(19):2503–2509, Nov 2002.

[288] I. K. Hornstra, S. Birge, B. Starcher, A. J. Bailey, R. P. Mecham, and S. D. Shapiro. Lysyl oxidase is required for vascular and diaphragmatic development in mice. *J. Biol. Chem.*, 278(16):14387–14393, Apr 2003.

[289] S. N. Gacheru, K. M. Thomas, S. A. Murray, K. Csiszar, L. I. Smith-Mungo, and H. M. Kagan. Transcriptional and post-transcriptional control of lysyl oxidase expression in vascular smooth muscle cells: effects of TGF-beta 1 and serum deprivation. *J. Cell. Biochem.*, 65(3):395–407, Jun 1997.

[290] C. J. Shanley, M. Gharaee-Kermani, R. Sarkar, T. H. Welling, A. Kriegel, J. W. Ford, J. C. Stanley, and S. H. Phan. Transforming growth factor-beta 1 increases lysyl oxidase enzyme activity and mRNA in rat aortic smooth muscle cells. *J. Vasc. Surg.*, 25(3):446–452, Mar 1997.

[291] R. S. Green, M. E. Lieb, A. S. Weintraub, S. N. Gacheru, C. L. Rosenfield, S. Shah, H. M. Kagan, and M. B. Taubman. Identification of lysyl oxidase and other platelet-derived growth factor-inducible genes in vascular smooth muscle cells by differential screening. *Lab. Invest.*, 73(4):476–482, Oct 1995.

[292] D. Y. Li, B. Brooke, E. C. Davis, R. P. Mecham, L. K. Sorensen, B. B. Boak, E. Eichwald, and M. T. Keating. Elastin is an essential determinant of arterial morphogenesis. *Nature*, 393(6682):276–280, May 1998.

[293] Z. S. Galis and J. J. Khatri. Matrix metalloproteinases in vascular remodeling and atherogenesis: the good, the bad, and the ugly. *Circ. Res.*, 90(3):251–262, Feb 2002.

[294] E. Allaire, B. Muscatelli-Groux, C. Mandet, A. M. Guinault, P. Bruneval, P. Desgranges, A. Clowes, D. Melliere, and J. P. Becquemin. Paracrine effect of vascular smooth muscle cells in the prevention of aortic aneurysm formation. *J. Vasc. Surg.*, 36(5):1018–1026, Nov 2002.

[295] B. Voss and J. Rauterberg. Localization of collagen types I, III, IV and V, fibronectin and laminin in human arteries by the indirect immunofluorescence method. *Pathol. Res. Pract.*, 181(5):568–575, Oct 1986.

[296] H. Koyama, E. W. Raines, K. E. Bornfeldt, J. M. Roberts, and R. Ross. Fibrillar collagen inhibits arterial smooth muscle proliferation through regulation of Cdk2 inhibitors. *Cell*, 87(6):1069–1078, Dec 1996.

[297] E. W. Raines, H. Koyama, and N. O. Carragher. The extracellular matrix dynamically regulates smooth muscle cell responsiveness to PDGF. *Ann. N. Y. Acad. Sci.*, 902:39–51, May 2000.

[298] L. C. Hofbauer and M. Schoppet. Clinical implications of the osteoprotegerin/RANKL/RANK system for bone and vascular diseases. *JAMA*, 292(4):490–495, Jul 2004.

[299] N. Bucay, I. Sarosi, C. R. Dunstan, S. Morony, J. Tarpley, C. Capparelli, S. Scully, H. L. Tan, W. Xu, D. L. Lacey, W. J. Boyle, and W. S. Simonet. osteoprotegerin-deficient mice develop early onset osteoporosis and arterial calcification. *Genes Dev.*, 12(9):1260–1268, May 1998.

[300] M. Schoppet, M. M. Kavurma, L. C. Hofbauer, and C. M. Shanahan. Crystallizing nanoparticles derived from vascular smooth muscle cells contain the calcification inhibitor osteoprotegerin. *Biochem. Biophys. Res. Commun.*, 407(1):103–107, Apr 2011.

[301] R. Candido, B. Toffoli, F. Corallini, S. Bernardi, D. Zella, R. Voltan, V. Grill, C. Celeghini, and B. Fabris. Human full-length osteoprotegerin induces the proliferation of rodent vascular smooth muscle cells both in vitro and in vivo. *J. Vasc. Res.*, 47(3):252–261, 2010.

[302] A. Lawrie, E. Waterman, M. Southwood, D. Evans, J. Suntharalingam, S. Francis, D. Crossman, P. Croucher, N. Morrell, and C. Newman. Evidence of a role for osteoprotegerin in the pathogenesis of pulmonary arterial hypertension. *Am. J. Pathol.*, 172(1):256–264, Jan 2008.

[303] J. Zhang, M. Fu, D. Myles, X. Zhu, J. Du, X. Cao, and Y. E. Chen. PDGF induces osteoprotegerin expression in vascular smooth muscle cells by multiple signal pathways. *FEBS Lett.*, 521(1-3):180–184, Jun 2002.

[304] C. M. Giachelli, L. Liaw, C. E. Murry, S. M. Schwartz, and M. Almeida. Osteopontin expression in cardiovascular diseases. *Ann. N. Y. Acad. Sci.*, 760:109–126, Apr 1995.

[305] M. Takemoto, K. Yokote, M. Nishimura, T. Shigematsu, T. Hasegawa, S. Kon, T. Uede, T. Matsumoto, Y. Saito, and S. Mori. Enhanced expression of osteopontin in human diabetic artery and analysis of its functional role in accelerated atherogenesis. *Arterioscler. Thromb. Vasc. Biol.*, 20(3):624–628, Mar 2000.

[306] T. X. Pedersen, M. Madsen, N. Junker, C. Christoffersen, J. Vikesa, S. Bro, A. Hultgardh-Nilsson, and L. B. Nielsen. Osteopontin deficiency dampens the pro-atherogenic effect of uraemia. *Cardiovasc. Res.*, 98(3):352–359, Jun 2013.

[307] C. M. Giachelli, D. Lombardi, R. J. Johnson, C. E. Murry, and M. Almeida. Evidence for a role of osteopontin in macrophage infiltration in response to pathological stimuli in vivo. *Am. J. Pathol.*, 152(2):353–358, Feb 1998.

[308] K. Fujinaga, K. Onoda, K. Yamamoto, K. Imanaka-Yoshida, M. Takao, T. Shimono, H. Shimpo, T. Yoshida, and I. Yada. Locally applied cilostazol suppresses neointimal hyperplasia by inhibiting tenascin-C synthesis and smooth muscle cell proliferation in free artery grafts. *J. Thorac. Cardiovasc. Surg.*, 128(3):357–363, Sep 2004.

[309] K. Yamamoto, K. Onoda, Y. Sawada, K. Fujinaga, K. Imanaka-Yoshida, H. Shimpo, T. Yoshida, and I. Yada. Tenascin-C is an essential factor for neointimal hyperplasia after aortotomy in mice. *Cardiovasc. Res.*, 65(3):737–742, Feb 2005.

[310] U. Hedin, J. Holm, and G. K. Hansson. Induction of tenascin in rat arterial injury. Relationship to altered smooth muscle cell phenotype. *Am. J. Pathol.*, 139(3):649–656, Sep 1991.

[311] P. Raynal and H. B. Pollard. Annexins: the problem of assessing the biological role for a gene family of multifunctional calcium- and phospholipid-binding proteins. *Biochim. Biophys. Acta*, 1197(1):63–93, Apr 1994.

[312] C. Y. Chung and H. P. Erickson. Cell surface annexin II is a high affinity receptor for the alternatively spliced segment of tenascin-C. *J. Cell Biol.*, 126(2):539–548, Jul 1994.

[313] K. A. Hajjar, A. T. Jacovina, and J. Chacko. An endothelial cell receptor for plasminogen/tissue plasminogen activator. I. Identity with annexin II. *J. Biol. Chem.*, 269(33):21191–21197, Aug 1994.

[314] C. Y. Chung, J. E. Murphy-Ullrich, and H. P. Erickson. Mitogenesis, cell migration, and loss of focal adhesions induced by tenascin-C interacting with its cell surface receptor, annexin II. *Mol. Biol. Cell*, 7(6):883–892, Jun 1996.

[315] S. Potteaux, C. Combadiere, B. Esposito, S. Casanova, R. Merval, P. Ardouin, J. L. Gao, P. M. Murphy, A. Tedgui, and Z. Mallat. Chemokine receptor CCR1 disruption in bone marrow cells enhances atherosclerotic lesion development and inflammation in mice. *Mol. Med.*, 11(1-12):16–20, 2005.

[316] R. Salcedo, H. A. Young, M. L. Ponce, J. M. Ward, H. K. Kleinman, W. J. Murphy, and J. J. Oppenheim. Eotaxin (CCL11) induces in vivo angiogenic responses by human CCR3+ endothelial cells. *J. Immunol.*, 166(12):7571–7578, Jun 2001.

[317] P. Joubert, S. Lajoie-Kadoch, M. Welman, S. Dragon, S. Letuvee, B. Tolloczko, A. J. Halayko, A. S. Gounni, K. Maghni, and Q. Hamid. Expression and regulation of CCR1 by airway smooth muscle cells in asthma. *J. Immunol.*, 180(2):1268–1275, Jan 2008.

[318] A. Zernecke and C. Weber. Chemokines in the vascular inflammatory response of atherosclerosis. *Cardiovasc. Res.*, 86(2):192–201, May 2010.

[319] A. Zernecke and C. Weber. Chemokines in atherosclerosis: proceedings resumed. *Arterioscler. Thromb. Vasc. Biol.*, 34(4):742–750, Apr 2014.

[320] V. Braunersreuther, A. Zernecke, C. Arnaud, E. A. Liehn, S. Steffens, E. Shagdarsuren, K. Bidzhekov, F. Burger, G. Pelli, B. Luckow, F. Mach, and C. Weber. Ccr5 but not Ccr1 deficiency reduces development of diet-induced atherosclerosis in mice. *Arterioscler. Thromb. Vasc. Biol.*, 27(2):373–379, Feb 2007.

[321] O. Soehnlein, M. Drechsler, Y. Doring, D. Lievens, H. Hartwig, K. Kemmerich, A. Ortega-Gomez, M. Mandl, S. Vijayan, D. Projahn, C. D. Garlichs, R. R. Koenen, M. Hristov, E. Lutgens, A. Zernecke, and C. Weber. Distinct functions of chemokine receptor axes in the atherogenic mobilization and recruitment of classical monocytes. *EMBO Mol Med*, 5(3):471–481, Mar 2013.

[322] M. Drechsler, R. T. Megens, M. van Zandvoort, C. Weber, and O. Soehnlein. Hyperlipidemia-triggered neutrophilia promotes early atherosclerosis. *Circulation*, 122(18):1837–1845, Nov 2010.

[323] N. R. Veillard, B. Kwak, G. Pelli, F. Mulhaupt, R. W. James, A. E. Proudfoot, and F. Mach. Antagonism of RANTES receptors reduces atherosclerotic plaque formation in mice. *Circ. Res.*, 94(2):253–261, Feb 2004.

[324] C. H. Lundgren, H. Sawa, B. E. Sobel, and S. Fujii. Modulation of expression of monocyte/macrophage plasminogen activator activity and its implications for attenuation of vasculopathy. *Circulation*, 90(4):1927–1934, Oct 1994.

[325] S. Demyanets, C. Kaun, K. Rychli, G. Rega, S. Pfaffenberger, T. Afonyushkin, V. N. Bochkov, G. Maurer, K. Huber, and J. Wojta. The inflammatory cytokine oncostatin M induces PAI-1 in human vascular smooth muscle cells in vitro via PI 3-kinase and ERK1/2-dependent pathways. *Am. J. Physiol. Heart Circ. Physiol.*, 293(3):H1962–1968, Sep 2007.

[326] G. Rega, C. Kaun, T. W. Weiss, S. Demyanets, G. Zorn, S. P. Kastl, S. Steiner, D. Seidinger, C. W. Kopp, M. Frey, R. Roehle, G. Maurer, K. Huber, and J. Wojta. Inflammatory cytokines interleukin-6 and oncostatin m induce plasminogen activator inhibitor-1 in human adipose tissue. *Circulation*, 111(15):1938–1945, Apr 2005.

[327] J. Ko, C. Y. Yun, J. S. Lee, J. H. Kim, and I. S. Kim. p38 MAPK and ERK activation by 9-cis-retinoic acid induces chemokine receptors CCR1 and CCR2 expression in human monocytic THP-1 cells. *Exp. Mol. Med.*, 39(2):129–138, Apr 2007.

[328] I. Boing, C. Stross, S. Radtke, B. E. Lippok, P. C. Heinrich, and H. M. Hermanns. Oncostatin M-induced activation of stress-activated MAP kinases depends on tyrosine 861 in the OSM receptor and requires Jak1 but not Src kinases. *Cell. Signal.*, 18(1):50–61, Jan 2006.

[329] W. Li, Z. Cai, M. Liu, C. Zhao, D. Li, C. Lv, Y. Wang, and T. Xu. Urotensin II contributes to collagen synthesis and up-regulates Egr-1 expression in cultured pulmonary arterial smooth muscle cells through the ERK1/2 pathway. *Biochem. Biophys. Res. Commun.*, 467(4):1076–1082, Nov 2015.

[330] M. S. Rahman, J. Yang, L. Y. Shan, H. Unruh, X. Yang, A. J. Halayko, and A. S. Gounni. IL-17R activation of human airway smooth muscle cells induces CXCL-8 production via a transcriptional-dependent mechanism. *Clin. Immunol.*, 115(3):268–276, Jun 2005.

[331] H. Renz, J. Domenico, and E. W. Gelfand. IL-4-dependent up-regulation of IL-4 receptor expression in murine T and B cells. *J. Immunol.*, 146(9):3049–3055, May 1991.

[332] J. Ohara and W. E. Paul. Up-regulation of interleukin 4/B-cell stimulatory factor 1 receptor expression. *Proc. Natl. Acad. Sci. U.S.A.*, 85(21):8221–8225, Nov 1988.

[333] H. Kotanides and N. C. Reich. Interleukin-4-induced STAT6 recognizes and activates a target site in the promoter of the interleukin-4 receptor gene. *J. Biol. Chem.*, 271(41):25555–25561, Oct 1996.

[334] P. Palmqvist, P. Lundberg, E. Persson, A. Johansson, I. Lundgren, A. Lie, H. H. Conaway, and U. H. Lerner. Inhibition of hormone and cytokine-stimulated osteoclastogenesis and bone resorption by interleukin-4 and interleukin-13 is associated with increased osteoprotegerin and decreased RANKL and RANK in a STAT6-dependent pathway. *J. Biol. Chem.*, 281(5):2414–2429, Feb 2006.

[335] N. C. Stein, C. Kreutzmann, S. P. Zimmermann, U. Niebergall, L. Hellmeyer, C. Goettsch, M. Schoppet, and L. C. Hofbauer. Interleukin-4 and interleukin-13 stimulate the osteoclast inhibitor osteoprotegerin by human endothelial cells through the STAT6 pathway. *J. Bone Miner. Res.*, 23(5):750–758, May 2008.

[336] D. Lin, L. Li, Y. Sun, W. Wang, X. Wang, Y. Ye, X. Chen, and Y. Xu. IL-17 regulates the expressions of RANKL and OPG in human periodontal ligament cells via TRAF6/TBK1-JNK/NF-B pathways. *Immunology*, Sep 2014.

[337] J. L. Ingram, D. Slade, T. D. Church, D. Francisco, K. Heck, R. W. Sigmon, M. Ghio, A. Murillo, R. Firszt, N. L. Lugogo, L. Que, M. E. Sunday, and M. Kraft. Matrix Metalloproteinases-1 and -2 Mediate IL-13-induced Suppression of Elastin in Airway Fibroblasts in Asthma. *Am. J. Respir. Cell Mol. Biol.*, Jun 2015.

[338] P. Gillery, C. Fertin, J. F. Nicolas, F. Chastang, B. Kalis, J. Banchereau, and F. X. Maquart. Interleukin-4 stimulates collagen gene expression in human fibroblast monolayer cultures. Potential role in fibrosis. *FEBS Lett.*, 302(3):231–234, May 1992.

[339] V. Salmon-Ehr, H. Serpier, B. Nawrocki, P. Gillery, C. Clavel, B. Kalis, P. Birembaut, and F. X. Maquart. Expression of interleukin-4 in scleroderma skin specimens and scleroderma fibroblast cultures. Potential role in fibrosis. *Arch Dermatol*, 132(7):802–806, Jul 1996.

[340] A. E. Postlethwaite, M. A. Holness, H. Katai, and R. Raghow. Human fibroblasts synthesize elevated levels of extracellular matrix proteins in response to interleukin 4. *J. Clin. Invest.*, 90(4):1479–1485, Oct 1992.

[341] M. Voss, L. Wolf, A. Kamyschnikow, B. Wonnenberg, A. Honecker, C. Herr, P. M. Lepper, M. Wegmann, M. D. Menger, R. Bals, and C. Beisswenger. Il-17A contributes to maintenance of pulmonary homeostasis in a murine model of cigarette smoke-induced emphysema. *Am. J. Physiol. Lung Cell Mol. Physiol.*, 309(2):L188–195, Jul 2015.

[342] A. L. Andrews, T. Nasir, F. Bucchieri, J. W. Holloway, S. T. Holgate, and D. E. Davies. IL-13 receptor alpha 2: a regulator of IL-13 and IL-4 signal transduction in primary human fibroblasts. *J. Allergy Clin. Immunol.*, 118(4):858–865, Oct 2006.

[343] T. Zheng, Z. Zhu, W. Liu, C. G. Lee, Q. Chen, R. J. Homer, and J. A. Elias. Cytokine regulation of IL-13Ralpha2 and IL-13Ralpha1 in vivo and in vitro. *J. Allergy Clin. Immunol.*, 111(4):720–728, Apr 2003.

[344] M. G. Chiaramonte, M. Mentink-Kane, B. A. Jacobson, A. W. Cheever, M. J. Whitters, M. E. Goad, A. Wong, M. Collins, D. D. Donaldson, M. J. Grusby, and T. A. Wynn. Regulation and function of the interleukin 13 receptor alpha 2 during a T helper cell type 2-dominant immune response. *J. Exp. Med.*, 197(6):687–701, Mar 2003.

[345] B. Schieffer, T. Selle, A. Hilfiker, D. Hilfiker-Kleiner, K. Grote, U. J. Tietge, C. Trautwein, M. Luchtefeld, C. Schmittkamp, S. Heeneman, M. J. Daemen, and H. Drexler. Impact of interleukin-6 on plaque development and morphology in experimental atherosclerosis. *Circulation*, 110(22):3493–3500, Nov 2004.

[346] T. Komori, M. Tanaka, E. Senba, A. Miyajima, and Y. Morikawa. Deficiency of oncostatin M receptor (OSMR) exacerbates high-fat diet-induced obesity and related metabolic disorders in mice. *J. Biol. Chem.*, 289(20):13821–13837, May 2014.

[347] M. Makishima, A. Y. Okamoto, J. J. Repa, H. Tu, R. M. Learned, A. Luk, M. V. Hull, K. D. Lustig, D. J. Mangelsdorf, and B. Shan. Identification of a nuclear receptor for bile acids. *Science*, 284(5418):1362–1365, May 1999.

[348] T. Kubin, J. Poling, S. Kostin, P. Gajawada, S. Hein, W. Rees, A. Wietelmann, M. Tanaka, H. Lorchner, S. Schimanski, M. Szibor, H. Warnecke, and T. Braun. Oncostatin M is a major mediator of cardiomyocyte dedifferentiation and remodeling. *Cell Stem Cell*, 9(5):420–432, Nov 2011.

6 Index of abbreviations

α	Alpha
β	Beta
γ	Gamma
°C	Degree Celsius
µg	Microgramm
µl	Microliter
µm	Micrometer
µM	Micromolar
Ab	Antibody
ABCA1	ATP-binding cassette transporter 1
ACC	Acetyl-CoA-Carboxylase
Ag	Antigen
Akt (PKB)	Protein kinase B
Amph B	Amphotericin B
ApoE	Apolipoprotein E
bp	Base pair
BSA	Bovine serum albumin
BSEP (ABCB11)	Bile Salt Export Pump (ATP Binding Cassette protein B11)
CAD	Coronary artery disease
CCR1	Chemokine receptor type 1
CO_2	Carbon dioxide
Col1α1	Collagen type I α 1
Col1α2	Collagen type I α 2
Col3α1	Collagen type III α 1
Ct	Cycle of threshold
Ctrl	Control
CXCR	Chemokine receptor

CYP7A1	Cholesterol 7 alpha-hydroxylase
DAPI	4',6-Diamidino-2-phenylindole
DC	Dendritic cell
ddW	Double destilled water
DMEM	Dulbecco's Modified Eagle Medium
DMSO	Dimethyl sulfoxide
DNA	Deoxyribonucleic acid
dNTP	Deoxyriobnuleotide triphosphate
EC	Endothelial cell
ECM	Extracellular matrix
e.g.	For example
EDTA	Ethylenediaminetetraacetic acid
Eln	Elastin
ELOVL6	Elongation of very long chain fatty acids protein 6
ERK1/2	Extracellular-signal regulated kinase 1/2
Fab	Fragment antigen binding
FACS	Fluorescence activated cell sorting
FASN	Fatty acid synthase
FBS/FCS	Foetal bovine serum/Fetal calf serum
Fig.	Figure
FN III	Fibronectin type III
Fwd primer	Forward primer
FXR	Farnesoid X receptor
g	Relative centrifugal force/ G force
g/gr	Gram
GAPDH	Glyceraldehyde 3-phosphate dehydrogenase
gDNA	genome DNA
GFP	Green fluorescent protein
GM-CSF	Granulocyte macrophage colony stimulating factor
gp130	Glycoprotein 130
GPCR	G protein-coupled receptor
h	Hour
H&E	Haematoxylin and Eosin
HBSS	Hank's balanced salt solution
HCl	Hydrochloric acid

HDL	High density lipoprotein
HFD	High fat diet
HPRT	Hypoxanthine-guanine phosphoribosyltransferase
HRP	Horse radish peroxidase
IF	Immunofluorescence
IFNγ	Interferon gamma
Ig	Immunoglobulin
IL-4	Interleukin-4
IL-6	Interleukin-6
IL-13	Interleukin-13
IL-17	Interleukin-17
JAK	Janus kinase
kb	Kilobase
kb	Kilobase
KO	Knockout
l	Liter
LDL	Low density lipoprotein
LDLR	Low density lipoprotein receptor
LIF	Leukemia inhibitory factor
LIFRβ	Leukemia inhibitory factor receptor beta
LN	Lymph node
LPS	Lipopolysaccharide
LXR	Liver X receptor
M	Molarity
MΦ	Macrophage
mAb	Monoclonal antibody
MAPK	Mitogen-activated protein kinases
MCV	Mean cell volume
MEK (MAPKK)	Mitogen-activated protein kinase kinase
mg	Milligram
$MgCl_2$	Magnesium chloride
MHC	Major histocompatibility complex
min	Minutes
ml	Milliliter
mm	Millimeter

mM	Millimolar
MMP	Matrix metalloproteinase
mRNA	Messenger RNA
MS	Multiple sclerosis
MS1 cells	"MILE SVEN 1" cells
N_2	Nitrogen
Na_2HPO_4	Disodium phosphate
Na_3VO_4	Sodium orthovanadate
NaCl	Sodium chloride
ng	Nanogram
NK cells	Natural killer cells
NKT cells	Natural killer T cells
nm	Nanometer
nM	Nanomolar
nt	Nucleotide
NTCP	Sodium-taurocholate co-transporting polypeptide
o/n	Overnight
oligo(dT)	Oligo desoythymidine
OPG	Osteoprotegerin
OPN	Osteopontin
OSM	Oncostatin M
OSMRβ	OSM receptor beta
oxLDL	Oxidized low density lipoprotein
p38	Mitogen-activated protein kinase p38 alpha
PAR	Protease activated receptor
pAb	Polyclonal antibody
PAMP	Pathogen associated molecular pattern
PBS	Phosphate buffered saline
PCR	Polymerase chain reaction
PE	Phycoerythrin
PFA	Paraformaldehyde
PI3K	Phosphatidylinositol 3-kinase
PLT	Platelet
PMSF	Phenylmethylsulfonyl fluoride
P/S	Penicillin and Streptomycin

PVDF	Polyvinylidene fluoride
qPCR	Quantitative real time PCR
RA	Rheumatoid arthritis
RBC	Red blood cell
Rev primer	Reverse primer
RNA	Ribonucleic acid
rpm	Rotations per minute
RPMI	Roswell park memorial institute
RT	Room temperature
RT-PCR	Reverse transcription PCR
SCD1	Stearoyl-coenzyme A desaturase-1
SD	Standard deviation
SDS	Sodium dodecyl sulfate
SM22α	smooth muscle protein 22-alpha
SEM	Standard error of mean
SerpinB2 (PAI-2)	Serine peptidase inhibitor, clade B, member 2 (Plasminogen activator inhibitor-2)
SHP	Small heterodimer partner
SMA	Smooth muscle actin
SMC	Smooth muscle cell
SN	Supernatant
STAT	Signal Transducers and Activators of Transcription
α-tubulin	Alpha tubulin
TAE	Tris-acetate-EDTA
TBS-T	Tris-buffered saline Tween 20
TEMED	N,N,N',N'-Tetramethylethylendiamin
TGFβ	Transforming growth factor beta
Th	Helper T cell
Thbs-4	Thrombospondin-4
TLR	Toll-like receptor
TnC	Tenascin C
TNFα	Tumour necrosis factor alpha
Treg	Regulatory T cell
TRIS	Tris(hydroxymethyl)aminomethane
unst.	Unstimulated

UT	Untreated
UV	Ultraviolet
VEGFR-2 (Kdr)	Vascular endothelial growth factor receptor-2
VLDL	Very low density lipoprotein
VSMC	Vascular smooth muscle cell
WB	Western blot
WBC	White blood cell
WD	Western diet
WT	Wild-type

7 Acknowledgements

First, I would like to thank PD Dr. Heike Hermanns for the opportunity to work in her laboratory and to conduct this thesis. Furthermore, her support and knowledge were always helpful during my PhD period.

I also want to thank my second supervisor Prof. Dr. Bernhard Nieswandt and my third supervisor Prof Dr. Thomas Rudel for helpful scientific discussions and for reviewing my thesis.

I am thankful for the great discussions with and support of my present and former lab members Dr. Christine Mais, Sabine Hergovits (née Walter), Dr. Johannes Drechsler, Dr. Christiane Erb, Daniela Kraemer, Desislava Koleva, and Dr. Christoph Hintzen. Dr. Christine Mais helped me a lot establishing and breeding my mouse lines. After I left the group, she maintained my mouse lines for further experiments. Beside the great discussions, Sabine Hergovits supported me with FACS analysis and the work-up of my mice on WD. Additionally I would like to thank all students who worked in our laboratory during my thesis establishing some important experiments.

I thank Dr. Koji Nakamura (LivTech Inc.), Prof. Dr. Thomas Braun and Dr. Thomas Kubin (MPI, Bad Nauheim) for receiving the *Osmr*$^{-/-}$ mouse and Prof. Dr. Alma Zernecke-Madsen for obtaining the *Ldlr*$^{-/-}$ mouse.

Additionally, I want to thank Prof. Dr. Alma Zernecke-Madsen and her group, especially Dr. Miriam Koch, Melanie Schott and Petra Werner for their support during the WD experiments.

I want to thank Prof. Dr. Andreas Geier and his group, for their cooperation and the meetings within the last years. During the WD experiments, I got a lot of support from Dr. Daniel Jahn and Donata Dorbath.

Furthermore, I want to thank Prof. Dr. Bernhard Nieswandt's group, especially Dr. Sebastian Dütting and Dr. Timo Vögtle, for the opportunity to work on their Grb2 and the Sax project.

My thanks also go to Prof. Dr. Thomas Müller and Dr. Viswanadham Duppatla. There, I had the chance to work on their IL-4 agonist project.

I want to thank all the members of the groups around our laboratories and office for the great time and many chats. It was a pleasure to work with you.

It is also important to thank the animal caretakers for running the animal facility and Dr. Katharina Remer who always gave helpful advice for handling mice.

Special thanks go to our IT persons Christian Weinberger and Bernhard Fröhlich for solving acute computer problems, to Hilke Gehret managing the post office, and to our company technicians Daniel Göbel, Mario Artmann and Sebastian Hämmerling.

My thanks also go to the "Graduate School of Life Sciences" (GSLS) and the *Rechenzentrum* from the University of Würzburg for organizing useful transferable skill and computer courses.

At the end, I want to thank my boyfriend Alex, my family, and friends for all their support during these years. Without their help and appreciation I would not be as far as I am today.

8 Danksagung

Zunächst möchte mich bei PD Dr. Heike Hermanns für die Möglichkeit bedanken, in ihrem Labor arbeiten zu dürfen und diese Doktorarbeit erhalten zu haben. Desweiteren waren ihre Unterstützung und Wissen immer sehr hilfreich während meiner Doktorandenzeit.

Ich möchte mich auch bei meinem Zweitbetreuer Prof. Dr. Bernhard Nieswandt und meinem Drittbetreuer Prof. Dr. Thomas Rudel für ihre hilfreichen wissenschaftlichen Diskussionen und für die Rezension meiner Doktorarbeit bedanken.

Ich bin dankbar für die tollen Diskussionen und Unterstützung seitens meiner jetzigen und ehemaligen Laborkollegen Dr. Christine Mais, Sabine Hergovits (geborene Walter), Dr. Johannes Drechsler, Dr. Christiane Erb, Daniela Kraemer, Desislava Koleva und Dr. Christoph Hintzen. Dr. Christine Mais half mir sehr bei der Etablierung und Zucht meiner Mauslinien. Nach Verlassen der Arbeitsgruppe, verwaltete sie meine Mauslinien für weitere Experimente. Neben zahlreichen Diskussionen, unterstützte mich Sabine Hergovits bei FACS Analysen und bei der Aufarbeitung der Mäuse für die WD-Experimente. Zusätzlich möchte ich allen Studenten danken, die während meiner Doktorarbeit in unserem Labor gearbeitet und einige wichtige Experimente etabliert haben.

Ich danke Dr. Koji Nakamura (LivTech Inc.), Prof. Dr. Thomas Braun und Dr. Thomas Kubin (MPI, Bad Nauheim) für den Erhalt der *Osmr*$^{-/-}$ Maus, ebenso Prof. Dr. Alma Zernecke-Madsen für den Erhalt der *Ldlr*$^{-/-}$ Maus.

Zusätzlich möchte ich Prof. Dr. Alma Zernecke-Madsen und ihrer Gruppe danken, vor allem aber Dr. Miriam Koch, Melanie Schott und Petra Werner für ihre Unterstützung während der WD-Experimente.

Ich möchte mich bei Prof.Dr. Andras Geier und seiner Gruppe für ihre Zusammenarbeit und den *meetings* in den letzten Jahren bedanken. Während der WD-Experimente erhielt ich von Dr. Daniel Jahn und Donata Dorbath viel Unterstützung.

Weiterhin möchte ich mich bei Prof. Dr. Bernhard Nieswandts Gruppe bedanken, vor allem bei Dr. Sebastian Dütting und Dr. Timo Vögtle für die Möglichkeit, an ihrem Grb2- und Sax-Projekt arbeiten zu dürfen.

Meinen Dank gilt auch Prof. Dr. Thomas Müller und Dr. Viswanadham Duppatla. Bei ihnen hatte ich die Chance, an ihrem Il-4-Agonisten-Projekt arbeiten zu dürfen.

Ich möchte mich bei allen benachbarten Gruppenmitgliedern für die tolle Zeit und den vielen Gesprächen bedanken. Es war mir ein Vergnügen, mit euch zu arbeiten.

Ebenso wichtig ist es den Tierpflegern für die Betreibung des Tiereinrichtung zu danken und Dr. Katharina Remer, die mir immer hilfreiche Ratschläge bei die Handhabung von Mäusen gab.

Besonderen Dank geht an unsere ITler Christian Weinberger und Bernhard Fröhlich für die Behebung akuter Computerprobleme, an Hilke Gehret für das Verwalten des Postbüros und an unsere Haustechniker Daniel Göbel, Mario Artmann and Sebastian Hämmerling.

Meinen Dank gilt auch der "*Graduate School of Life Sciences*" (GSLS) und dem Rechenzentrum der Universität Würzburg für die Organisation nützlicher Fortbildungs- und Computerkurse.

Zum Schluss möchte ich meinem Freund Alex, meiner Familie und meinen Freunden für ihre Unterstützung während all den Jahren danken. Ohne ihre Hilfe und ihr Verständnis wäre ich nicht so weit gekommen.

9 Publications

Dütting S, Vögtle T, Morowski M, Schiessl S, **Schäfer CM**, Watson SK, Hughes CE, Ackermann JA, Radtke D, Hermanns HM, Watson SP, Nitschke L, Nieswandt B. Growth factor receptor-bound protein 2 contributes to (hem)immunoreceptor tyrosine-based activation motif-mediated signaling in platelets. *Circ. Res.*, 114(3):444-453, Jan 2014.

Duppatla V, Gjorgjevikj M, Schmitz W, Hermanns HM, **Schäfer CM**, Kottmair M, Müller T, Sebald W. IL-4 analogues with site-specific chemical modification at position 121 inhibit IL-4 and IL-13 biological activities. *Bioconjug. Chem.*, 25(1):52-62, Jan 2014.

Affidavit

I hereby confirm that my thesis entitled "Influence of interleukin-6-type cytokine oncostatin M on murine aortic vascular smooth muscle cells" is the result of my own work. I did not receive any help or support from commercial consultants. All sources and/or materials applied are listed and specified in the thesis.

Furthermore, I confirm that this thesis has not yet been submitted as part of another examination process neither in identical nor in similar form.

Würzburg,

Eidesstattliche Erklärung

Hiermit erkläre ich an Eides statt, die Dissertation "Einfluss des Interleukin-6-Typ Zytokins Oncostatin M auf murine vaskuläre glatte Muskelzellen der Aorta" eigenständig, d.h. insbesondere selbstständig und ohne Hilfe eines kommerziellen Promotionsberaters angefertigt und keine anderen als die von mir angegebenen Quellen und Hilfsmittel verwendet zu haben.

Ich erkläre außerdem, dass die Dissertation weder in gleicher noch in ähnlicher Form bereits in einem anderen Prüfungsverfahren vorgelegen hat.

Würzburg,